BEHAVIOR OF IODINE IN THE PRESENCE OF SODIUM OXIDE AEROSOLS*

L. Baurmash
C. Nelson
J. Granger
R. Koontz

Atomics International,
A Division of North American Rockwell Corporation
Canoga Park, California

ABSTRACT

The agglomeration of iodine-131 and sodium oxide particulates has been studied for two types of hypothetical Liquid Metal Fast Breeder Reactor (LMFBR) accidents. In the first test, the iodine was in the form of sodium iodide-131, and was released simultaneously with sodium oxide aerosol produced from a pool fire. In the second, the sodium oxide aerosol was released into an atmosphere containing molecular iodine-131 vapor.

The first type of release simulates an incident in which the fission product iodine has reacted to form sodium iodide before the accident. The released aerosol consists of sodium oxide and sodium iodide-131. Observations of the airborne concentration, fallout rate, plating rate, and particle size show that the sodium iodide-131 was agglomerated with the sodium oxide, and the aerosol behaved as though it were one material. The second experiment simulates a fuel accident in which fission products are released separately from the oxide. As the sodium oxide aerosol particles were mixed with iodine-131 vapor, the oxide rapidly scavenged a large fraction of the available iodine, reducing the free molecular iodine concentration by a factor of 10^3 in a few minutes. The molecular iodine activity was preferentially associated with the smaller sodium oxide particles. The sedimentation, filtration, and plating rates were measured, and the iodine and the mixed aerosol behaved as had been noted previously. A plating rate was also established for the iodine vapor before the oxide was released. A small residual amount of unagglomerated iodine was detected, which was not identifiable as molecular iodine. The particulate oxide-iodine aerosol was filterable, with an efficiency better than 0.99, while the unagglomerated iodine compound could not be filtered by a molecular membrane filter.

I. INTRODUCTION

The release of radioactive iodine following a hypothetical Liquid Metal Fast Breeder Reactor accident could result in excessive environmental exposures, if the iodine were to remain as a vapor or as very small particles, and were to leak from the containment structure as air does. If, at the same time, the sodium coolant burns and produces a

*Work performed under USAEC Contract AT(04-3)-701.

sodium oxide aerosol, the resulting mixture of sodium oxide and radioiodine should behave differently. Under these conditions, the aerosol particles and the iodine agglomerate with each other, and are removed from the airborne phase, mainly by gravitational settling. A series of tests have been performed to study these removal effects for radioiodine - sodium oxide systems.

Two types of reactor accidents were simulated in these studies. The first tests simulated an incident in which the fission product iodine had reacted to form sodium iodide, and was released during the pool burning of sodium coolant. The second group of tests simulated the release of fission products separately from the sodium oxide aerosol, which is subsequently generated from a pool fire.

II. EXPERIMENTAL DESCRIPTION

The first type of incident was simulated by the pool burning of metallic sodium containing sodium iodide-131, and the second by pool burning metallic sodium and the release of sodium oxide into an atmosphere containing elemental iodine-131. All experiments were performed in the Laboratory Test Chamber (LTC), which has a height of 180 cm and a volume of 1.1×10^6 cm^3. The chamber is instrumented for air sampling at a number of elevations, for automatic sequential fallout sampling, and for automatic sequential wall plating sampling.* In the sodium iodide release studies, air samples were taken with 0.2-μ "Gelman" millipore filters; while in the elemental iodine releases, the air samples were taken with 0.8-μ "Gelman" millipore filter backed with "H. Reeves Angel" Type AGB-1 charcoal filter paper. The activity was measured by means of a sodium iodide detector, and the sodium was measured with a flame photometer.

The sodium iodide aerosol releases were initiated by adding dry sodium iodide containing I-131 to metallic sodium. The sodium was heated to 1000°F under an inert atmosphere. At the start of the release, the molten sodium was exposed to the air atmosphere of the chamber and ignited spontaneously, releasing a mixture of sodium iodide and sodium oxide.

The pure elemental iodine was prepared by a molten-state oxidation of sodium iodide. An aliquot of the condensed iodine crystals from this oxidation was placed in a glass vial which could be heated separately in the test chamber. The test was initiated by first vaporizing the iodine crystals; then, after 20 min, the hot sodium was burned, releasing the sodium oxide. Prior to the release of iodine for Test No. 2, the atmosphere in the chamber had been filtered and dried to ~ 1 nuclei/cm^3 and 1500 ppm of water vapor.

A third test of radioiodine - sodium oxide agglomeration was evaluated. In this test, the iodine was in the same form as for the iodine vapor study, but the atmosphere had not been precleaned, so that the elemental

*C. T. Nelson, L. Baurmash, and R. L. Koontz, "Technique for Sampling Sodium Smoke and Fission Products," Proc. 9th AEC Air Cleaning Conference, AEC 660904 (1966)

iodine could agglomerate on naturally occurring atmospheric nuclei before the sodium oxide aerosol was produced.

III. DISCUSSION OF RESULTS

Air Concentration

The sodium oxide and sodium iodide released from the burning molten sodium in the first type of experiment came off at the same rates, and, after the maximum concentrations, decayed at similar rates, as shown in Figure 1. The peak concentration of sodium, as sodium oxide, was 1.6 $\mu g/cm^3$, and it took ~40 min to decay to 50% of this value. The comparable data for the sodium iodide was 8.4×10^{-4} $\mu Ci/cm^3$, and 40 min for the first 50% value. The concentrations were measured for 6 hr, when both sodium oxide and sodium iodide were 0.5% of their maximum values.

In the iodine vapor - sodium oxide experiment, sodium oxide was not produced until 20 min after the iodine had been vaporized. The initial airborne iodine activity was ~1340 dpm/cm^3, or 6.1×10^{-4} $\mu Ci/cm^3$, which is equivalent to 148 mg of iodine in the test chamber volume (13 $\mu g/cm^3$) (Figure 2). During the time when only iodine vapor was present in the chamber (20 min), the concentration of activity collected on charcoal filters decreased, with a half-time of 400 min. During this initial phase of the experiment, only 30% of the total activity was collected on the millipore filter. When the heated sodium in the pot was exposed to the air in the chamber, at about 20 min, 0.92 gm of sodium was immediately released to the chamber as oxides of sodium, with the peak (sodium) concentration of 0.77 $\mu g/cm^3$ occurring at ~21 min. As shown in Figure 2, the radioactive level which was airborne increased during the sodium release. Immediately upon the release of sodium oxide, ~99% of the total airborne activity was found on the millipore filter, while the balance was on the charcoal backup filter. The level of activity retained on the charcoal filter had immediately been decreased by about a factor of 100 by the addition of particulate sodium oxide, showing the rapid scavenging effect of the particulate oxide. After the peak concentration of sodium had been reached, both the sodium concentration and the iodine concentration decreased at the same rate. The initial half-time was 60 min for both components. The iodine concentration collected on charcoal filters leveled off at ~1.6 dpm/cm^3 (a reduction of the initial value by $\sim 10^3$). After 15 hr, the major fraction of the airborne iodine activity was on the charcoal filter.

When elemental iodine is condensed on "Aitken" nuclei, as in the third experiment, the peak concentration of iodine-131 was 7.5×10^{-4} $\mu Ci/cm^3$, and the half-time of the activity retained on the molecular filter was >100 min, as shown in Figure 3. During the time that only iodine was present (20 min), ~2 to 3% of the total activity was retained on the charcoal filter, as compared to 70% for the second test. Immediately after the molten sodium was ignited, the iodine concentration decreased more rapidly, with an air concentration half-time of 10 min. The peak sodium oxide concentration, as sodium, was 6.4 $\mu g/cm^3$, with a half-time of ~15 min. The activity collected on the charcoal backup filters

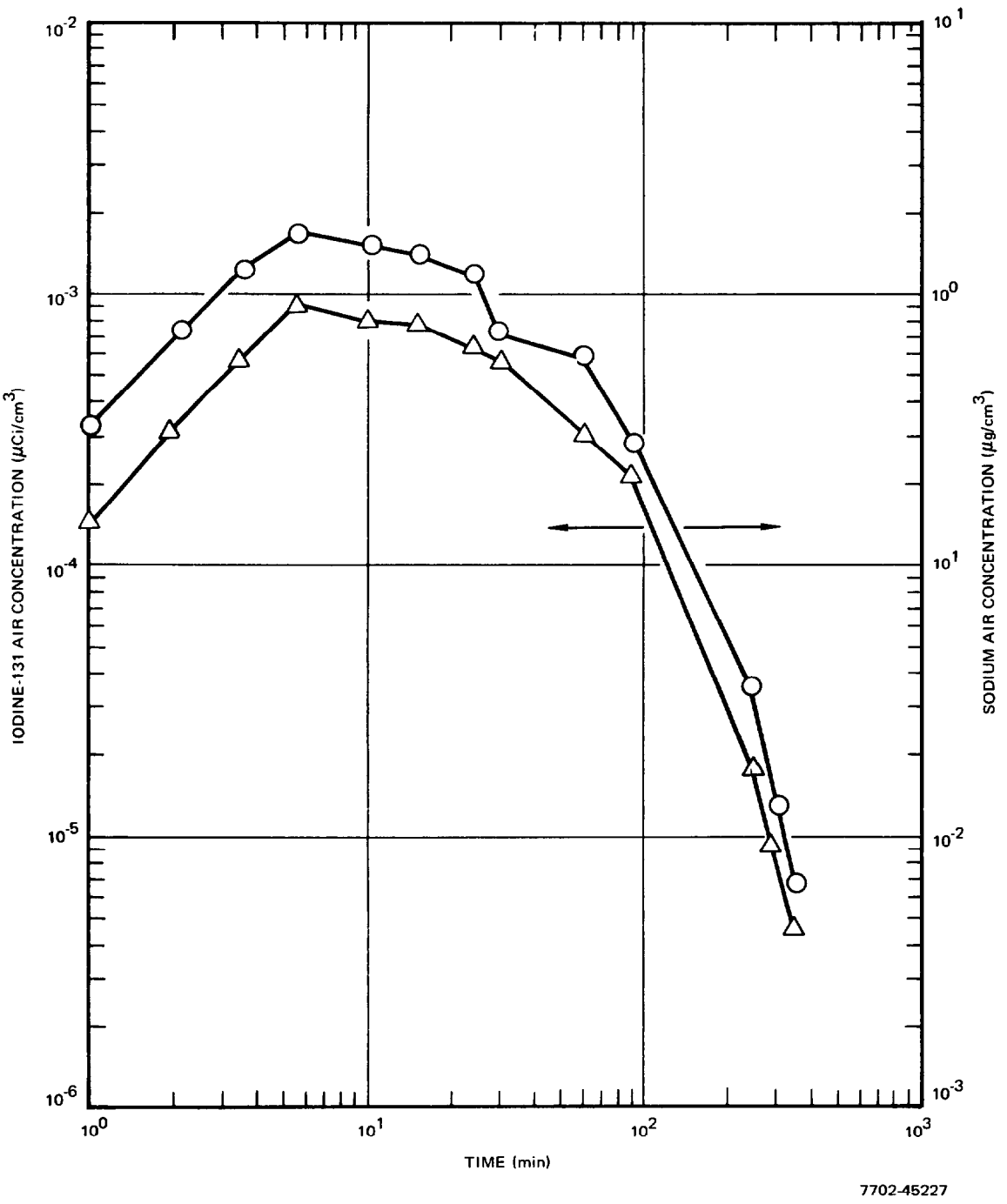

Figure 1. Air Concentration for Sodium Iodide - Sodium Oxide System

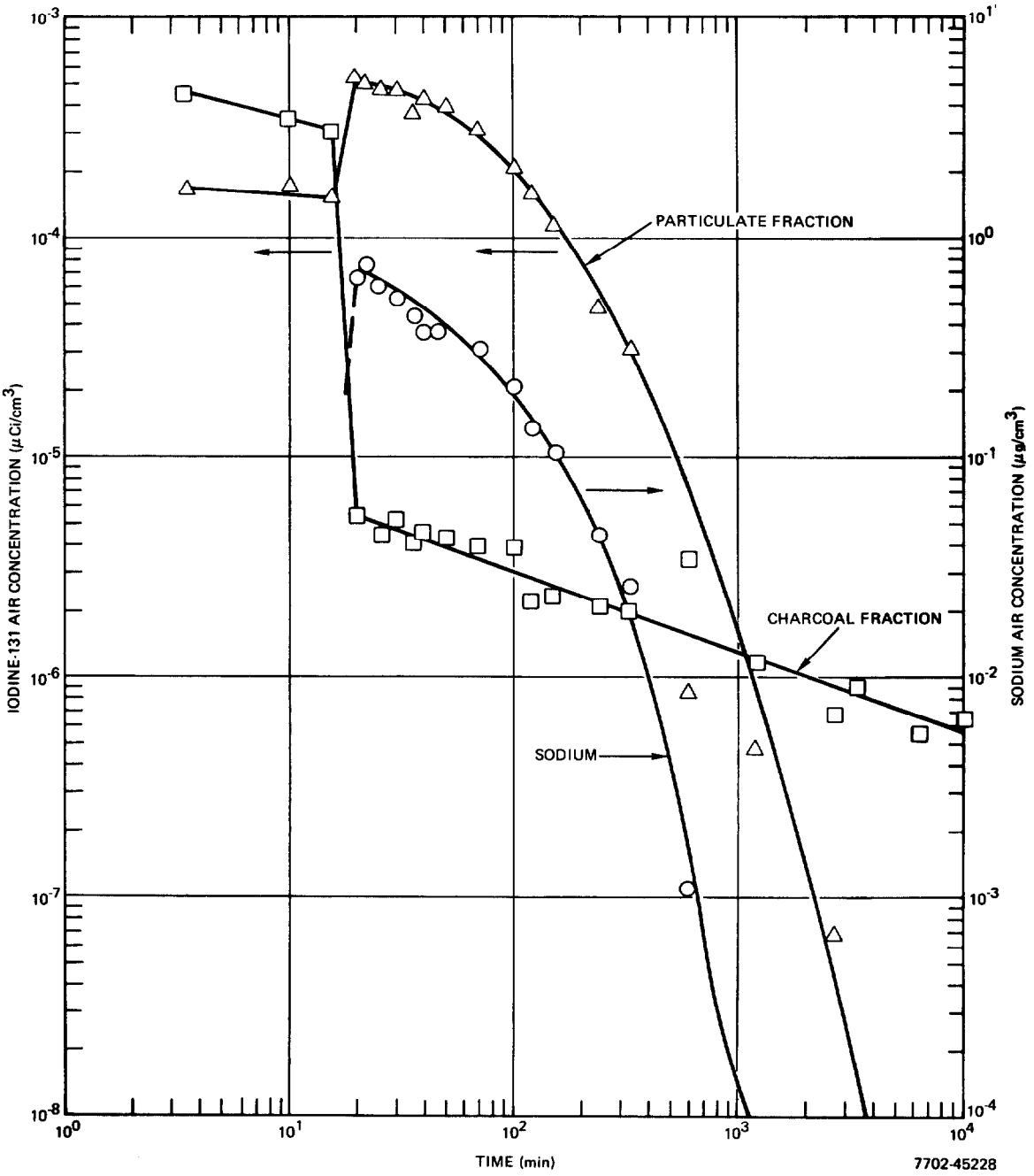

Figure 2. Air Concentration for Iodine Vapor - Sodium Oxide System

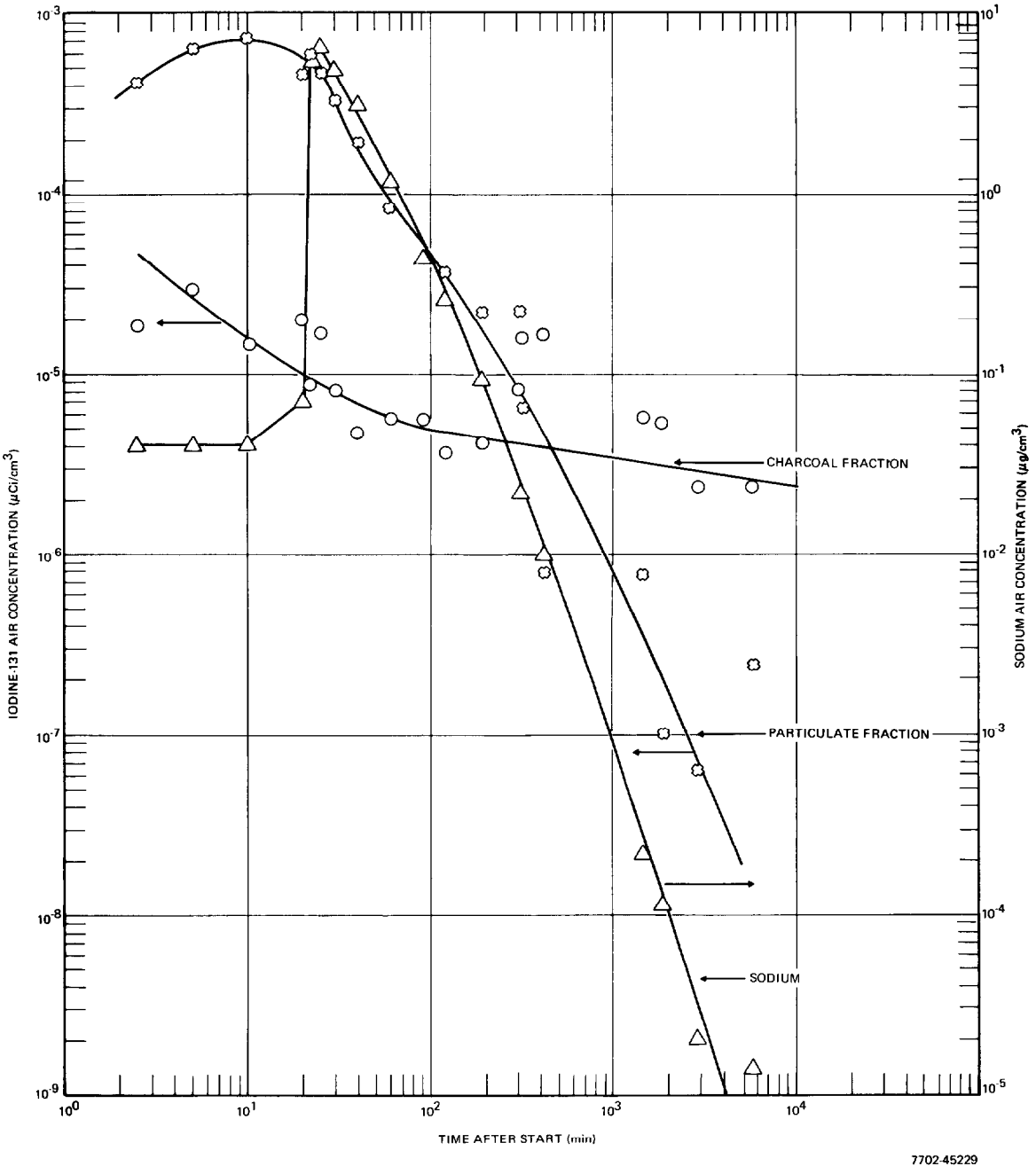

Figure 3. Air Concentration for Particulate Iodine - Sodium Oxide System

did not change markedly during the time the particulate iodine was decreasing; and, after 2 hr, the charcoal fraction was the dominant airborne component.

Particle Size Studies

Particle size studies of the airborne activity and sodium oxide, made by means of cascade impactors, showed that the radioiodine component was associated with sodium on all stages. For the sodium iodide - sodium pool fire, it was found that the distributions, whether measured by activity or mass of sodium, showed the same trends, and indicate a maximum AED of 3.3 was reached in ~50 to 60 min, as shown in Figure 4. This effect is also typical for the iodine - sodium pool fire, which reached a peak size (measured by activity and mass) of 3.7 at 50 min.

In Test No. 2 (before the release of sodium oxide), cascade impactor samples had 94% of the total activity on the last stage, indicating that most of the airborne iodine was not associated with particulates with radii >0.3 μ. Immediately after the release of the sodium oxide, analysis of cascade impactor slides showed that the radioactive iodine was now associated with sodium. The activity and mass median aerodynamic diameters grew to a peak AED, at 50 min, of 3.7 (Figure 5). Both sodium oxide and iodine distributions show the same trends with time, but the iodine activity median sizes were slightly less than those of the oxide. Figure 6 is a representation of the specific activity of sodium (dpm/μg Na) as a function of the collector stage constants (mean size collected) in aerodynamic diameter units, which shows that the iodine agglomeration is size dependent. As the size of the particles increased, the specific activity decreased. Figure 7 is a plot of the specific activity per stage constant. The specific activity per unit size is shown to be:

$$\frac{SA}{d} = \frac{K}{d^{\alpha}}$$

where:

SA = dpm/μg on a collector stage

d = aerodynamic diameter, AED

α = proportionality constant

K = constant.

The slope of the curve in Figure 7, for stage constants with AED <2, is 0.9. The slope for larger stage constants is 0.7. The specific activity of particles with an AED <2 is therefore directly proportional to the diameter, while, for larger particles, the specific activity is proportional to the diameter to the 2/3 power.

In the experiment in which sodium iodide and sodium oxide were released simultaneously from a pool fire, no attempt was made to identify the chemical form of the radioactive iodine, but it was assumed to be still in the form of sodium iodide. When iodine vapor was used in the experiment, an attempt was made to measure the elemental iodine present in the aerosol. The iodine fractions collected on the charcoal filter papers and extracted with benzene were analyzed for elemental

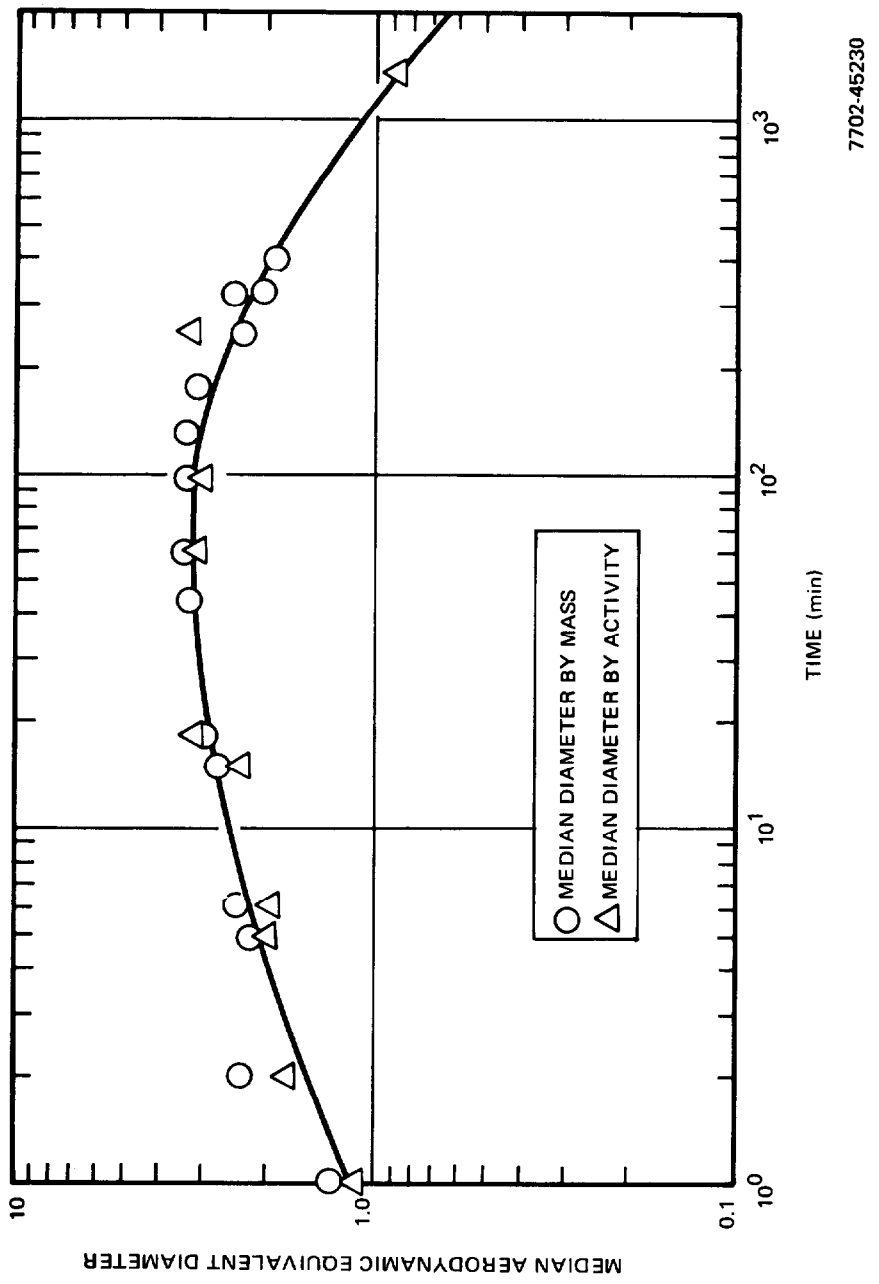

Figure 4. Median Diameter by Mass and Activity for Sodium Iodide - Sodium Oxide System

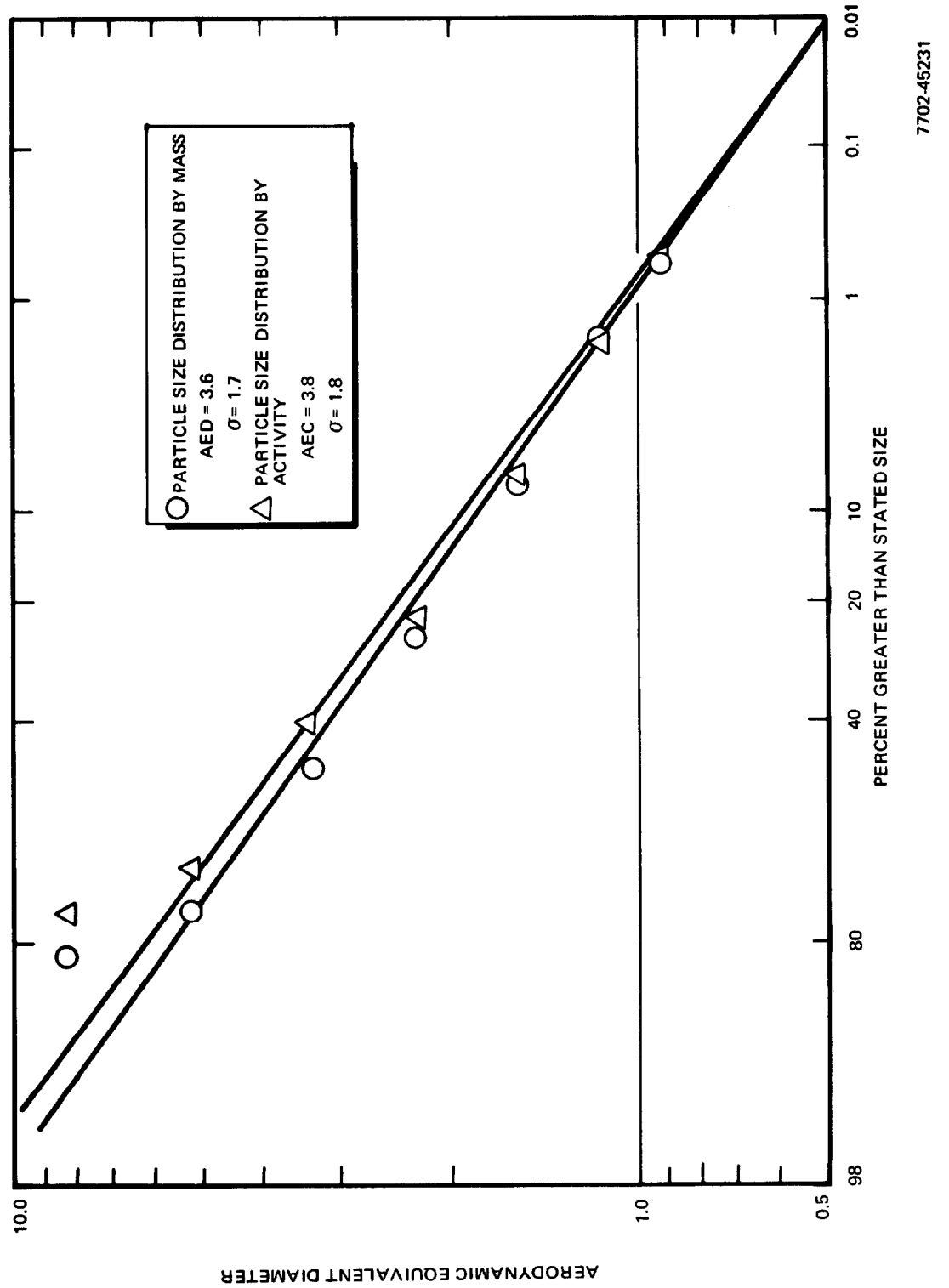

Figure 5. Particle Size Distribution for Iodine Vapor - Sodium Oxide System

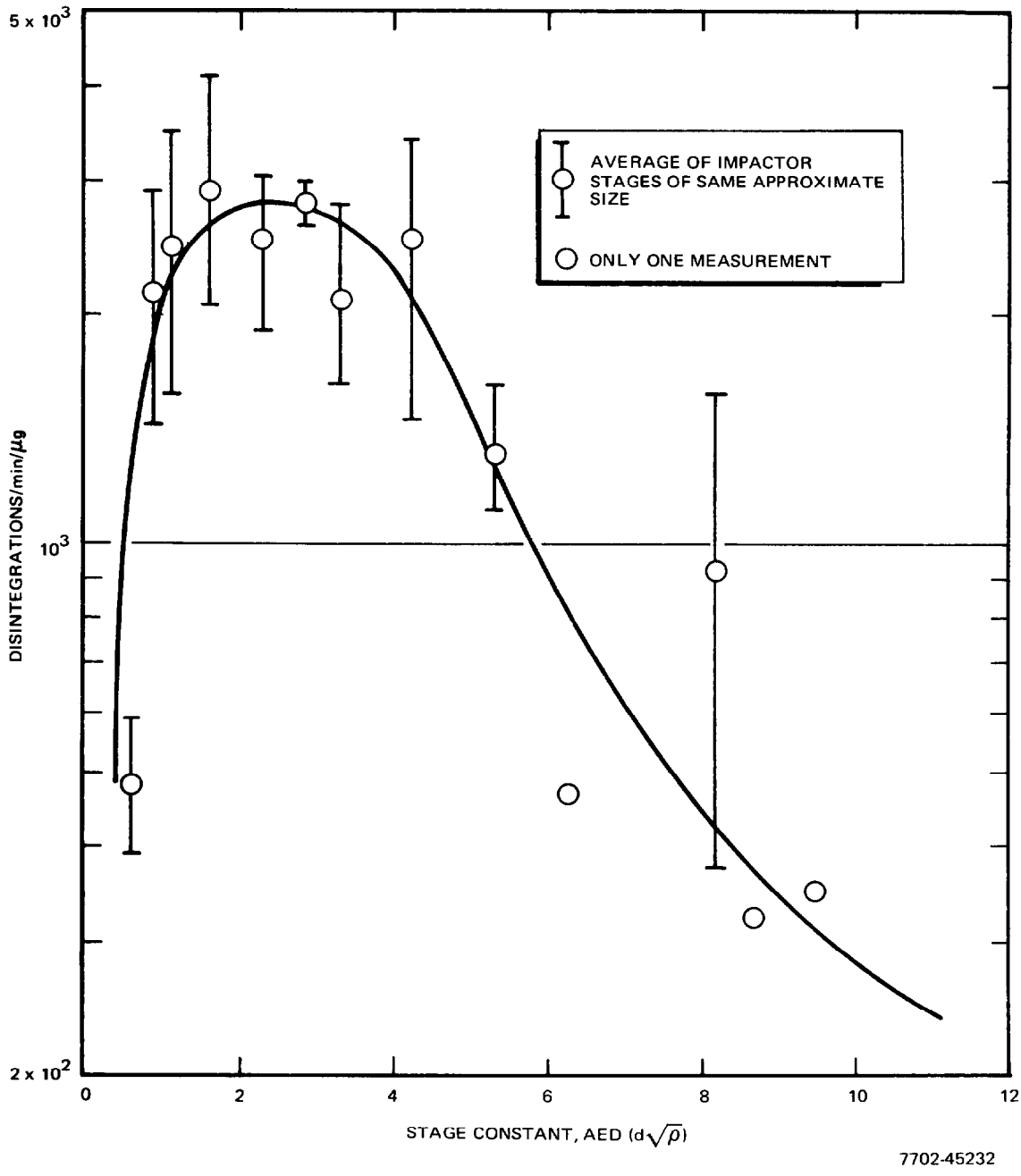

Figure 6. Specific Activity vs Impactor Stage Constants

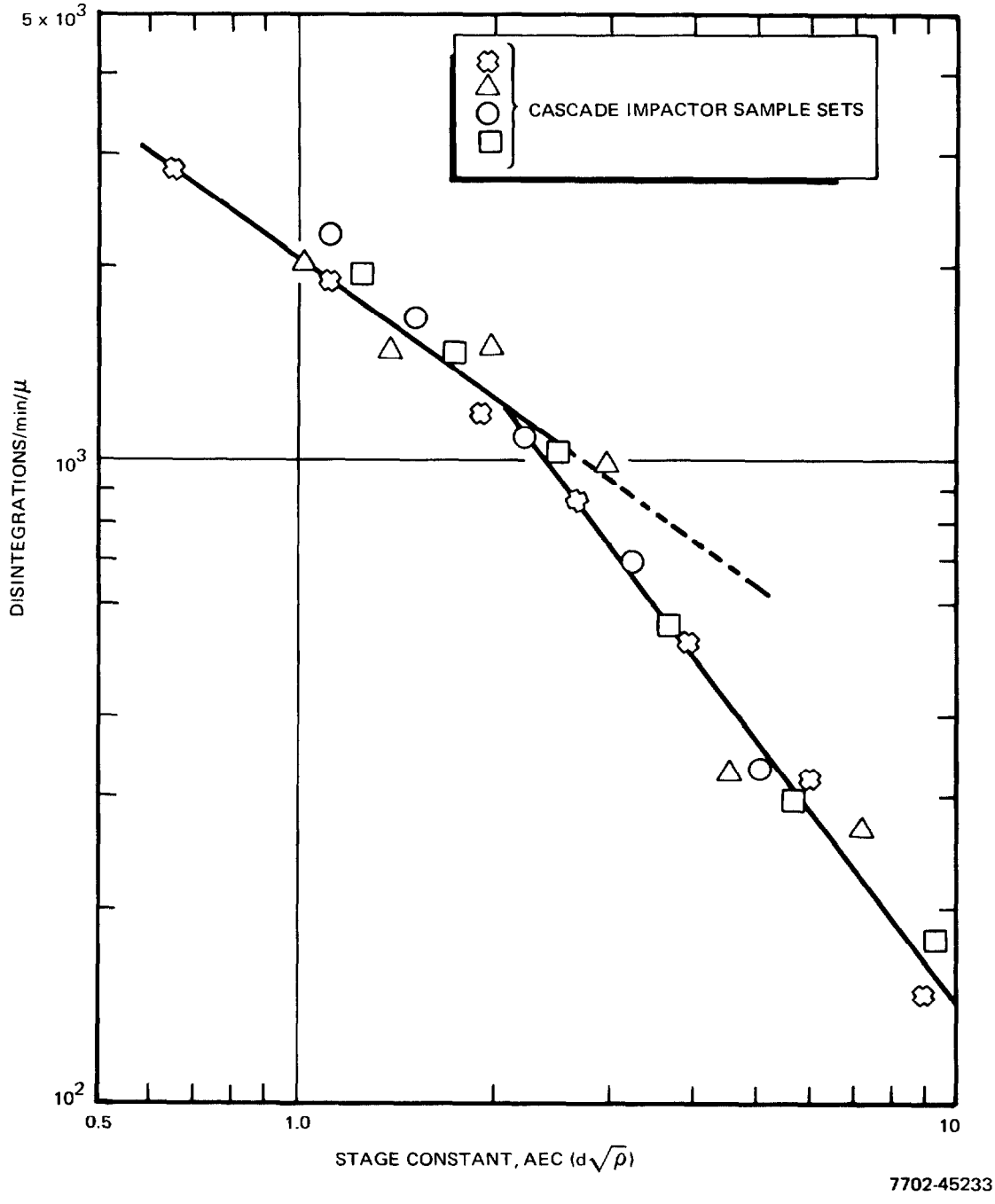

Figure 7. Specific Activity per Unit Size for Cascade Impactor Samples

iodine content by spectrophotometry. Benzene extracts of samples collected before the sodium was released contained 20 to 30% of the activity, but analysis indicated that no elemental iodine (<2.5 μg) was present. A sample of iodine, collected after sodium had been burned but late enough for most of the total airborne activity to be on the charcoal, was also extracted with benzene. The extract contained 75% of the radioactivity, but did not contain any detectable elemental iodine; 22% of the iodine activity which was in the fallout component was extractable, but again no elemental iodine was identified. In order to verify the initial chemical form of the iodine used in this experiment, an aliquot of the original material was analyzed and shown to be molecular iodine.

Fallout and Wall Plating

Sequential samples of the fallout material and wall plating material were analyzed for sodium and for radioactivity. The results for the sodium pool fire containing sodium iodide are shown in Figures 8 and 9. The curves for the various components show that the radioactive sodium iodide and the sodium oxide show the same trends, and indicate that the aerosol particle is composed of both components. Table 1 shows the distribution of the sodium iodide and sodium oxide at the end of the experiment.

TABLE 1

DISTRIBUTION OF SODIUM AND I^{131} FOR SODIUM OXIDE - SODIUM IODIDE RELEASE (Test No. 1)

Material	Total	Floor Fraction	Wall Fraction
Sodium Oxide (as sodium)	2.1 gm	0.66	0.34
I^{131} (as sodium iodide)	1.13 mCi	0.54	0.46

The results from Test No. 2 are shown in Figures 10 and 11, and indicate that, after sodium oxide is released into an iodine atmosphere, the iodine and sodium oxide behave the same. This again shows that the aerosol particle is composed of sodium oxide and radioiodine. A summary of the results is shown in Table 2.

TABLE 2

DISTRIBUTION FOR SODIUM AND I^{131} FOR SODIUM OXIDE - IODINE RELEASE (Test No. 2)

Material	Total	Floor Fraction	Wall Fraction
Sodium Oxide (as sodium)	0.92 gm	0.78	0.22
I^{131} (as I_2)	0.91 mCi	0.60	0.40

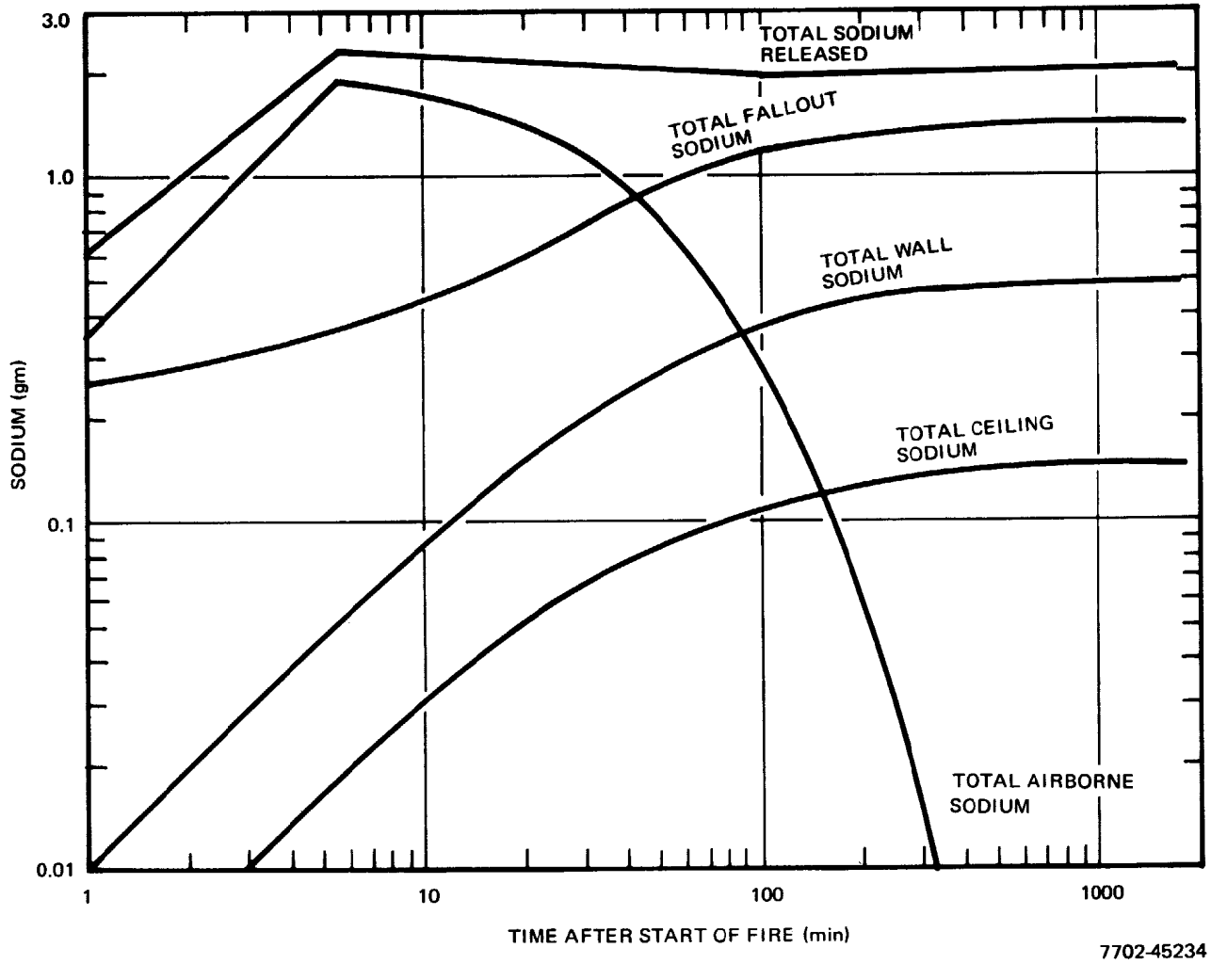

Figure 8. Sodium Mass Balance for Sodium Iodide - Sodium Oxide System

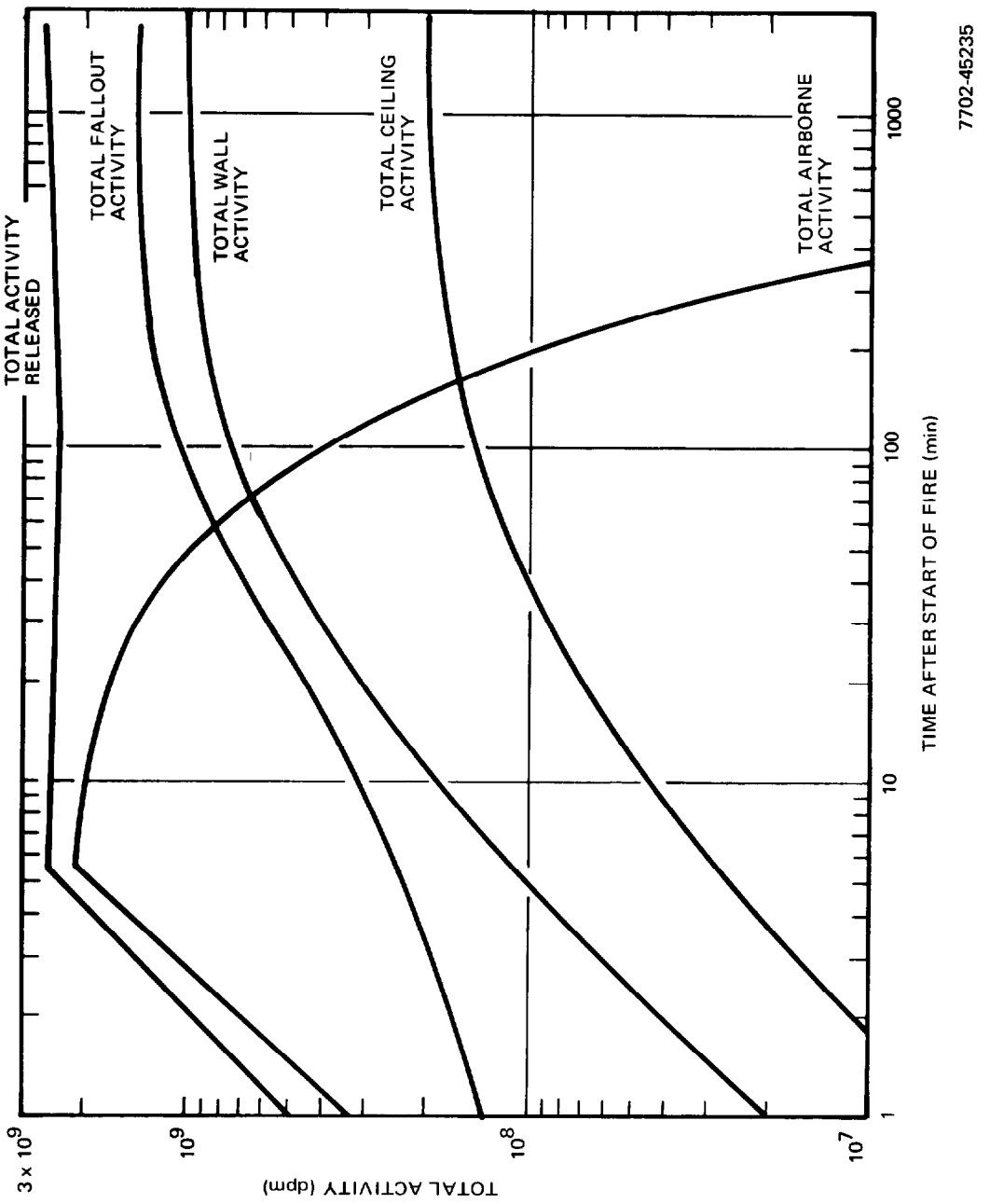

Figure 9. Activity Balance for Sodium Iodide - Sodium Oxide System

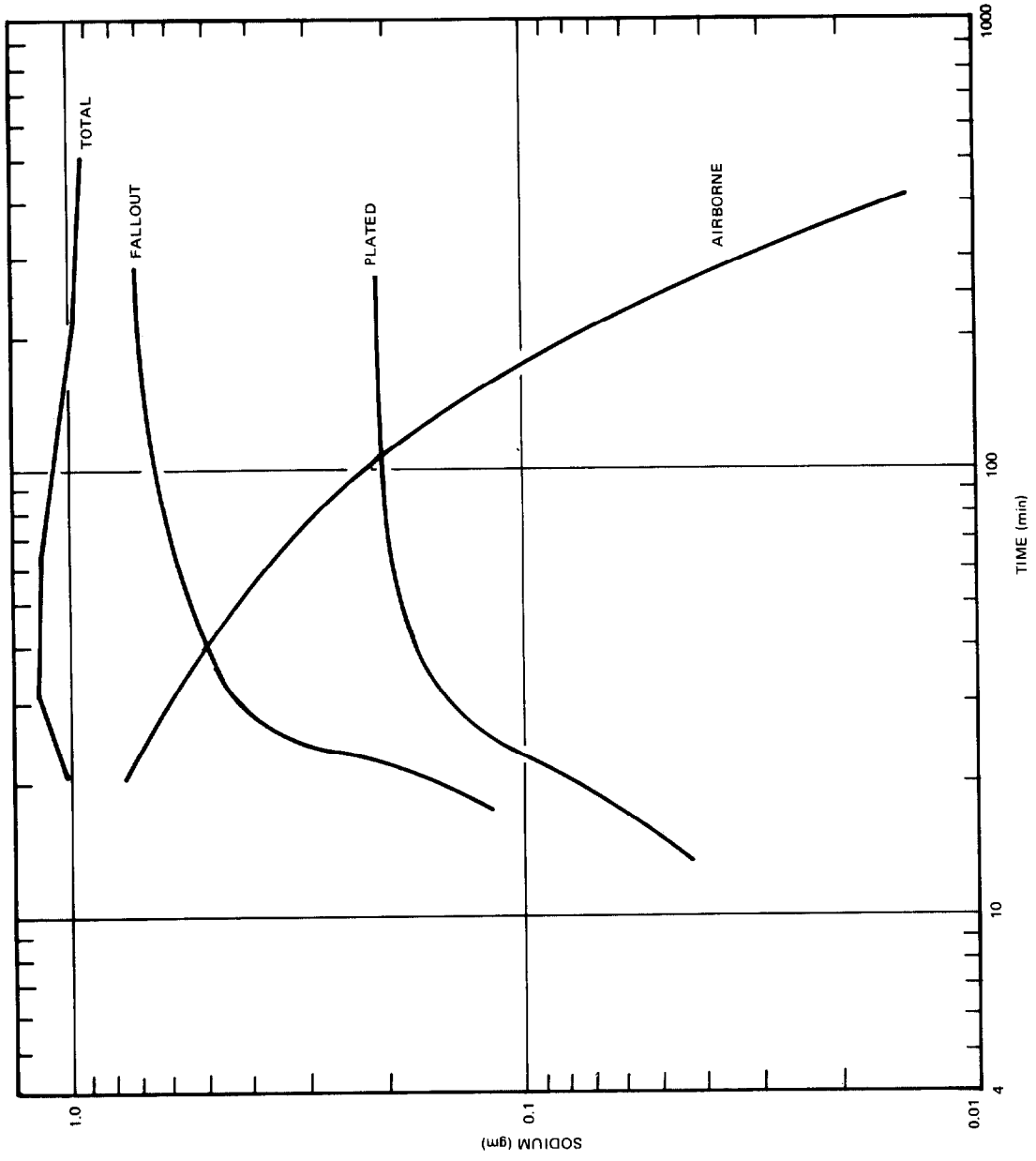

Figure 10. Sodium Mass Balance for Iodine Vapor - Sodium Oxide System

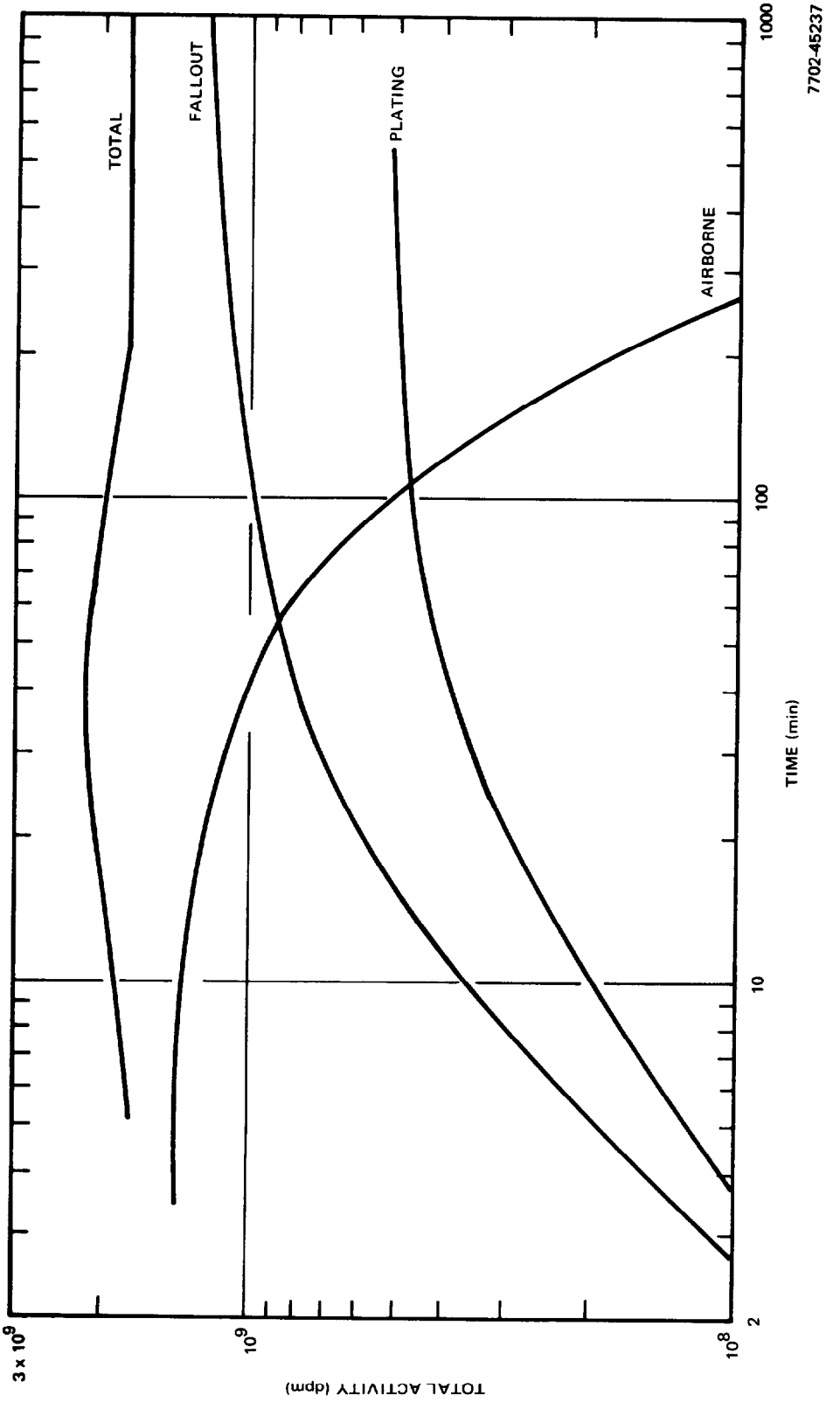

Figure 11. Activity Balance for Iodine Vapor - Sodium Oxide System

IV. CONCLUSIONS

Sodium oxide particles, generated in an air atmosphere at the same time that sodium iodide is released, agglomerate with the iodide to form a particle whose behavior is determined by the characteristics of the mixed aerosol particle. Similar behavior is exhibited when sodium oxide particles are released into an air atmosphere containing elemental iodine absorbed on atmospheric nuclei. The sodium oxide particles which are released into an atmosphere containing iodine vapor scavenge a large fraction of the airborne iodine. In this case, the iodine component which can be collected on a charcoal filter was immediately reduced by a factor of 100, which increased in time to a factor of 1000. The activity collected on the charcoal filter, for both Test No. 2 and No. 3, ultimately reached an equilibrium concentration, while the agglomerated component which could be collected on a molecular filter decreased in direct proportion to the sodium oxide. The airborne activity and sodium oxide, collected on molecular filters, decreased at the same rates, for each system, regardless of the original form of the radioiodine.

Particle size data for sodium oxide and radioactive iodine aerosols show that the iodine is agglomerated by sodium oxide. In the second test, the elemental iodine has been shown to be preferentially agglomerated on small particles. This was verified by comparison of the specific activities of the plated and settled sodium oxide, which show that the plated material, which is composed of mostly small particles, has a higher specific activity than the fallout material.

These studies indicate that the analyses of hypothetical reactor accidents which could produce aerosols of radioiodine and sodium oxide, such as for LMFBR, should take credit for the reduction of the airborne concentration of the iodine due to its agglomeration with sodium oxide and subsequent fallout to the floor of the containment structure. The removal times due to this mechanism are shorter than radioactive decay, and will have a large effect on the amount of iodine which can leak from a containment building.

DISCUSSION

BEATTIE: I do not quarrel at all with what Dr. Baurmash says. I'm in favor. What I'm raising now is a point of principal which I think is important. I'm not being nationalistic either this time because what I've got to say applies to Mr. Clough's paper which is coming up, and he is from my country. Dr. Baurmash, I think you said something about your DBA, or design basis accident, I think in some circles this is described as energy release or the energy released by a reactivity excursion. Right? I can go on from there, I've established that. The point of principal which concerns me is that all the papers around this part of the session seem to be concerned with iodine, and in the case of Mr. Clough, my good friend (sorry Bill) with Caesium. Now, we all know what this energy the release excursion means. It's a vaporization. So what about the plutonium was the one question, why has nobody mentioned plutonium? And finally, this is the nasty one, why has no one mentioned the mixed fission products? Long lived solid fission products. I believe that the plutonium is more important than the Iodine in the DBA, and I believe, going farther, that the long lived fission products are more important than Plutonium unless there are special factors such as deposition and filtration to produce differential effects. The problem that concerns me about these mixed fission products is the external radiation from the long lived activity deposited on the ground and I just really wanted to raise this general point of principal and bring it to your notice. I know I'm not the only person who has thought of this; I'm sure there is somebody else in this audience waiting to add something. It will be interesting to see who it is.

BAURMASH: Can I discuss the point first about the plutonium. I don't think the intent was purposely to leave out the plutonium problem. I know that 2 years ago at the IAEA meeting in New York I gave a paper on uranium oxide experiments. The purpose was to study the removal factors that go with particle agglomeration, settling and wall plating using UO_2 or U_3O_8 as a simulant for plutonium (our facility can handle uranium oxide but not plutonium). There is other work going on in this field. I am not going to apologize for everybody else; I'm just going to tell you what our facility has been doing. We are using uranium oxide as a simulant for plutonium or the mixed fuel. We are also looking at the aerosol problem with sodium oxide aerosol. We are using at the time iodine as a simulant for the volatile fission product species. I'm not saying that this is the only reason for using iodine.

The experiments that were described were basically confirmation or developmental experiments to get information about agglomeration of mixed aerosols, how they behave with one another and it is incidental

that it happens to be iodine which was selected. I could have made the Ruthenium oxide or Caesium, and reached similar conclusions. However, iodine is a hazardous material in reactor accidents and therefore the one that we have used to simulate other volatile materials.

FIRST: I'd like to offer a little rebuttal here. I think the maximum accident you refer to is of course terribly important, an event to look at, but it's not the only kind of accident that may occur and I think the more serious the accident the more improbable it becomes. It is quite likely that there will be large numbers of accidental spills of sodium from all kinds of places and all kinds of activity which will not be contaminated with the products which you mentioned. These also must be handled in an expeditious manner and some of these experiments are designed to look at that aspect as well as to shed more light on the type of accident you describe.

BAURMASH: I made a point about that. I think I'm going to agree with you on the DBA being important. Under the present state of licensing requirements, one must show the DBA is taken care of or one doesn't have a reactor.

BEATTIE: I would agree with what Dr. Baurmash has said. I agree with everything you have said in reply. I would like to tangle with Dr. First, if he doesn't mind. You may know that the basis of the F. R. Farmer probability idea is that all accidents count, from the biggest to the smallest and we certainly in the United Kingdom Atomic Energy Authority take account of and examine very closely all these small accidents. The design basis accident is only one of many important accidents. So it seems to me you may become a "probability man" yet, Dr. First.

CLOUGH: This isn't to defend ourselves Jack, I just want to say something. Everybody is talking about accidents here. I think it isn't necessary always to speak about accidents, hopefully we will one day run fast reactors without the fuel and in that case we are going release fission products both in the liquid sodium and in the gas phase. I think in this case, when this does happen the behavior of fission products like iodine and caesium may well assume importance from the economic point of view than from a nuisance value point of view rather than a large accident situation and any knowledge we have about the behaviors of these things in liquid sodium at this stage will be useful at that stage when we get to it.

FIRST: I want to ask you a question that refers to the manner in which you determined gaseous iodine. Do I understand that you filtered a sample through a millipore filter and then put the effluent through charcoal paper to determine the nonparticulate iodine? How did you determine that you were not removing iodine on the particulate filter

because of very intimate contact between gas and the sodium collected on the filter? How can you be certain that you got the same iodine passage through the sodium-loaded filter as you had in the air mass in the chamber?

BAURMASH: We had confirmation from our cascade impactor samples, taken before the oxide was released, in which the iodine penetrated to the eighth stage which was a charcoal paper filter. We had collected less than six percent of the iodine on the first seven stages and more than 94 percent of the iodine on the charcoal.

FIRST: Even with a cascade impactor, the iodine-containing air stream could be sweeping across a coating of deposited sodium or sodium oxide.

BAURMASH: There is not enough oxide to filter the iodine. It is not really in very great contract because it is only the top of the deposit that will be exposed and besides there was no indication of any deposit on any of the glass slides. As I said in my paper, when iodine vapor was sampled 94 percent was collected on the charcoal filter stage of the impactor. Thirty percent was collected on the millipore filter of the millipore-charcoal combination after the oxide was released. In the experiment in which the iodine had agglomerated on "Aitken" nuclei we get 99 percent collected on the millipore with no collection on the charcoal paper. Same iodine, same filter - in one case six percent on the millipore and the next case 99 percent.

CAESIUM BEHAVIOUR IN LIQUID SODIUM - THE EFFECT OF CARBON

W.S. Clough and S.W. Wade

Health Physics and Medical Division,
A.E.R.E. Harwell, Didcot, Berks.

ABSTRACT

On the basis of previous thermodynamic calculations and experimental work, caesium has been identified as the most volatile major fission product with respect to release from liquid sodium into the gas phase. Sorption of the caesium by graphite has been shown to be very effective in reducing the volatility of the caesium and the formation of stable caesium-graphite compounds reduces the escaping tendency of caesium to less than that of iodine in liquid sodium. The caesium forms two compounds one of which is relatively unstable in liquid sodium and is probably a surface adsorption compound. The more stable fraction of the adsorbed caesium is probably a lamellar caesium-graphite compound and is almost fully stable in vacuum at 500°C in the absence of sodium. The rate of reaction for the break down of the more stable caesium-graphite compound in sodium has been measured over a range of temperatures and the corresponding activation energy has been calculated. Graphite has been found to be equally effective for caesium sorption when it is used in the gas phase above the liquid sodium.

Charcoal has been shown to be even more efficient than graphite in trapping caesium and the caesium-charcoal compound which is formed is almost fully stable in sodium at 500°C and in air at the same temperature. Pre-treatment of the charcoal with sodium at 500°C for 3 days has little effect on its performance with respect to caesium sorption.

1. Introduction

The release of fission products from a fast reactor, either in accident conditions or in uncanned fuel operation, can be considered in three stages

(a) Release from the fuel into the liquid sodium,

(b) Partition of the fission product between the liquid sodium and the gas phase,

(c) Transport in the gas phase.

Except in the unlikely event of a catastrophic accident involving the vaporisation of both the fuel and a large portion of the coolant, the liquid sodium can be expected to modify the fission product release. Data on fission product behaviour in liquid sodium will be of use in the assessment of the safety of the fast reactor and in deciding which fission products are of importance in the gas phase above the coolant. The chemical state of the fission product in the liquid sodium can have a profound effect on its release into the gas phase. Thus if caesium reacted with the trace amounts of oxygen in the reactor coolant then the oxide formed would be involatile and the caesium would be trapped in the liquid phase. If no caesium-oxygen reaction occurs the volatile caesium metal would be quickly released into the gas phase. Standard state thermodynamic calculations have been used(4) to predict the chemical state of the fission products in liquid sodium and they can be used in conjunction with fission product concentration data to show that iodine will exist as sodium iodide, barium and strontium as the oxide and caesium as caesium metal. The calculations suggest that there is very little chance of forming a caesium compound of low volatility in the same phase as the liquid sodium. Even though involatile compounds can be found (e.g. CsI) which are stable in sodium when present in their standard state, in the real case the vast excess of sodium moves the equilibrium in favour of the sodium compound and free caesium (e.g. in dilute solution CsI breaks down to form NaI + Cs).

Experimental work on the sodium-iodide system has shown that iodine volatility in liquid sodium corresponds to that expected for sodium iodide(5,1). The presence of oxygen in the sodium does not modify the iodine volatility but the effect of decreasing the iodine concentration is to increase its volatility. Attempts have been made to calculate the volatility of sodium iodide in liquid sodium using activity coefficients obtained from solubility data(1,6). The calculations agree with the experimental results in indicating that the liquid sodium greatly reduces the volatility of fission product iodine released from the fuel. Caesium then remains as potentially the most hazardous fission product due to its high volatility from a large excess of sodium. From vapour pressure data and by estimating activity coefficients(1) the relative volatility of caesium and sodium (α) has been calculated to be about 70 at 500°C. Experimental verification of the high volatility of caesium in liquid sodium has been obtained(1,7). It is about two hundred times more volatile than iodine and therefore requires careful consideration in the analysis of the early stages of a fast reactor accident or in deliberate release in uncanned fuel operation. A method for retaining the caesium in the liquid phase or trapping it in the gas phase would greatly reduce the hazard from caesium.

2. Experimental

The apparatus used was a bench-scale vacuum distillation apparatus shown schematically in Fig. 1. Its use has been described previously(5).

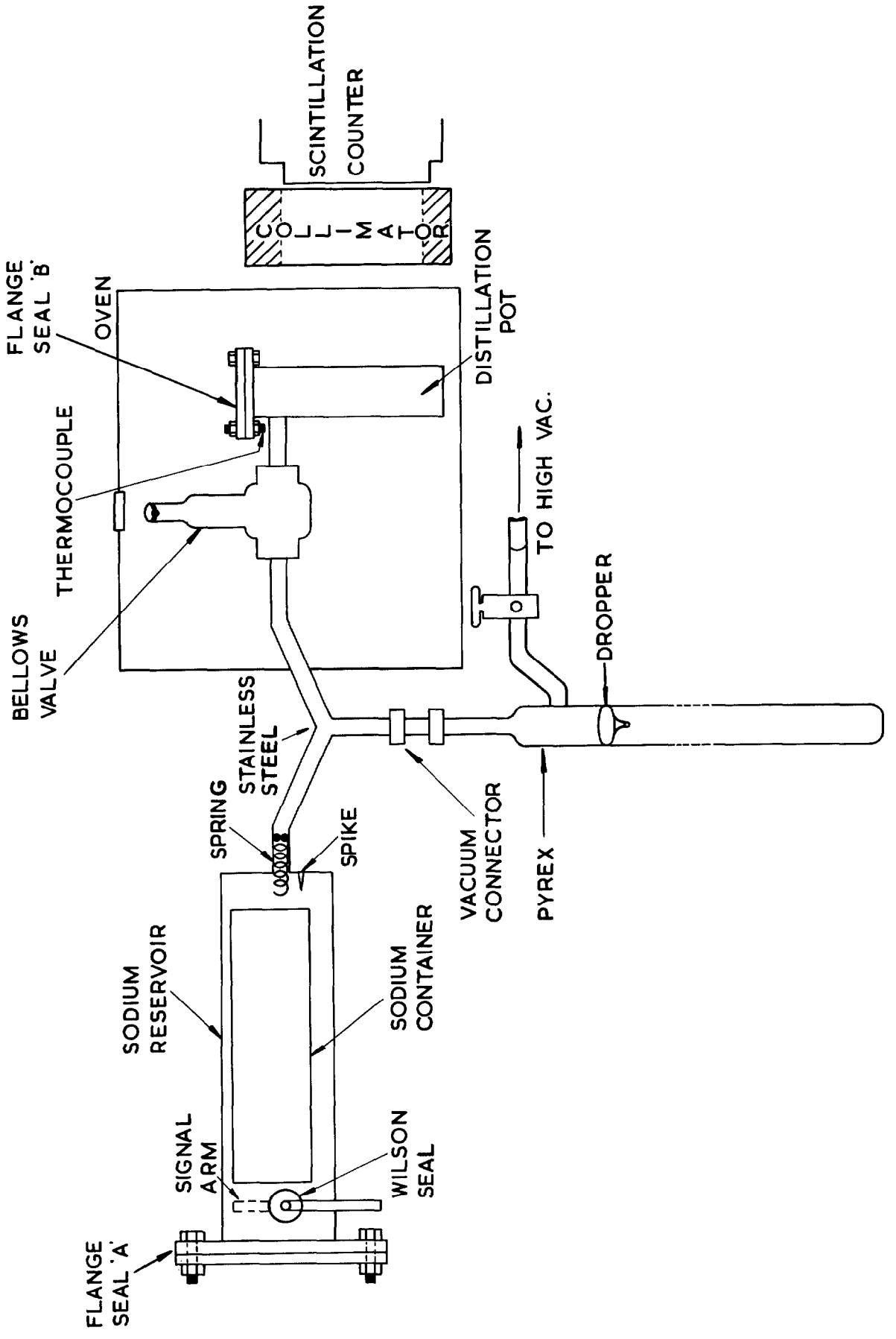

FIG. 1. DISTILLATION APPARATUS.

Radioactive caesium (as $^{137}CsCl$ solution) was placed in the distillation pot before the apparatus was evacuated. Pure sodium was transferred to the distillation pot by bursting the can containing the pure sodium and tilting the apparatus so that the sodium ran into the pot under gravity. The rate of distillation of the caesium was measured radioactively by the γ counter shown. In the first experiments the rate of distillation of the caesium was so high that the gravimetric techniques used previously[5] to measure the rate of sodium distillation could not be used. The sodium was labelled with Na^{24} and the rate of distillation of both the caesium and the sodium was measured radioactively. In later experiments, when graphite was used in the sodium, the rate of caesium distillation was slow enough to make the gravimetric technique again applicable. The pure graphite used was U.K.A.E.A. Pile Graphite "A".

3. Results

3.1 The volatility of caesium in pure sodium at 500°C

Results typical of those obtained are shown in Fig. 2. These results were calculated from the measured values of the activity remaining in the pot at given times after the start of the distillation. In the case of Cs137 the γ count originates in the decay scheme.

$$Cs^{137} \xrightarrow[\beta]{32a} Ba^{137m} \xrightarrow[\gamma]{2.6\ min} Ba^{137}$$

When distillation is in progress the Cs is removed by both physical transport and radioactive decay

$$N_1\ Cs^{137} \xrightarrow{\lambda_1} N_2 Ba^{137m} \xrightarrow{\lambda_2} Ba^{137}$$

$$\text{Distillation} \quad (\lambda_3)$$

Where N_1 and N_2 are the numbers of atoms of the species shown and λ_1, and λ_2 and λ_3 are rate constants.

$$\text{Now } \frac{dN_2}{dt} = \lambda_1 N_1 - \lambda_2 N_2 = N_1^{\,o} e^{-\lambda_3 t} - \lambda_2 N_2 \text{ as } \lambda_1 << \lambda_3.$$

$N_1^{\,o}$ is the value of N_1 at the start of the distillation. Solving the above equation for N_2 gives

$$N_2 = \frac{\lambda_2}{\lambda_2 - \lambda_2} N_2^{\,o} (e^{-\lambda_3 t} - e^{-\lambda_2 t}) + N_2^{\,o} e^{-\lambda_2 t}$$

Where $N_2^{\,o}$ is the value of N_2 at the start of the distillation. λ_3 can be calculated from this expression using the experimental values of $\frac{N_2}{N_2^{\,o}}$ and t. The results are shown in Fig. 2 plotted as fraction

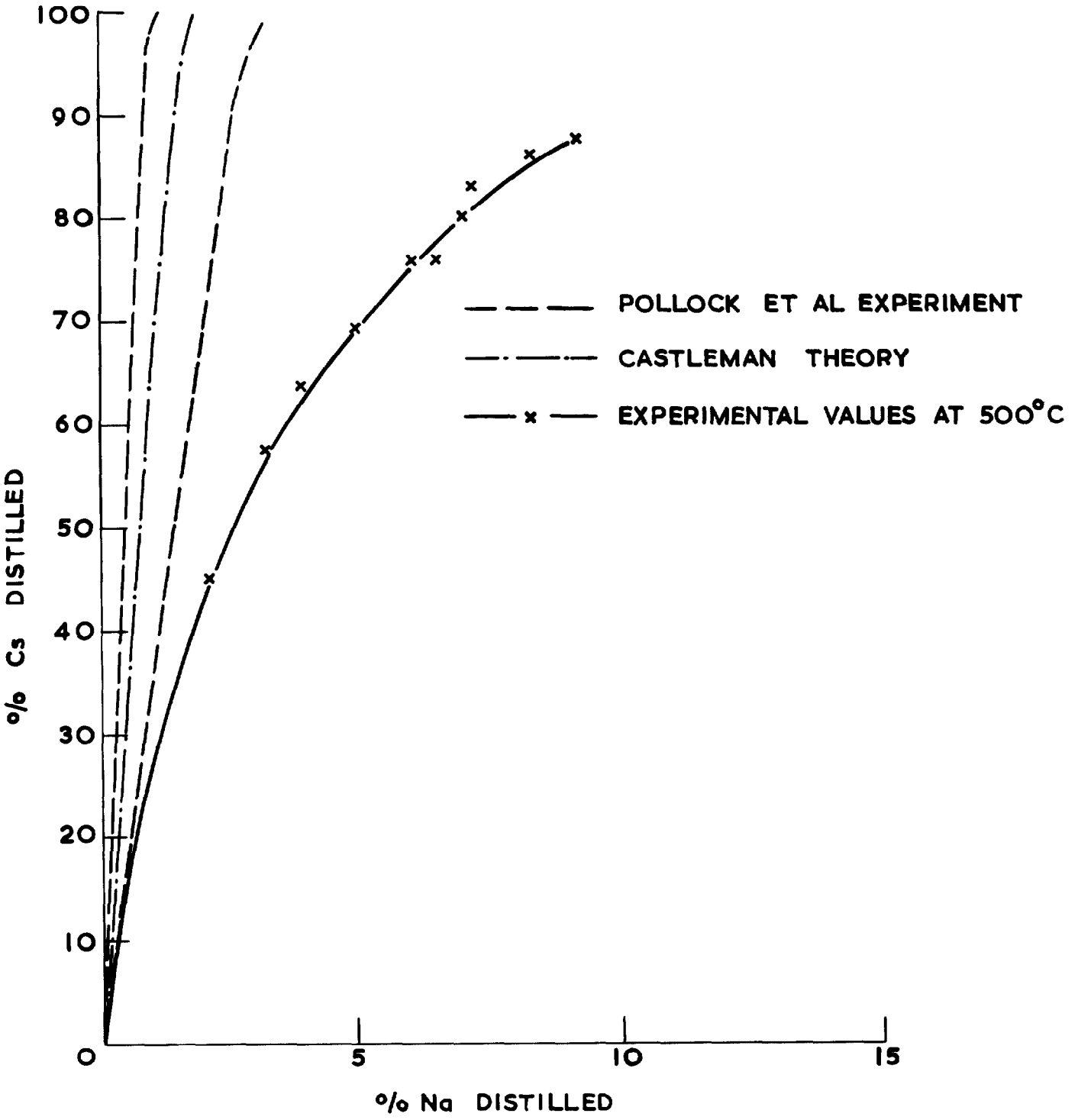

FIG.2 THE VOLATILITY OF Cs IN LIQUID SODIUM.

of caesium distilled against fraction of sodium distilled. The relative volatility (α) was found to be high (about 20) but not so high as that predicted from thermodynamic data by Castleman[1] and found experimentally by Pollock et al.[7] (see Fig. 2). Castleman[2] has shown that the diffusion rate of caesium in either the liquid or gas phase can limit the distillation rate of caesium in liquid sodium. It is probable that diffusion in the liquid phase or the presence of trace amounts of carbon in the apparatus (see next section) is responsible for the experimental results being smaller than the predicted maximum value.

3.2 The effect of graphite on the volatility of caesium in sodium

The distillation pot was contaminated with carbon and, even after prolonged washing, subsequent results obtained were like those shown in Fig. 3. The results can be analysed in two sections. Section A closely resembles the behaviour of caesium before the pot was contaminated. Section B was ascribed to the presence of graphite on the pot walls. Caesium is known to form inter-lamellar compounds with graphite and the break down of these compounds has been measured kinetically at 500°C in vacuum[8]. Sorption of caesium on graphite in a flowing sodium loop has been reported[3].

The deliberate addition of graphite modified the caesium emission in the way shown in Fig. 4. 5.8 g of graphite was used in the form of 2 sticks with dimensions 4 cm x $\frac{1}{2}$ cm in 48 g of sodium. While the sodium was distilling the caesium was evolved at a rate less than that measured previously for iodine (see ref. (5)) and when all the sodium was removed the remaining caesium was fixed in the graphite. The behaviour of the caesium in the presence of graphite and sodium is compared to that in pure sodium in Fig. 4. The graphite acts as an excellent hot trapping device for caesium.

3.3 The rate of break down of the caesium-graphite compounds in sodium

Further experiments using less graphite (1 g) provided evidence that the caesium forms two compounds with graphite in sodium. Thus Fig. 5 shows that one of the compounds, A, (possibly a surface adsorption layer) breaks down at a rate of about 120%/hr in sodium at 500°C when the sodium is distilled. The more stable compound (probably a true inter-lamellar compound) breaks down at the rate of 6.5%/hr. Kinetic measurements of the rate of break down of the more stable compound B have been made over the temperature range 400°C - 600°C and the results are shown in the form of an Arrhenius plot in Fig. 6. The activation energy calculated from the graph is 14 K cal/mole. The spreadof results is probably mainly explained by the fact that each point was obtained from a separate experiment using different graphite samples.

3.4 Caesium sorption from sodium by graphite in the gas phase

In considering the possible use of graphite in fast reactor sodium some problems arise.

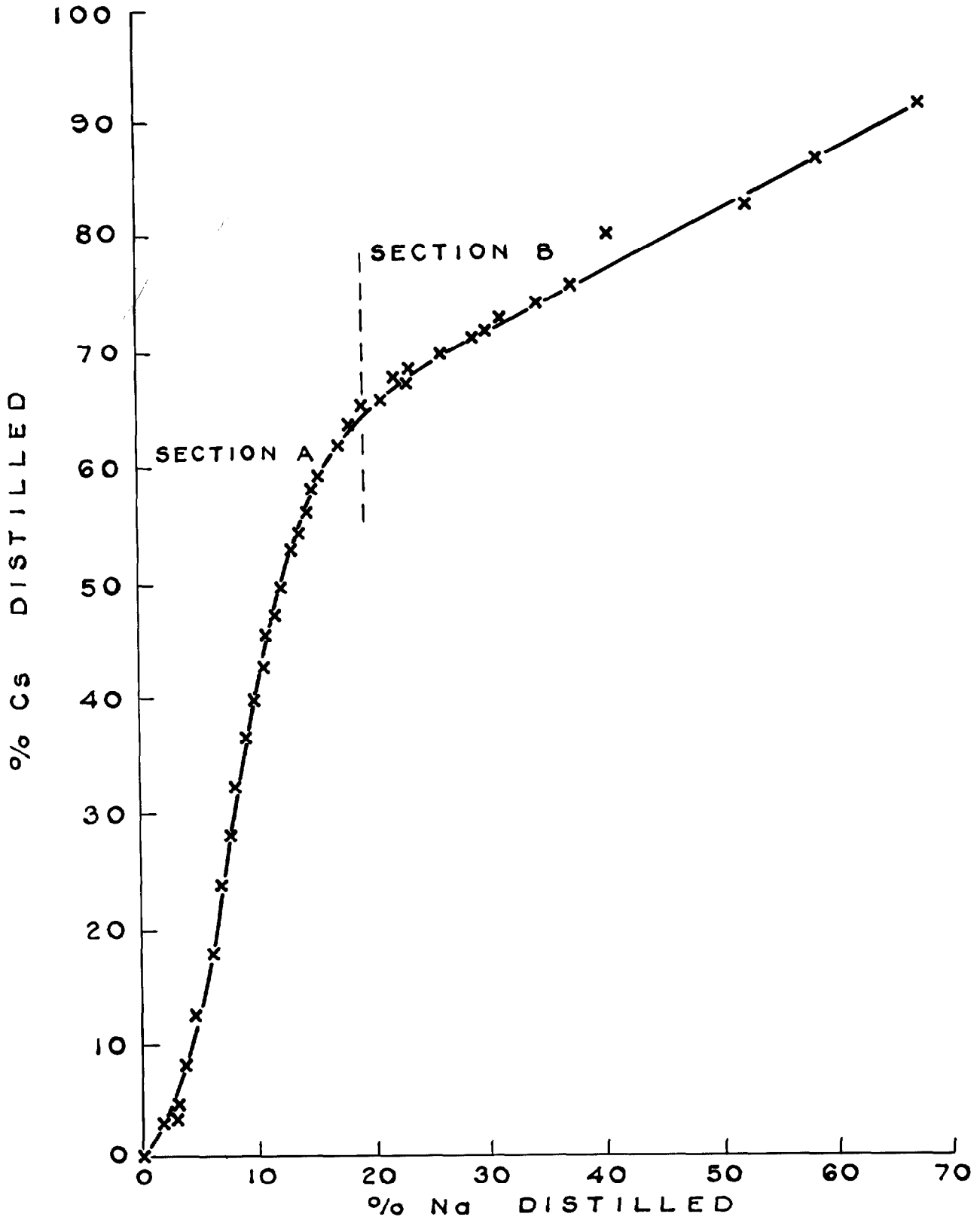

FIG. 3.

THE EFFECT OF CARBON CONTAMINATION ON THE VOLATILITY OF Cs IN LIQUID SODIUM.

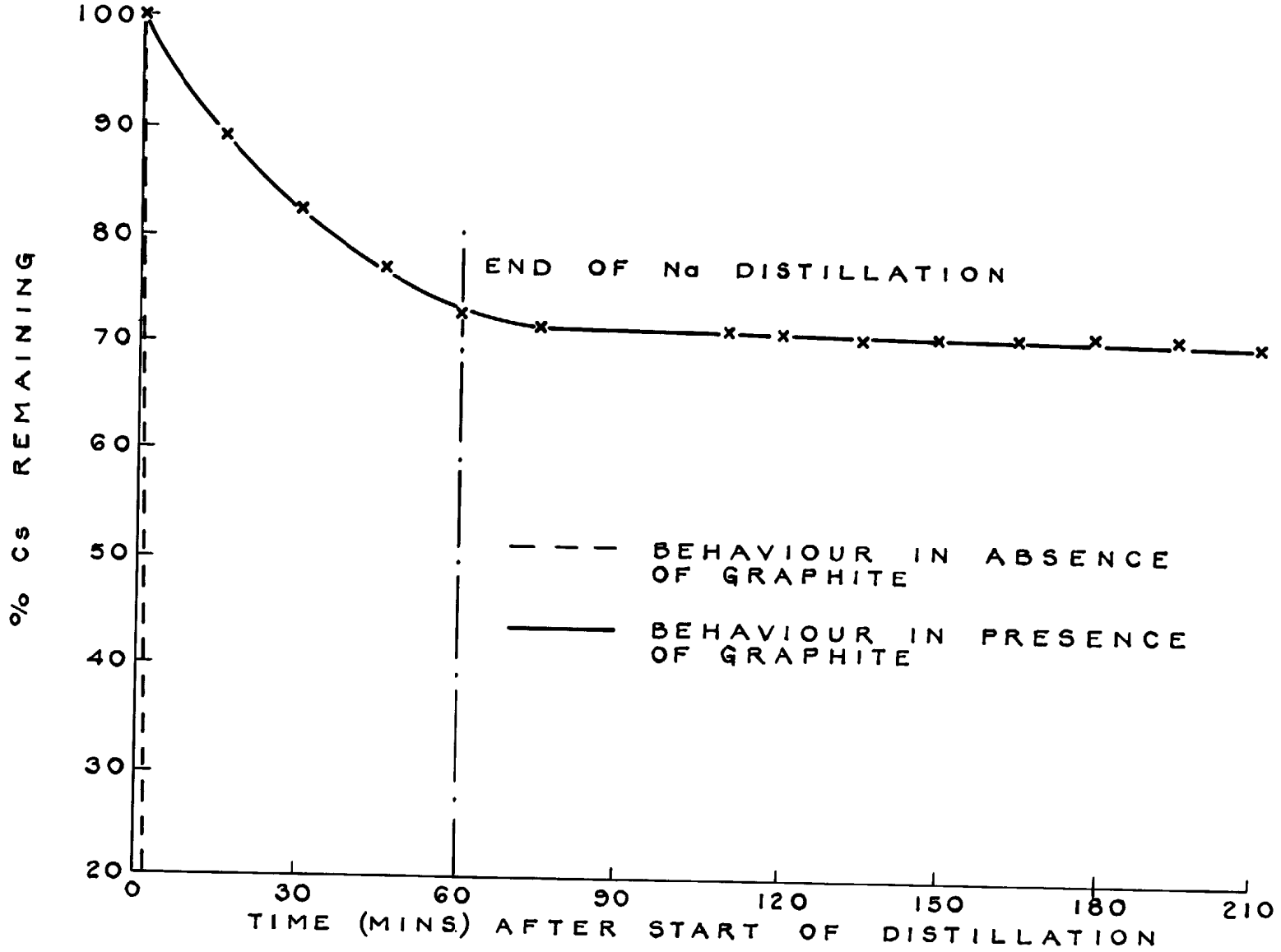

FIG. 4.

THE EFFECT OF GRAPHITE ON THE VOLATILITY OF Cs IN LIQUID SODIUM.

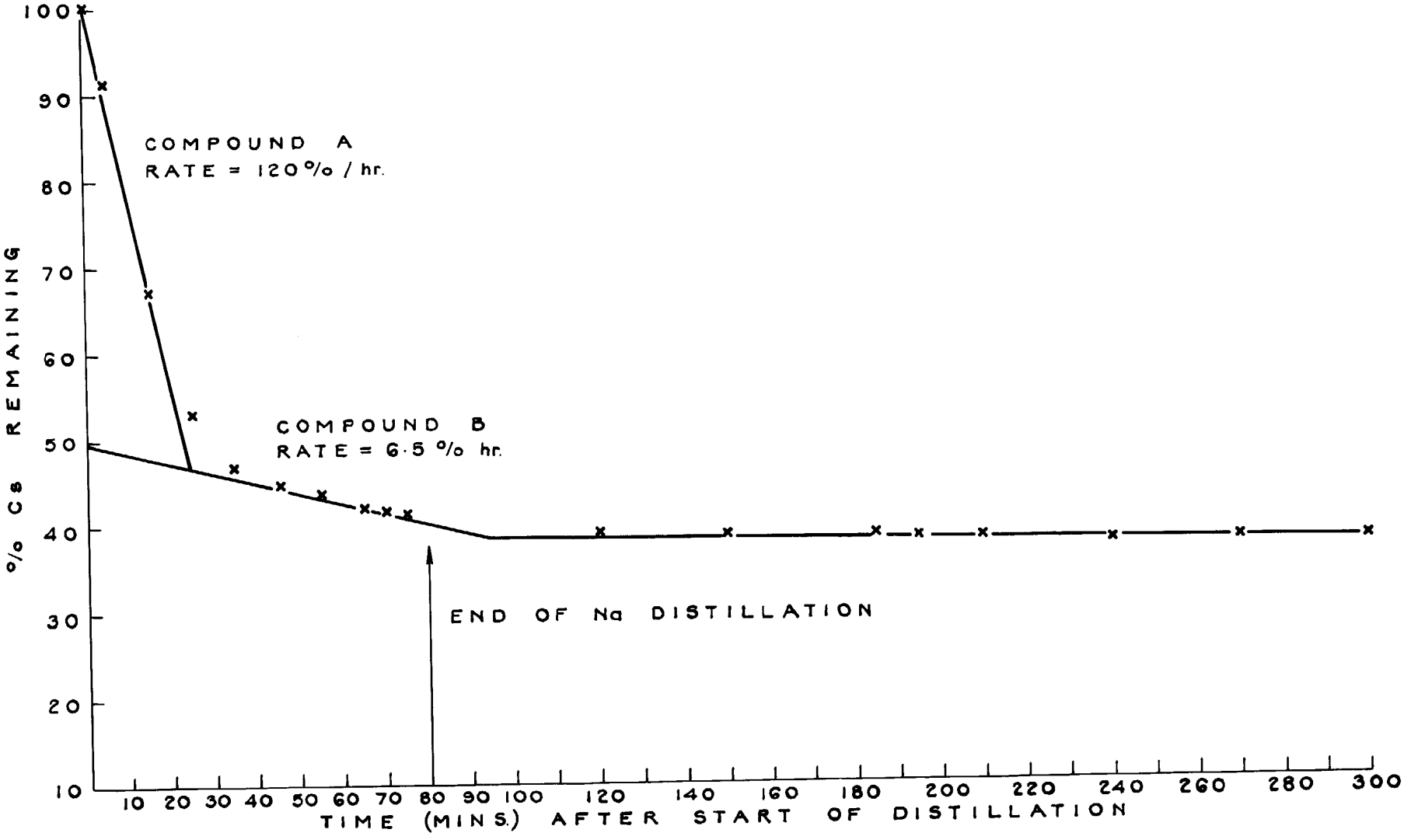

FIG. 5. DECOMPOSITION OF Cs–GRAPHITE COMPOUND IN DISTILLATION AT 500°C. GRAPHITE IN LIQUID PHASE

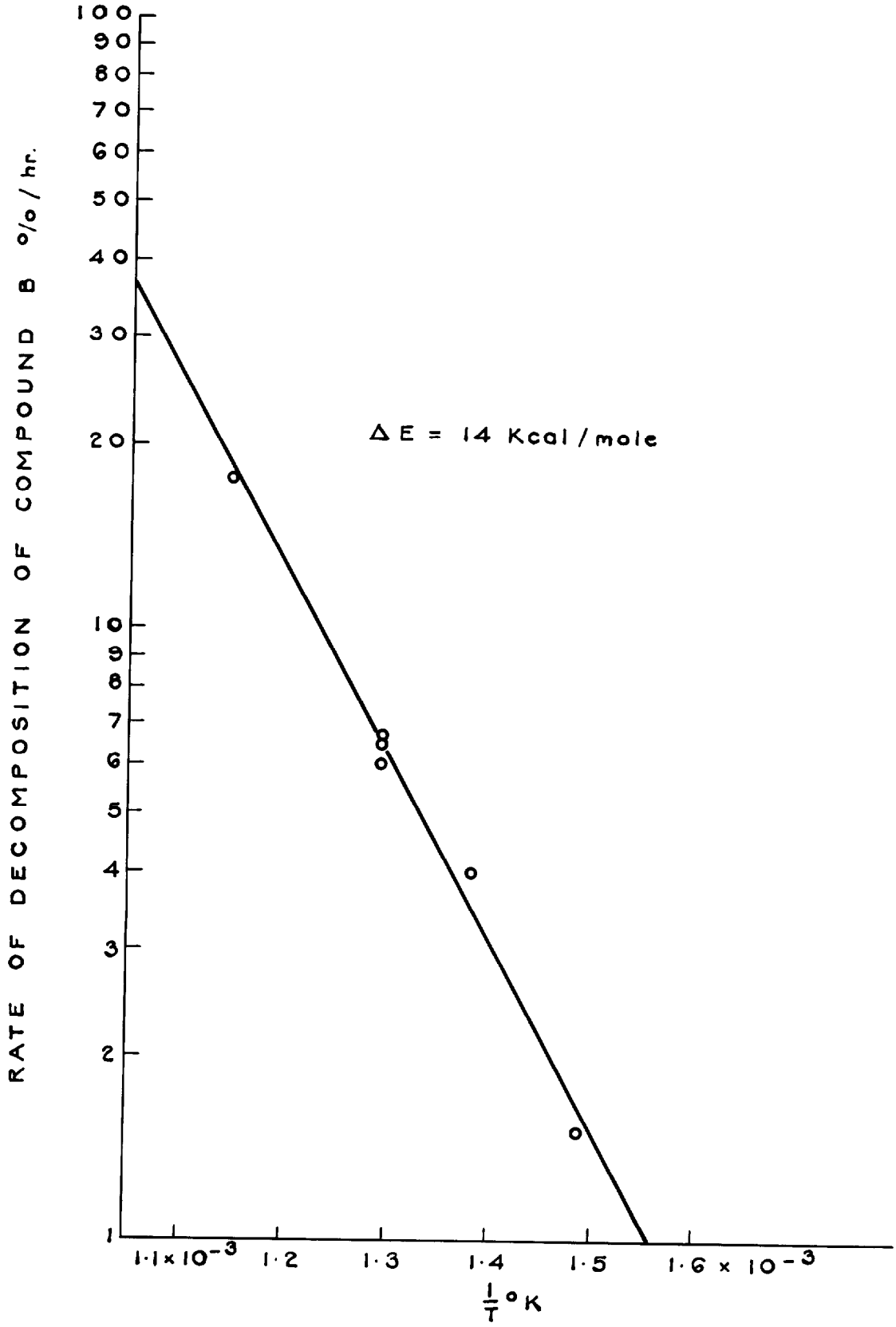

FIG. 6. ARRHENIUS PLOT FOR COMPOUND B

(i) Graphite is a neutron moderator and the use of massive quantities near the fuel is undesirable.

(ii) The volatility of caesium in sodium is so high that the trapping system would have to be carefully designed to allow the graphite to react with the caesium before the caesium escaped to the gas phase.

(iii) The presence of carbon in the liquid sodium may increase the rate of carbon transport between structural metals in the liquid sodium.

Points (i) and (ii) might be effectively dealt with by careful design. However, in view of the difficulties which might arise from point (iii) it was decided to test the effect of graphite in the gas phase, in equilibrium with liquid sodium and its vapour at 500°C.

A piece of graphite (mass 1 g) was fixed to the lid of the distillation pot and the caesium sorption experiment was carried out in exactly the same way as in previous experiments. With the pot sealed the graphite was held at 500°C in the gas phase above the sodium for three hours before the distillation was started. The results of the experiment are shown in Fig. 7 and should be compared with those in Fig. 5 where the conditions were the same except that the graphite is in the gas phase in Fig. 7 and in the liquid phase in Fig. 5. The similarity between the two results indicates that the graphite could be used, with equal efficiency, in the inert gas blanket of a fast reactor.

3.5 The sorption of caesium by charcoal

Experiments with solid and granulated graphite indicated that the formation of the more stable caesium-graphite (compound B in section 3.2) could be enhanced by an increase in the surface area of graphite used. It was therefore decided to investigate the effect of using high surface area gas absorption charcoal.

A carrier-free solution of Cs^{137} was dried down in the pot and one gram of charcoal (surface area 1000 m^2) was added. Pure sodium was introduced and the pot was held at 500°C for two hours before the sodium was distilled in the usual way. The results, shown in Fig. 8, demonstrate the very large retention of caesium which is possible using charcoal. The small increase in activity in the cell after all the sodium is distilled is probably due to migration of activity from the walls onto the charcoal. All the activity was found to be associated with the charcoal at the end of the experiment. The dotted line in Fig. 8 shows the rate at which caesium would be expected to distill out of the sodium in the absence of charcoal. The caesium deposited on charcoal is fully stable at 500°C in the absence of sodium.

The effect of charcoal in the gas phase was studied by placing one gram of charcoal in a steel cage fixed to the lid of the

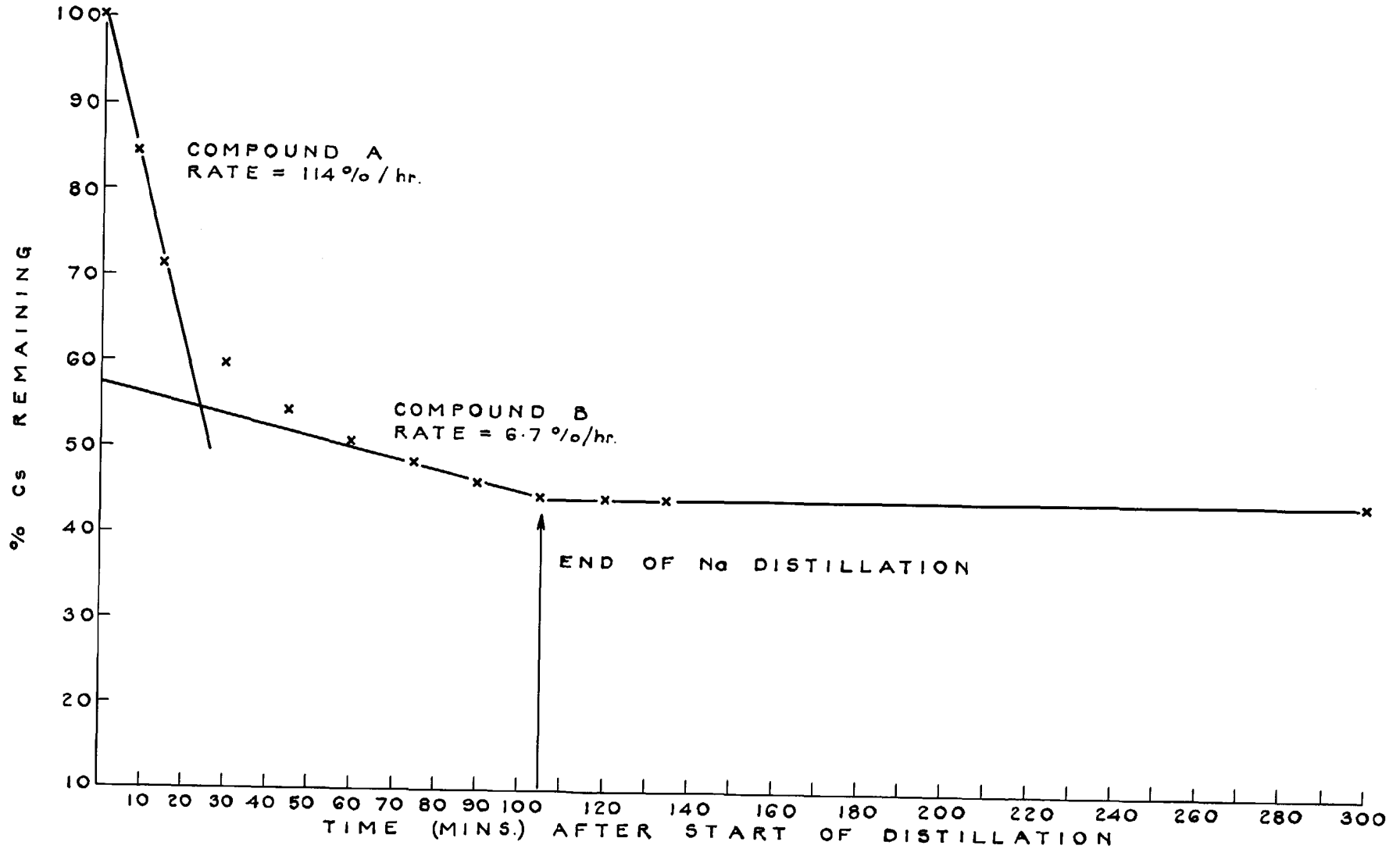

FIG. 7. DECOMPOSITION OF Cs-GRAPHITE COMPOUND IN DISTILLATION AT 500°C. GRAPHITE IN GAS PHASE

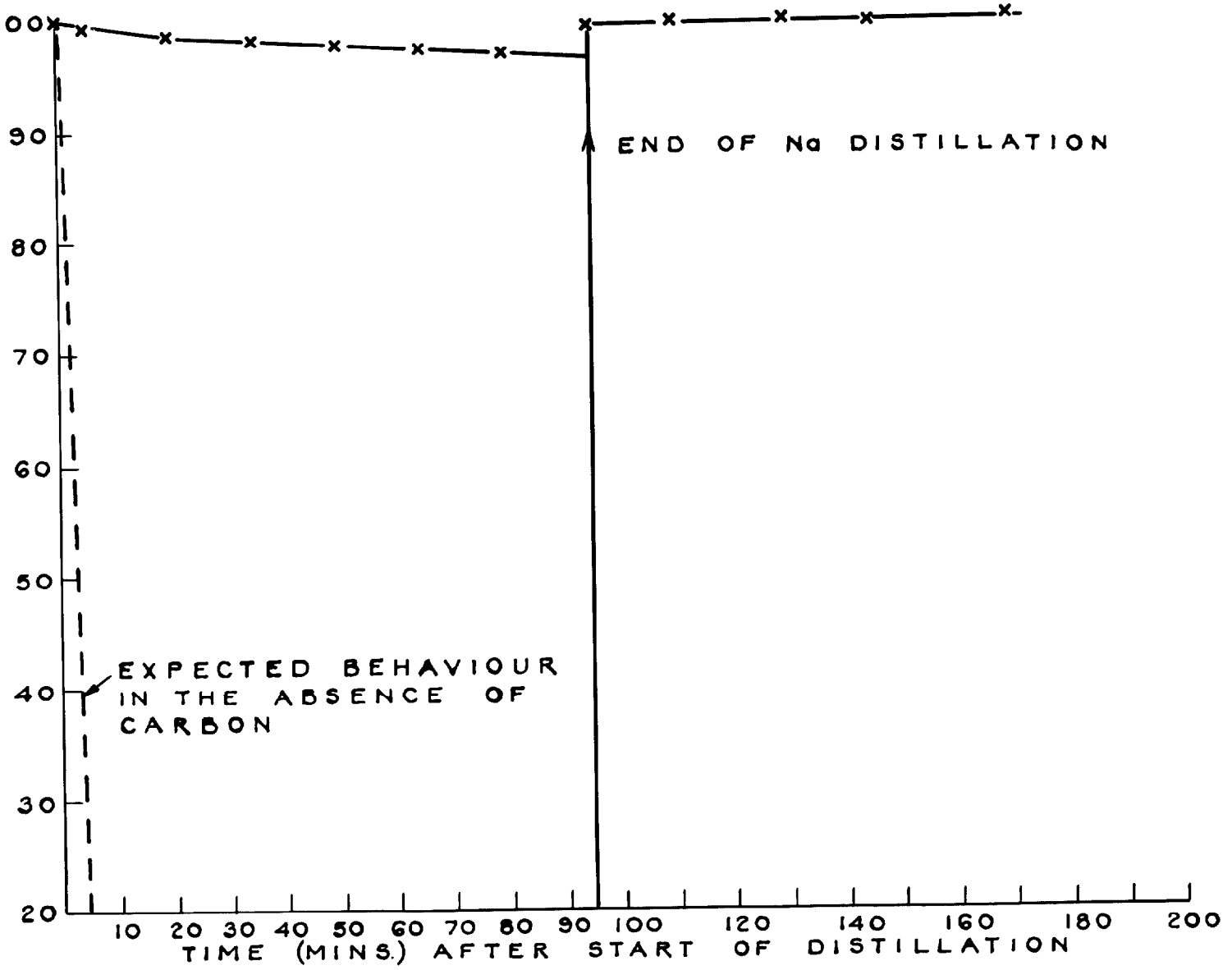

FIG.8. DECOMPOSITION OF Cs-CHARCOAL COMPOUND IN DISTILLATION AT 500°C. CHARCOAL IN LIQUID PHASE

distillation pot. The charcoal was then held above the level of the liquid while the distillation of the sodium containing active caesium was performed in the usual way. Results typical of those obtained are shown in Fig. 9. While the sodium was distilling the caesium was removed from the charcoal at the rate of 6%/hr. When all the sodium (60 g) was distilled 87% of the caesium remained on the charcoal and no further reduction was obtained by heating and evacuating for a further three hours.

Fig. 10 shows the results for the same experiment performed at 600°C. In this case the rate of break down of the caesium-charcoal compound was 15%/hr and 67% of the caesium was retained after all the sodium was distilled. In both cases all the activity remaining in the pot was subsequently shown to be associated with the charcoal.

If charcoal is to be of use for fission product trapping then it is essential that its absorbing properties do not rapidly deteriorate in the presence of hot sodium (e.g. by loss of surface area). Fig. 11 shows the results of an experiment to test the effect of pretreatment of the charcoal with sodium at 500°C. The charcoal was fixed to the lid of the distillation pot as in the previous experiment but no activity was placed in the pot before the sodium was introduced. The pot containing sodium and charcoal was kept at 500°C for three days before it was cooled and the lid removed. The active caesium solution was dried down on a steel disc and placed on top of the solid sodium in the pot then the lid was replaced and the pot was heated and evacuated at 250°C before the bellows valve was closed and the sodium was heated to 500°C. After two hours at 500°C the valve was opened and the rate of distillation was measured in the usual way. Comparison of Fig. 11 with Fig. 9 shows that pre-treatment with sodium had no discernible effect on the sorption of caesium by charcoal in the gas phase - 87% of the caesium was retained on the charcoal at the end of the distillation. The method used to obtain the results shown in Fig. 11 caused the sodium to be contaminated with oxygen to the level of 651 ppm at the start of the distillation. The similarity of the results shown in Fig. 11 to those in Fig. 9 (oxygen level 302 ppm) suggested that oxygen has no great effect on the sorption of caesium by charcoal. The absence of any oxygen effect was confirmed by the results shown in Fig. 12 for which the oxygen concentration was 39 ppm. In this experiment charcoal which contained active caesium (from a previous experiment) was fixed to the lid of the pot and pure sodium was run into the pot in the usual way. The charcoal containing the caesium was left for two days in the sodium vapour at 500°C, during which time no loss of caesium from the charcoal occurred. When the distillation was started the rate of break down of the caesium-charcoal compound was similar to that which had been obtained previously (Fig. 9, Fig. 11) at much higher oxygen levels. When all the sodium had distilled about 91% of the caesium remained on the charcoal. Subsequent treatment of the activity fixed on the charcoal with air at 500°C caused no further loss of caesium.

The experiments using graphite in sodium at 500°C (section 3.2)

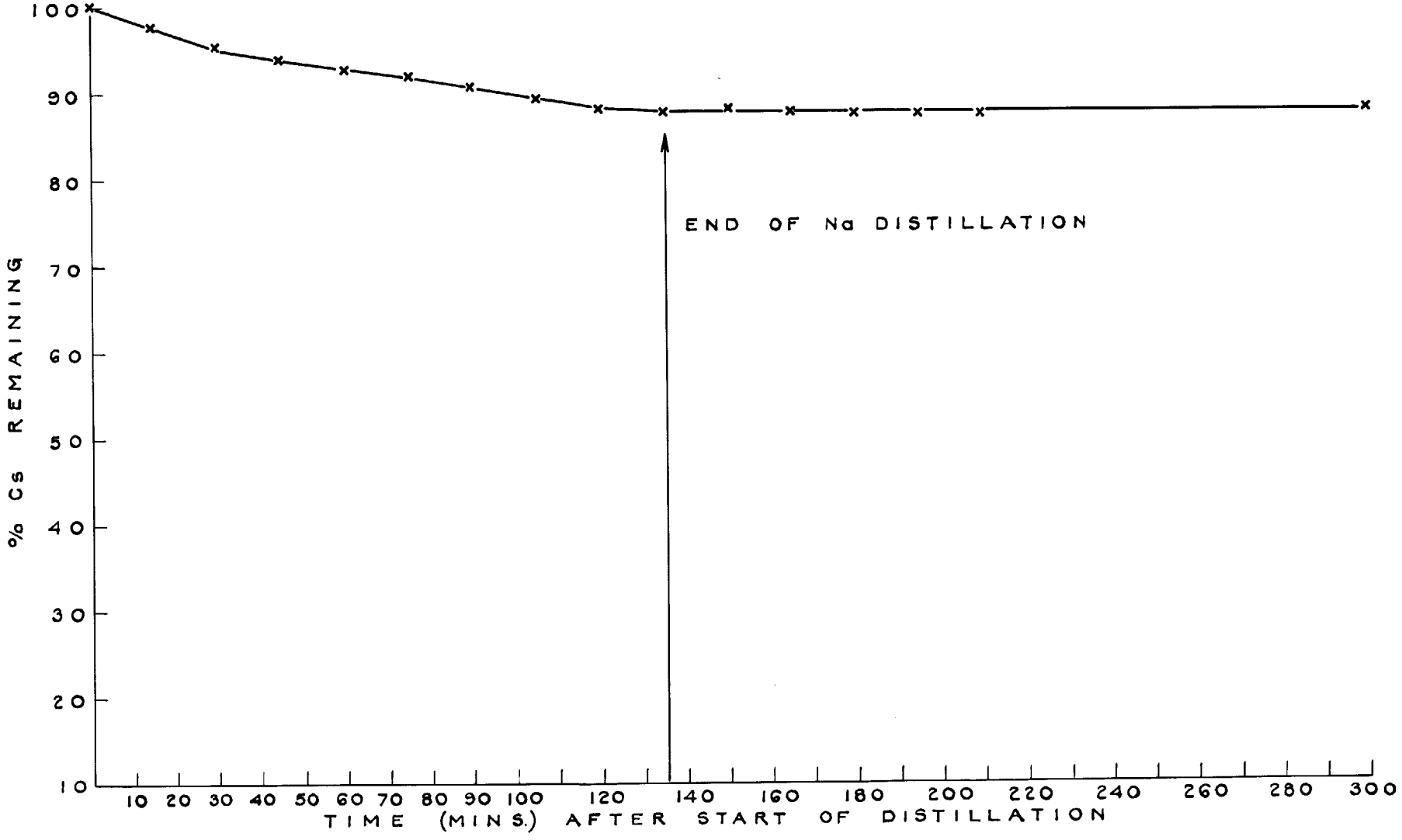

FIG. 9 . DECOMPOSITION OF Cs-CHARCOAL COMPOUND IN DISTILLATION AT 500°C. CHARCOAL IN GAS PHASE OXYGEN CONTENT 302 p.p.m.

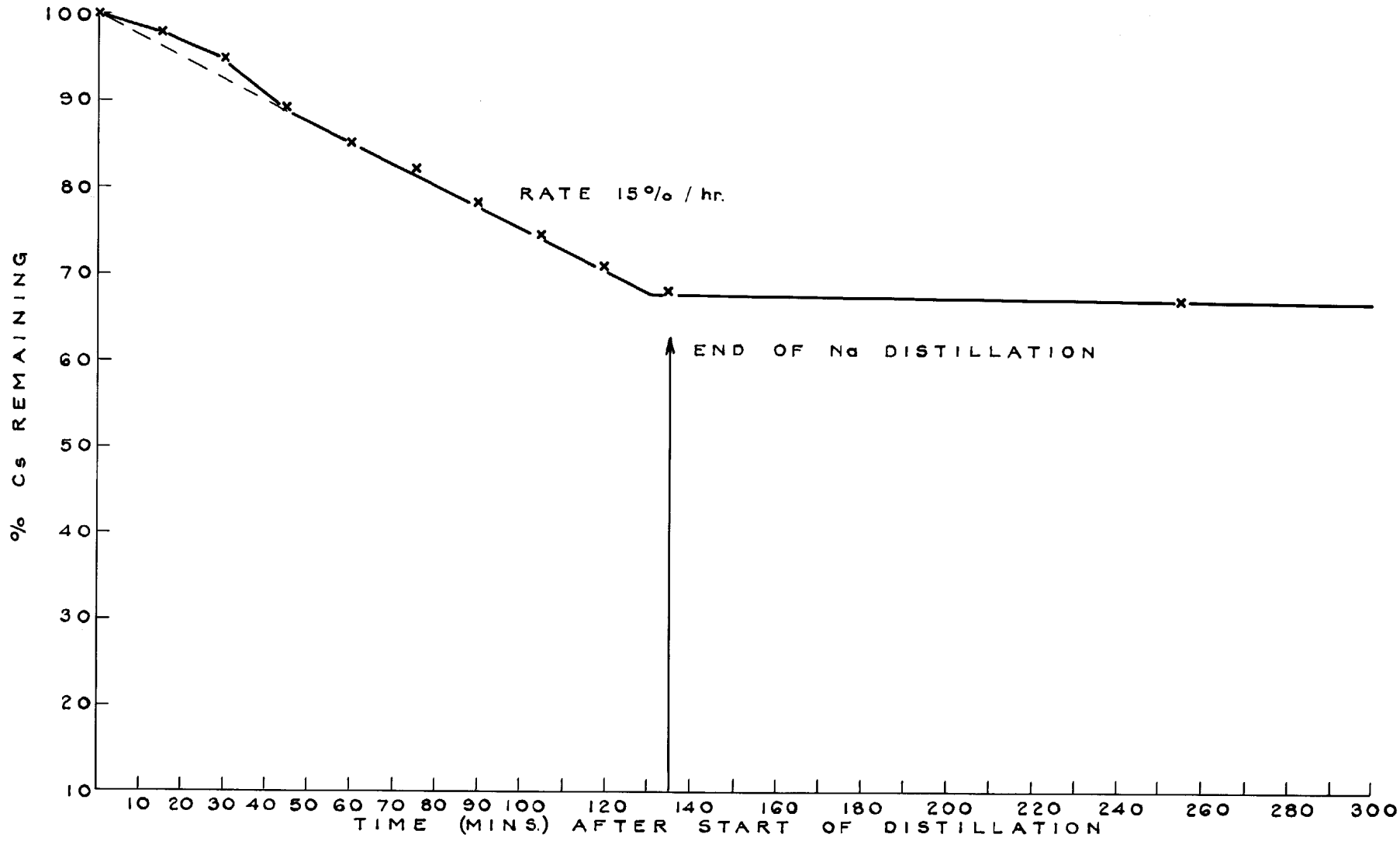

FIG. 10. DECOMPOSITION OF Cs-CHARCOAL COMPOUND IN DISTILLATION AT 600°C. CHARCOAL IN GAS PHASE

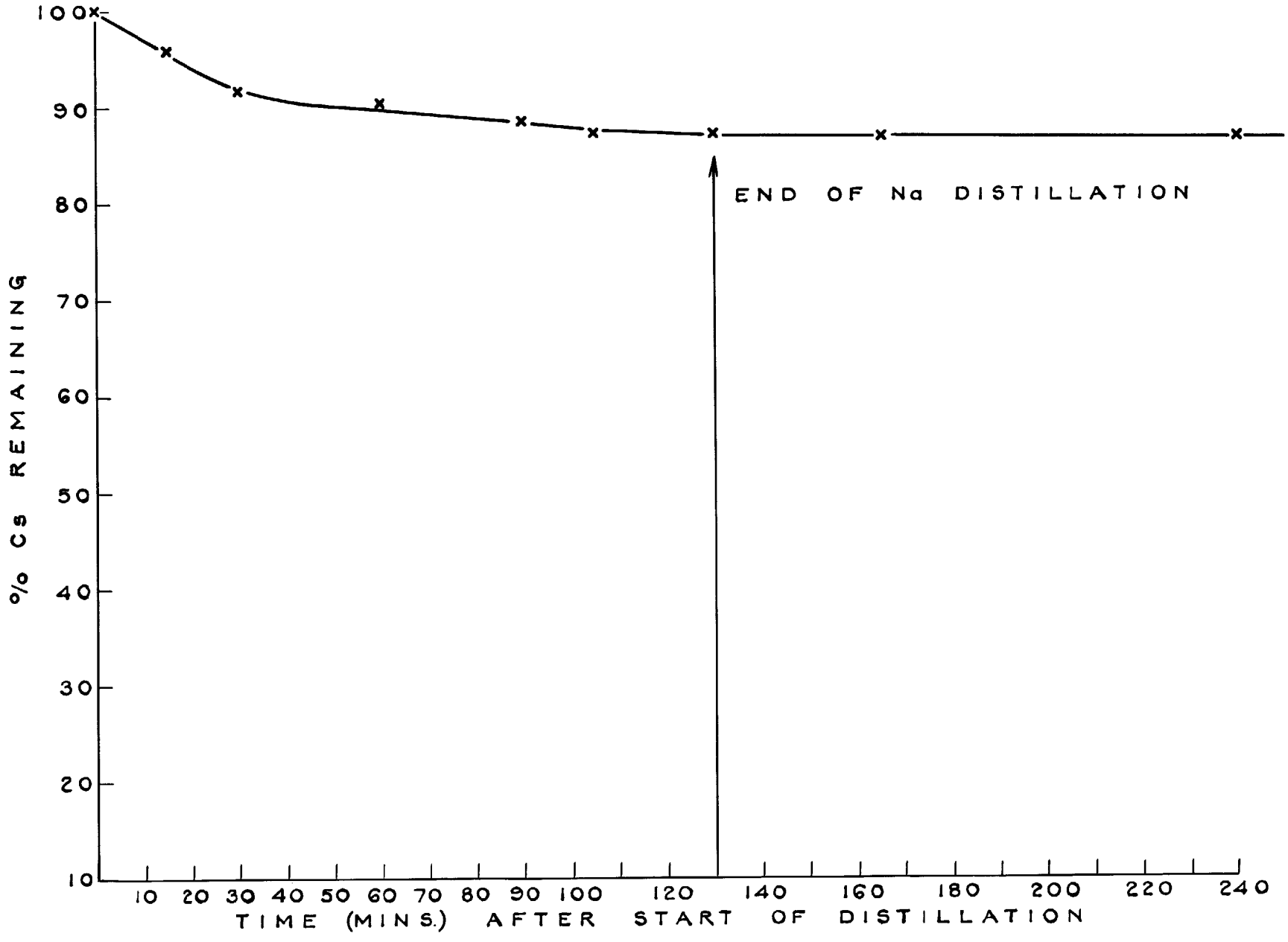

FIG. 11 DECOMPOSITION OF Cs-CHARCOAL COMPOUND IN DISTILLATION AT 500°C. CHARCOAL IN GAS PHASE PRE-TREATED WITH SODIUM
OXYGEN CONTENT 651 p.p.m.

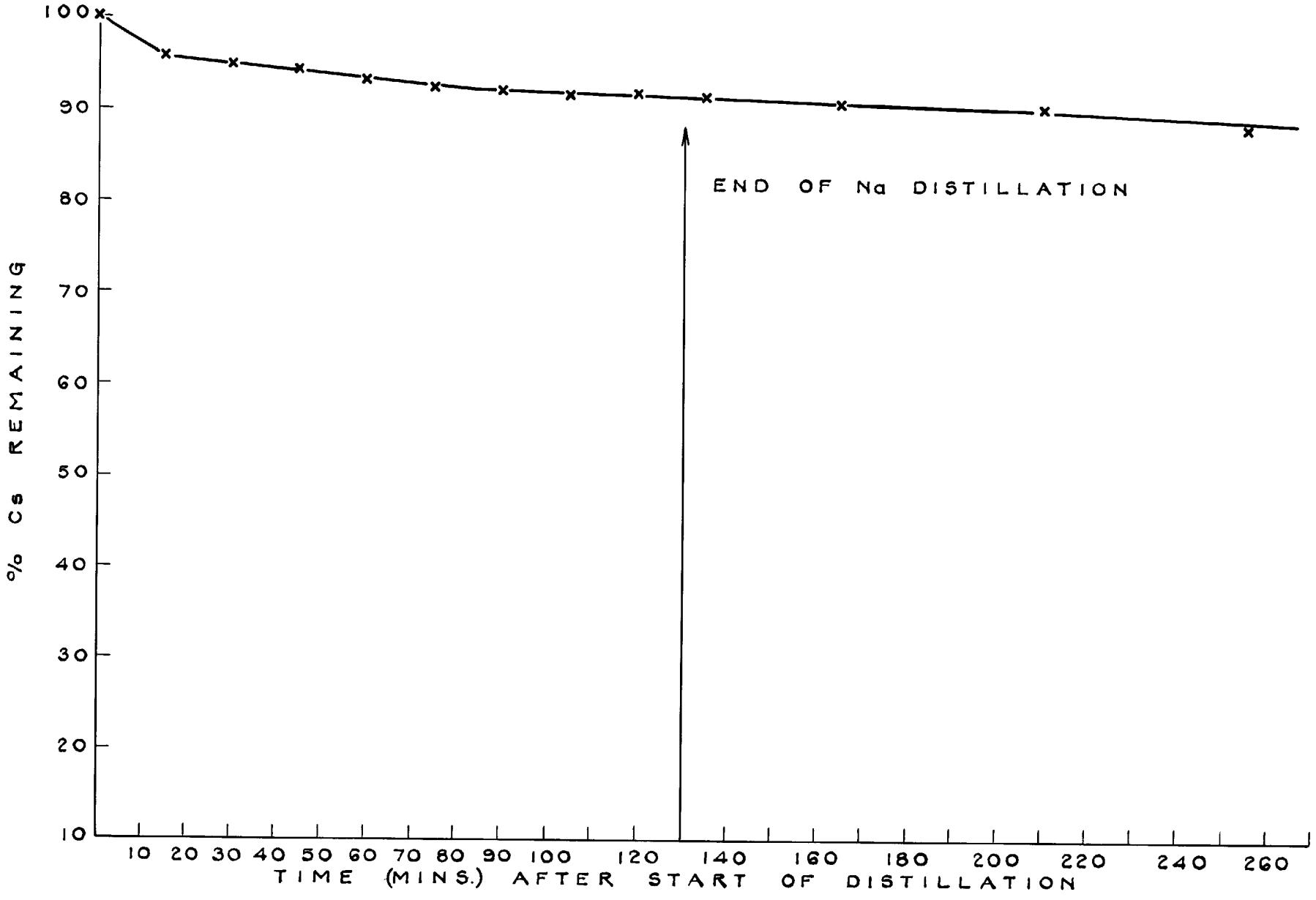

FIG. 12. DECOMPOSITION OF Cs – CHARCOAL COMPOUND IN DISTILLATION AT 500°C. CHARCOAL IN GAS PHASE PRE-TREATED WITH SODIUM
OXYGEN CONTENT 39 p.p.m.

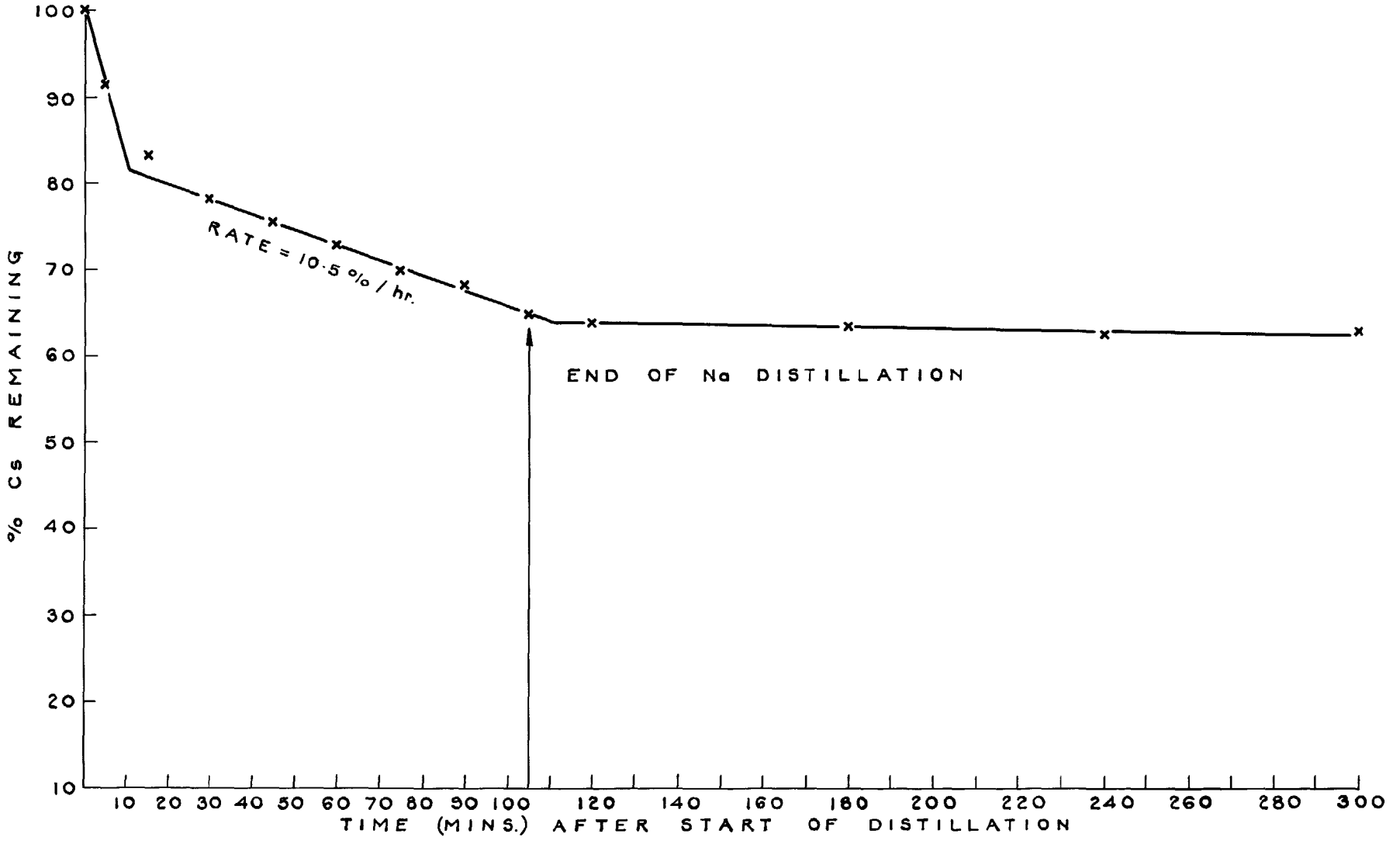

FIG. 13. THE DECOMPOSITION OF THE TWO Cs–CHARCOAL COMPOUNDS IN DISTILLATION AT 500°C.

provided evidence that the sorption of caesium occurs in two stages, one of which has been postulated as a surface adsorption and the other as a true inter-lamellar compound. In most of the experiments using charcoal in sodium the pot was held at 500°C for at least two hours before the start of the distillation and no evidence for a weakly attached surface layer of caesium on the charcoal was found. However, in one experiment the distillation was started as soon as the temperature reached 500°C and the result is shown in Fig. 13. The graph is similar in shape to those obtained previously using graphite (see for example Fig. 9) in that the break down of the caesium-graphite compound occurs in two sections, one fast (about 100%/hr) and the other slow (10.5%/hr). The data in Fig. 12 are not sufficient to establish accurately the rate of break down of the weakly bound caesium charcoal compound but the value for the more stable caesium charcoal compound (10.5%/hr) can be compared to the values obtained in the same conditions for the graphite caesium compound (6-7%/hr see Fig. 6). These results indicate that the mechanism of caesium sorption by charcoal is the same as that for caesium sorption on graphite. Charcoal is more efficient because the rate of formation of the interlamellar compound from the surface adsorption layer is more rapid in the case of charcoal than for graphite.

4. Conclusion

Graphite or charcoal in liquid sodium or in the vapour phase above the liquid sodium, forms an efficient trapping device for caesium at temperatures at least up to 600°C. The mechanism for the formation of the caesium-carbon compounds formed in sodium has been suggested and the rate of break down of the stable compound, as a function of temperature, has been measured. Oxygen has been shown to have little effect on either the formation or rate of decomposition of the caesium-carbon compounds and, in the absence of sodium, they are fully stable in air and vacuum at 500°C.

5. References

1. Castleman, A.W. et al. (1966) I.A.E.A. Symposium on Alkali Metal Coolants, Vienna.
2. Castleman, A.W. et al. (1968) BNL 13099.
3. Clifford, J.C. (1967) A.N.S. Trans. 10 (1).
4. Clough, W.S. (1967) J. of Nuclear Energy, 21, 225.
5. Clough, W.S. (1969) J. Nuc. Energy, 23, 495.
6. Pitzer, K.S. (1962) J. Am. Chem. Soc. 84, 2085.
7. Pollock, B.D. (1967) AI-AEC-12687, 51.
8. Salzano and Aronson (1965) J. Chem. Phys. 42, No. 4, 1323.

HEAT TRANSFER OF SODIUM COMPOUNDS DEPOSITED ON SURFACES FROM AEROSOLS*

Melvin W. First
Hideo Yusa**

Harvard School of Public Health
665 Huntington Avenue
Boston, Massachusetts 02115

ABSTRACT

Methods and apparatus have been developed to measure the coefficient of thermal conductivity of layers of elemental sodium combustion products deposited on heat exchange surfaces with an accuracy satisfactory for engineering design studies.

I. INTRODUCTION: Need for Thermal Conductivity Measurements of Deposited Sodium Aerosol Particles.

Heat dissipation from sealed spaces is a requirement for sodium cooled power reactors during normal operations and following accidental coolant releases.[1] Heat exchangers in sealed and inerted cells will absorb substantial amounts of heat when the reactor is functioning normally and this heat must be removed promptly to prevent an excessive temperature buildup inside the space which otherwise would result in premature failure of electric motors, gaskets, bearings, etc. Current plans for dissipating this heat include: (a) continuous recirculation of cell air through an air cooling coil sized to match the estimated heat release rate and (b) inducing heat flow through metal cell walls, ceiling, and floor to cooling air circulated in adequate quantities around all the exterior surfaces of the cell. No special difficulties are anticipated in designing systems for heat dissipation when there is clean air or nitrogen in the sealed spaces but sodium leaks of variable magnitude must be provided for in the design of the heat dissipation facility if the reactor is to continue to operate normally during and following minor sodium leaks. Sodium leaks will produce a mixture of sodium, sodium oxide, sodium peroxide, sodium hydroxide, and sodium carbonate particles in the cell air[2] which will coat the heat exchanger

*The work reported upon herein was performed under terms of Contract AT (30-1) 841 between Harvard University and the U.S. Atomic Energy Commission.

**Now at Hitachi Research Laboratory, Ltd., Hitachi-Shi, Ibaraki-Ken, 317, Japan.

surfaces, be they finned coils or cell walls, and inhibit the release of heat. The reduction in heat flow will be proportional to the amount of sodium coolant that leaks into the cell atmosphere and the effect will tend to be cumulative between service periods although the reaction of sodium products deposited on heat exchange surfaces for long periods is poorly understood at the present time.

Following a major sodium release which would interfere with normal operations, it is planned that emergency cooling and fume collection systems will go into operation to minimize release of radionuclides to the environment and hasten resumption of normal function. For these conditions, it is anticipated that large amounts of airborne sodium compounds will be generated and protection of heat exchange surfaces will become a major problem in the design of accident recovery systems. Installation of air filters upstream of heat exchangers is the protective measure most frequently specified for these recirculation systems. This appears to be satisfactory for handling small sodium releases as the heat generated by sodium reacting with atmospheric gases will not exceed the temperature limits of the materials of construction nor will the amount of airborne sodium fume exceed the dust holding capacity of the filter installation. For large sodium releases, high temperatures and high sodium particle concentrations will be generated inside the sealed spaces. This will call for filters having high fume holding capacity or, more likely, automatically cleanable filters resembling industrial bag filter units. Commercially available cleanable fabric filter units have a maximum temperature tolerance around 450°-550°F[3] although the upper temperature limit may be greater for brief service periods. Therefore, utilization of cleanable filters to protect heat exchangers is dependent upon the utilization of some method of protecting the filters from excessive temperatures.

One possibility is to use a pebble bed heat sink upstream of the filter unit sized to prevent passage of hot gases having temperatures in excess of the filter tolerance.[4] Static beds or movable self-cleaning pebble beds may be utilized but in either case, the pebbles will become coated with aerosol particles and the heat transfer rate will decline. Therefore, the particle deposition rate and the heat transfer characteristics of the material deposited on the surfaces must be known if pebble bed coolers are to be designed on a rational basis. Identical considerations apply to heat releases from sealed cells through the medium of cooling air circulation around the outside of the metal cell walls in the manner outlined earlier. Necessary allowances for

additional wall surface or lower cooling air temperatures must be made to account for expected particle deposition on walls, floor, and ceiling and the resulting modification of the heat transfer characteristics of the coated metal surfaces.

Although the thermal conductivity of elemental sodium and many of its common reaction products can be found in handbooks and similar sources, these values refer to the behavior of pure substances when compacted to their theoretical density and have no close or predictable relationship to the thermal conductivity of these same materials when deposited as highly porous films composed of finely divided particles of mixed chemical oxides and hydroxide. A familiar example will serve to illustrate this difference: ice with a density of 57.5 lb/cu.ft. has a thermal conductivity of 1.3 Btu/hr(sq.ft.)(°F/ft.) whereas compacted snow has a bulk density of 34.7 lb./cu.ft. and a thermal conductivity of only 0.27; showing the enormous change which occurs in heat flow characteristics when the bulk density of the material differs significantly from its true density. Freshly fallen snow, which often has a bulk density as low as 6 lb/cu.ft., will have even poorer heat flow characteristics, indicating the overriding influence of tiny occluded air spaces on heat transmission rates through porous materials. Therefore, it is necessary to measure the bulk density of deposited aerosol particles from sodium releases, as well as film thickness and thermal conductivity, to define fully the thermal characteristics of these deposits as it is anticipated that the density of the deposit will vary depending on (a) the temperature of the released sodium metal, (b) the rate of sodium emission (as this controls the rate of flocculation and the density of the resulting flocs), (c) the amount of oxygen available for sodium reaction, and (d) whether the sodium release may be characterized as a pool fire or spray fire.

II. EXPERIMENTAL METHOD

A. Heat Flow Measurements. The apparatus shown in Figure 1 was constructed to measure the thermal conductivity of sodium reaction products deposited from the airborne state. The basic element (A) is a solid block of 303 stainless steel having cross-sectional dimensions of 5 3/4 in.x 5 3/4 in., a thickness of 3 1/4 in., and a thermal conductivity of 9.4 Btu/hr.(sq.ft.)(°F/ft.). Thermocouples (B,C,D) were inserted in the steel block at three points 3.0 in. apart to measure temperature at known distances along the heat flow path while the block was heated from below with

an electric heating coil (E). A one inch thickness of closed cell polyurethane insulation was foamed in place (I) around the four sides of the steel block to minimize heat losses through this pathway and the entire assembly enclosed in an aluminum channel frame (G) for structural strength and ease in handling. The top surface of the stainless steel block on which the fume would be deposited was machined flat and polished smooth. The polyurethane foamed insulation was poured flush with the top surface with one depression (F) in each of four top surfaces that was sized to accommodate a 1x3 in. glass microscope slide with its exposed surface flush with the top surface of the steel block. These glass inserts were designed to be removed after the surface was coated with aerosol particles for measurement of (a) coating thickness, (b) weight per unit volume, and (c) chemical composition. After coating the upper surface of the block with sodium fume particles, the entire assembly was placed immediately inside a gloved box and maintained under an atmosphere of dry nitrogen to avoid oxidation and hydration of the deposit during measurement of thermal conductivity. After the initial heat flow measurements, the atmosphere inside the gloved box could be controlled by adding known amounts of water vapor and oxygen to the dry nitrogen stream flowing through the box and serial measurements of heat flow made as the chemical composition and density of the coating changed under the influence of the controlled environment. These serial measurements were considered especially important as it was observed that the deposited coating underwent rapid and profound physical and chemical changes when exposed to ventilation air containing the usual amounts of water vapor.

B. Heat Flow Calculations. Measurements of thermal conductivity were made by placing the side-insulated block on top of an electric heating coil (E, Figure 1) with the deposit up and heating the bottom of the stainless steel block. After suitable calibration, a simultaneous reading of the temperature near the bottom and top of the steel block, when steady state conditions have been reached, indicates the total heat flow rate without the need for accurate control or measurement of the heat input to the bottom heating coil or the small heat losses through the insulated sides of the block and magnesia block insulation around the electric heater (H).

Knowing the thermal conductivity of the stainless steel block and the distance between the measuring thermo-

FIGURE 1

HEAT TRANSFER MEASURING APPARATUS

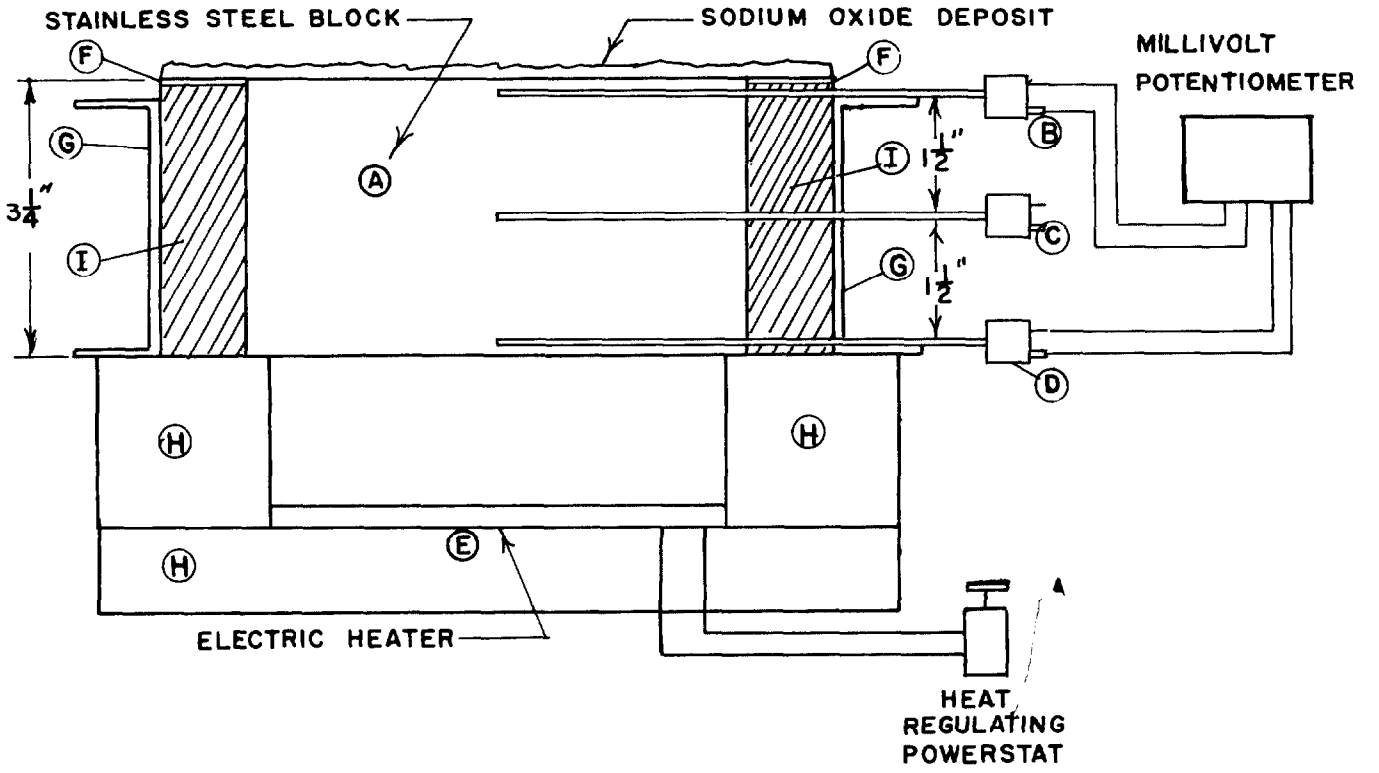

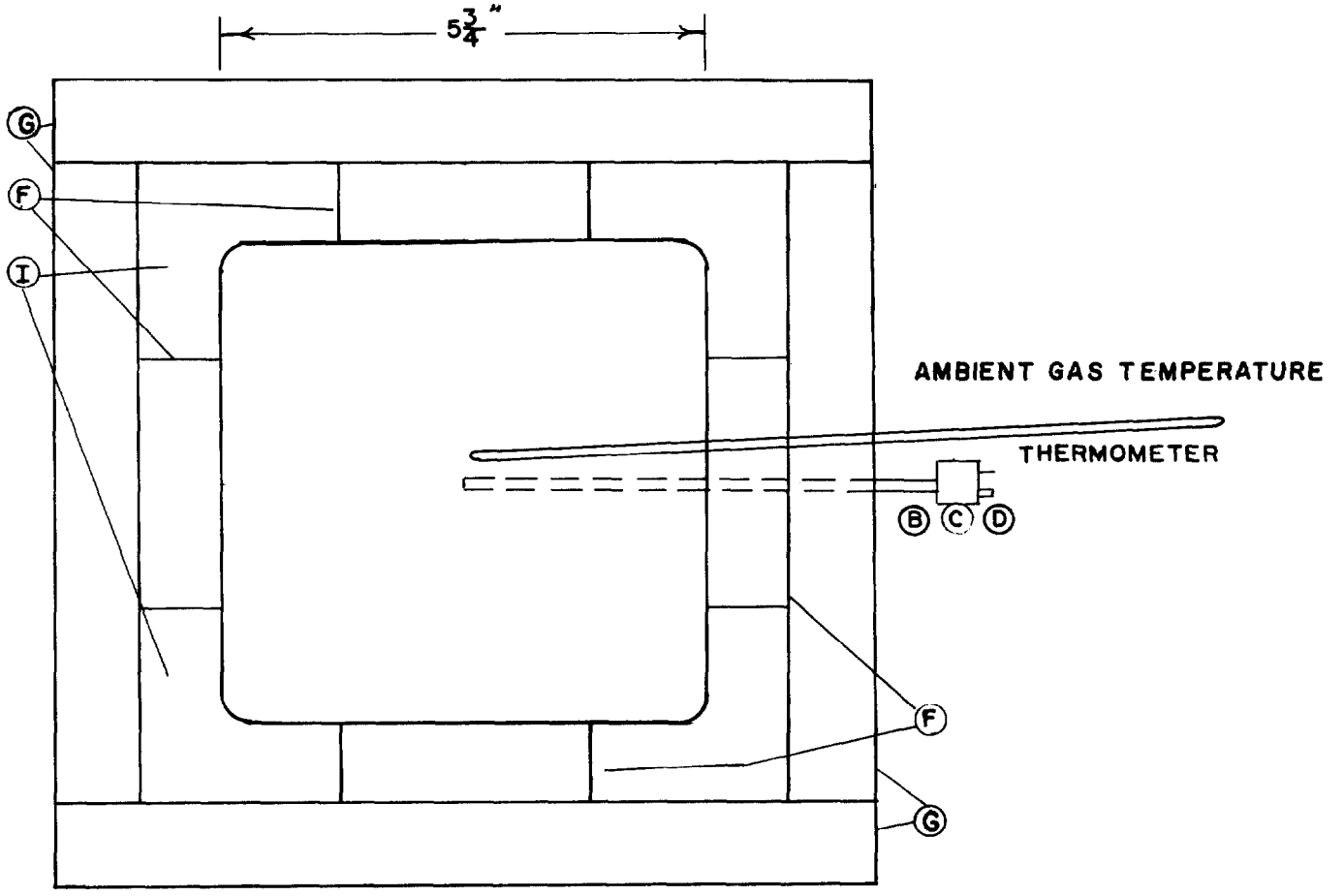

couples, it is possible to calculate the total amount of heat flow per unit time (Q) by the formula

$$Q = \frac{k}{\ell} A(\Delta t) \qquad (1)$$

where

k = thermal conductivity of the stainless steel block (Btu/hr)(sq.ft.)(°F/ft. of thickness)
ℓ = distance between thermocouples (ft.)
Δt = temperature difference between thermocouples (°F)
A = cross-sectional area at right angles to direction of heat flow (sq.ft.)

In Equation 1, all factors on the right side of the Equation are known (k, ℓ, and A) or measurable (Δt).

Heat flowing upward through the steel block leaves the upper surface by convective transfer to the air above it. The equation for this heat flow is

$$Q = hA(\Delta t_c) \qquad (2)$$

where

h = overall coefficient of convective heat transfer (Btu/hr.)(sq.ft.)(°F)
Δt_c = temperature difference between the upper surface of the plate (t_s) and the bulk temperature of the air mass(t_a) in contact with it(°F)

and the other symbols are as previously defined.

As the quantity of heat (Q) flowing through the steel block is the same as the amount lost from the upper surface by convection and the area through which the heat flows is the same in both cases, it follows that Equations 1 and 2 are equal and the value of h may be calculated from Equation 3.

$$h = \frac{k}{\ell} \frac{(\Delta t)}{(\Delta t_c)} \qquad (3)$$

The surface temperature at the top of the block is virtually identical with the temperature measured at the upper thermocouple but, if desired, a correction for the depth of the measuring point below the surface can be made

from Equation 1 and noting the distance between the top of the plate and the upper thermocouple, e.g.,

$$Q = \frac{k}{\ell_{1-2}} A\Delta t_{1-2} = \frac{k}{\ell_{2-s}} A\Delta t_{2-s} \tag{4}$$

where the subscripts (1-2) and (2-s) refer to the distance and temperature difference between the upper and lower thermocouples buried in the block, and the upper thermocouple and the surface, respectively. Thus, the unmeasured surface temperature, (t_s) becomes

$$t_s = t_2 - \frac{\ell_{2-s}}{\ell_{1-2}} \Delta t_{1-2} \tag{5}$$

When a layer of particles is applied to the top of the steel block, heat must flow from the steel block to and through the particle layer by conduction and then from the top of the particle layer by convection. Since the rate of heat flow is necessarily the same through all three zones, the following equation may be used:

$$Q_{1-2} = \frac{k}{\ell_{1-2}} (\Delta t_{1-2}) = \frac{k'}{\ell'} (\Delta t_{2-s}) = h(\Delta t_{s-a}) \tag{6}$$

where

k' and ℓ' are the coefficient of thermal conductivity and thickness of the deposited particle layer, respectively. t_s now refers to the upper surface of the deposited particle layer.

It is not possible to determine the temperature of the top of the particle layer without additional measurements of the values of both k' and t_s, which are related, but this difficulty may be avoided by using an overall coefficient of heat transfer for the combination of serial heat flow by steel block conduction, particle layer conduction, and particle layer to air convection in the following manner:

$$\frac{1}{U_{1-a}} = \frac{\ell}{k} + \frac{\ell'}{k'} + \frac{1}{h} \tag{7}$$

where

U = overall coefficient of heat transfer from the bottom of the steel block to the air above the block in the same units as h.

The value of "h", the convective heat transfer coefficient from the top of the bare steel block to the air can be measured precisely using Equation 3 and was found to be 1.6 Btu/hr.(sq.ft.)(°F). It has been assumed that the same value of "h" may be applied to the heat release to the air from the top of the particle deposition layer. This assumption has not been tested but it is believed that whatever differences exist in the texture of the top of the particle layer will not result in a significant deviation from the value derived experimentally for the bare steel block.

Using the overall coefficient of heat transfer, the design equation for measuring the heat transfer coefficient of a deposited layer of sodium reaction particles is:

$$Q = \frac{k}{\ell} A(\Delta t_{1-2}) = U_{1-a} A(\Delta t_{1-a}) \tag{8}$$

$$\frac{1}{U_{1-a}} = \frac{\Delta t_{1-a}}{\Delta t_{1-2}} \cdot \frac{\ell}{k} = \frac{\ell}{k} + \frac{\ell'}{k'} + \frac{1}{h} \tag{9}$$

and the value sought, k', the heat transfer coefficient of the deposited layer, may be determined from Equation 10 for which all of the quantities on the right side of the equation are known or measurable:

$$k' = \frac{\ell'}{\frac{\ell}{k}\left[\frac{\Delta t_{1-a}}{\Delta t_{1-2}} - 1\right] - \frac{1}{h}} \tag{10}$$

C. Deposition of Particle Layers. It is possible to generate airborne sodium reaction products in many ways and to simulate a variety of real accident situations very realistically with respect to the size, shape, porosity,

and chemical composition of the products that are formed. Four situations of major concern are pool and spray fires in air and in reduced oxygen atmospheres.

Particle deposition on the surface of the stainless steel block may be accomplished in a number of ways, including gravitational settling, electrostatic precipitation, and thermal precipitation, but perhaps the most realistic and the most useful method of deposition is to impact the particles on the measuring surface in the manner shown in Figure 2. This deposition method produces thick coatings of uniform density and thickness which are excellent for measurement and simulates closely the mode of deposition on pebble bed cooler packings, finned cooling coils, etc. Figure 2 illustrates aerosol generation from a small pool fire but the apparatus is equally useful for depositing particles from a spray fire. An air jet containing suspended particles impinges on the face of the steel block which is located 3 jet diameters downstream in a large plenum chamber which reproduces conditions resembling the discharge of a free jet. Air flow measurements indicate that the jet impinges on the face of the plate with a very nearly uniform velocity in excess of 2000 fpm. A more highly agglomerated particle can be deposited on the surface of the plate by moving the generating source farther away so that the particles will have longer to age and agglomerate before entering the apparatus. As a general rule, greater agglomeration results in a more fluffy and porous deposited layer but if the delay is greatly prolonged, the opposite effect will be noted because the largest flocs will settle out of the air rapidly and entrain many lesser flocs in the process.

III. RESULTS

Measurements have been made of the coefficient of thermal conductivity of layers of particles deposited on surfaces by impaction, electrostatic precipitation, and thermophoresis from aerosols generated by exposing hot sodium to air in a small pool-type sodium fire. The thickness of the deposited films has ranged from .004 to .025 in. Air temperature during particle deposition ranged from 88 to 110°F and the air had a dew point of 40°F, equivalent to 0.005 lbs. moisture per pound of dry air. When the deposit was exposed to these temperature and humidity conditions, it was noted that hydroxide formation occured within 30-40 minutes of exposure

METHOD OF DEPOSITING A LAYER OF FRESHLY FORMED FUME ON HEAT TRANSFER MEASURING APPARATUS

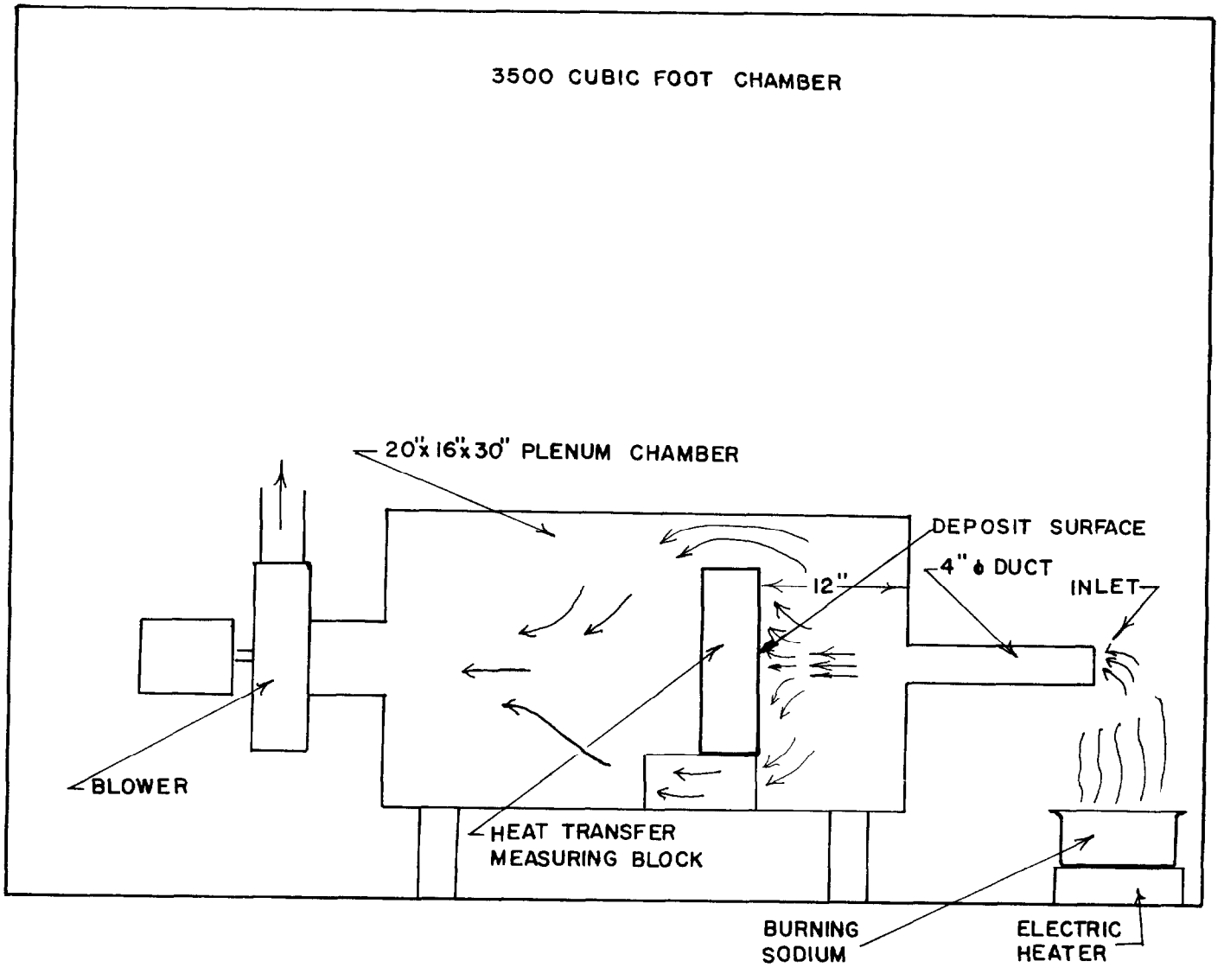

FIGURE 2

and this produced a wet sludge having obviously altered physical characteristics. Therefore, an experimental procedure was developed whereby an initial charge of sodium was burned in the exposure chamber (3500 cu.ft.) to tie up the remaining water vapor and then a second charge was ignited and the resulting aerosol drawn through the deposition apparatus, shown in Figure 2. Immediately after deposition, the steel block with its deposited layer was placed in a gloved box filled with dry nitrogen and heat flow measurements were begun. The test plaques in the upper surface of the foamed insulation were removed for thickness measurement, weighing, and analysis of chemical composition (oxide, peroxide and carbonate).

IV. SUMMARY AND CONCLUSIONS

Methods and apparatus have been developed to measure the coefficient of thermal conductivity of layers of elemental sodium combustion products deposited on heat exchange surfaces with an accuracy satisfactory for engineering design studies.

Measurements of surface deposits derived from small pool fires in air show that freshly formed deposits have a bulk density of 20 lb/cu.ft. and a coefficient of thermal conductivity equal to 0.52 Btu/hr(sq.ft.)(°F/ft.). After exposure to humid air (dew point, 60°F) for 30-45 minutes, water adsorption and chemical reaction change the appearance of the deposit to that of a moist paste. Thermal conductivity increases and approaches that of water as deposit becomes wetter and wetter.

More measurements are needed to explore all of the situations under which sodium aerosols may form and deposit on heat exchange surfaces and this study is continuing.

REFERENCES

1. Shaver, B.O. "Fast Flux Test Facility, Conceptual System Design for the Heating and Ventilating System", Pacific Northwest Laboratory Report BNWL-500, Volume 25, Richland, Washington (December 5, 1968).

2. First, M.W. et. al. "Semiannual Progress Report, March 1 - August 31, 1969", Harvard Air Cleaning Laboratory Report NYO-841-20, Boston, Massachusetts (October, 1969).

3. First, M.W. et. al. "Semiannual Progress Report, September 1, 1969 - February 28, 1970", Harvard Air Cleaning Laboratory Report NYO-841-22, Boston, Massachusetts, (April, 1970).

4. Bulba, E. and Underhill, D.W. "Application of a Pebble Bed Heat-Sink to the Fast Flux Test Facility Cleanup System", Harvard Air Cleaning Laboratory Report NYO-841-17, Boston, Massachusetts (March, 1969).

OPTICAL PROPERTIES OF SODIUM AEROSOLS

Parker C. Reist and William C. Hinds

Harvard University
School of Public Health
Boston, Massachusetts

ABSTRACT

One of the consequences of burning metallic sodium is the production of a dense white smoke. This paper discusses the optical properties of this aerosol, developing the relationship between visibility, aerosol concentration and time, as well as identifying light scattering properties of the cloud.

Black discs on white targets were used to determine visual range at different cloud concentrations. Light transmission measurements were made using a laser. At high aerosol concentrations multiple scattering was evident. Angular light scattering measurements were made which showed that the aerosol particles scattered light very strongly in the forward direction. All data indicate the opaque nature of the aerosol cloud. At concentrations above one gram per cubic meter, vision would be restricted to four meters or less, making walking through the cloud difficult and potentially hazardous. With concentrations of 0.1 gram per cubic meter, maximum visibility would be limited to about 40 meters, or roughly into the middle of a 200 foot diameter containment vessel. Typical overhead lights could be distinguished at distances three to four times greater than nonlit objects in the same cloud concentration.

At low concentrations, transmission measurements could be used to deduce the apparent aerosol particle density, which was found to be 1.2 grams per cubic centimeter. Scanning electron microscope photographs appear to confirm this conclusion.

Introduction

One of the consequences of burning metallic sodium is the production of a dense white smoke comprised of Na_2O, Na_2O_2 and

perhaps some NaOH and Na_2CO_3. If radioactive metallic sodium coolant burns in a closed space, the usual limitation on entry caused by the hazardous nature of the radioactive sodium aerosol is compounded by the practical limitations imposed by the very poor visibility in the resultant cloud. Low visibility greatly increases the risk factor in the risk-benefit analysis of when to enter the chamber. Two visibility considerations are important. The first is the visibility required to safely walk within the cloud without falling, getting lost, etc; while the second is the visibility required to see objects in a room which contains the cloud, when viewing from outside the room. In a reactor accident examples would be to see where damage occurred, whether valves are open or closed, or if anyone is still inside the room.

It is the purpose of this paper to discuss the optical properties of the aerosol produced by burning sodium in order to develop relationships between visibility, aerosol concentration and time, as well as identifying light scattering properties of the aerosol which could lead to methods for improving visibility in the cloud at a given aerosol concentration.

Experimental

a. Aerosol generation

The test aerosols for all experimental work reported here were generated by heating 1 to 2 pounds of sodium to ignition temperature in an open pan and then allowing the sodium to burn itself out. This burning took place in a closed room approximately 5 meters high, having a volume of about 94 cubic meters. Runs were made at initial relative humidities within the room of 20, 22, and 46 percent.

The initial room temperature in all cases was about 85°F. Most work was carried out at 46% relative humidity which was felt to be representative of potential accident conditions.

The total burning time for the three runs was 30 to 50 minutes, the end point being impossible to judge because the extremely dense cloud completely obscured the intense sodium flame. Concentrations were measured gravimetrically from a sampling port approximately two feet above the chamber floor using fiberglas filters (MSA type 1106B). Figure 1 is the aerosol concentration time history of the cloud in the chamber. It can be seen that after about 100 minutes for the quantities of sodium we used, the aerosol concentration becomes independent of the initial conditions and the shape of the curve is

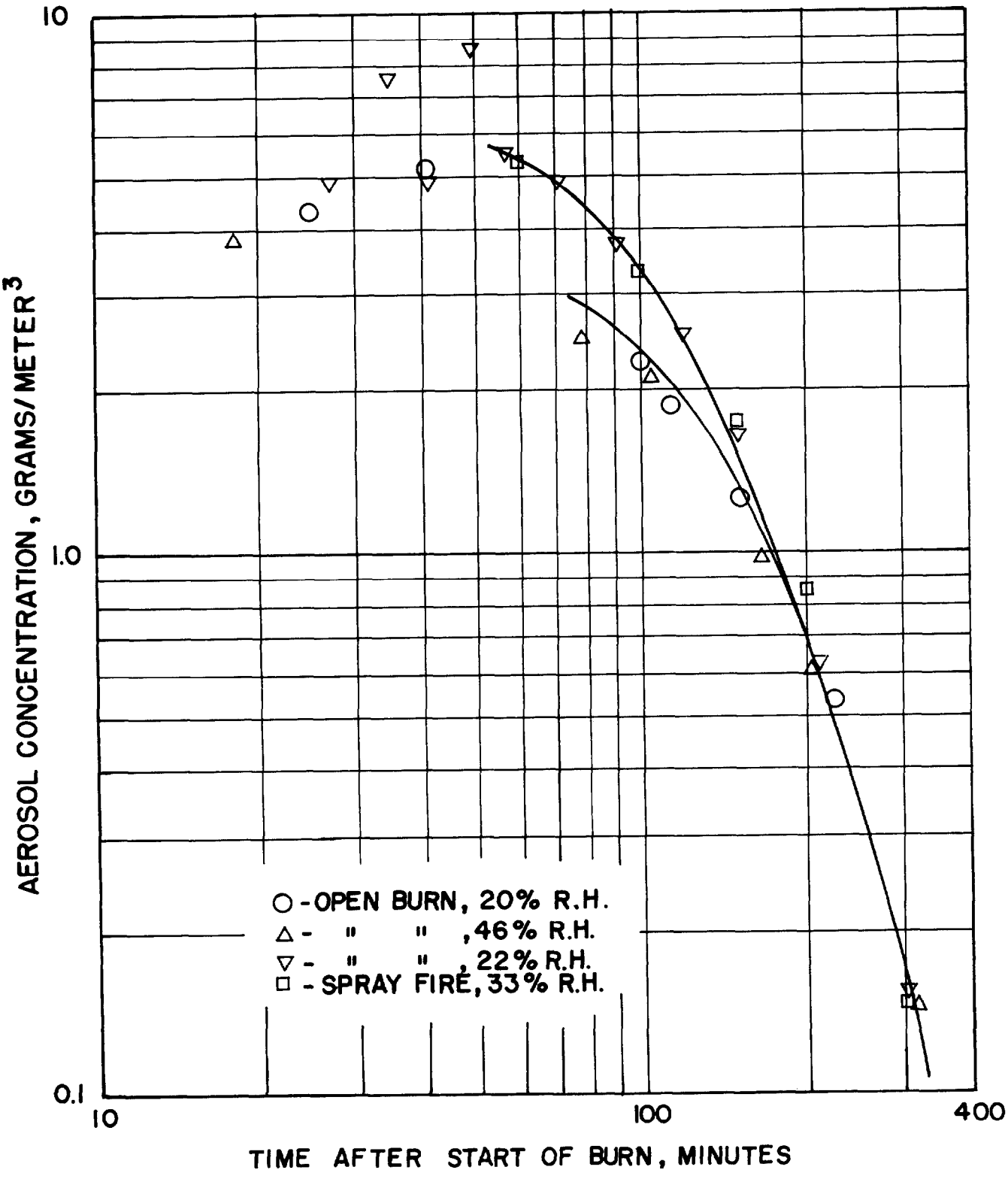

FIG. 1 - TIME-CONCENTRATION HISTORY OF AEROSOL

similar to the data of others[1,2]. The initial variability of the data was most likely due to concentration fluctuations as the cloud descended to our sampling height.

Samples of the aerosol cloud were collected for electron microscopy using a point-to-plane electrostatic precipitator. Figure 2 is a typical electron micrograph of the collected particles at 195 minutes following the start of a burn. In subsequent analysis it was assumed that this distribution was preserved over the time 100 to 300 minutes. Size analysis studies of the aerosol showed a fairly close fit to a log-normal distribution with some tailing off at the higher and lower ends of the curve as shown in Figure 3. From this curve a count median diameter of 1.6 microns was determined with a distribution having a geometric standard deviation of 2.3.

No chemical composition data were collected on the aerosol. However, the white-yellow color of all samples collected for weighing indicated a predominance of sodium peroxide. This is consistent with data collected from other runs so that we assume in the following that the aerosol is principally in the peroxide form[3].

b. Visibility studies

A series of observation targets were placed in the aerosol chamber at distances of 0.5, 1, 2, 3, and 4 meters from a viewing window. Each target consisted of a dull-finished white sheet on which were painted two black discs, one 8.5 centimeters in diameter and the other 2.5 centimeters in diameter. Visibility was then defined as that point where there was sufficient contrast between the large black disc and its background so that the large disc could be distinguished, although the small one could not. This visibility was related to aerosol concentration. As an aid to making this judgment, we used two discs; the smaller one being used to insure that the visibility was not greater than the target range since the little disc could be distinguished only at a slightly lower concentration than the larger one.

Figure 4 shows the data from the two runs on which visibility information was recorded. It is interesting to note the small amount of spread in the data points, even though visibility measurements had to be made at specific distances, or, at best, estimated as half the distance between two specific distances.

The visibility, or more accurately the visual range, can be approximated by a straight line having the form

$$D = \alpha C_m^{-1}$$

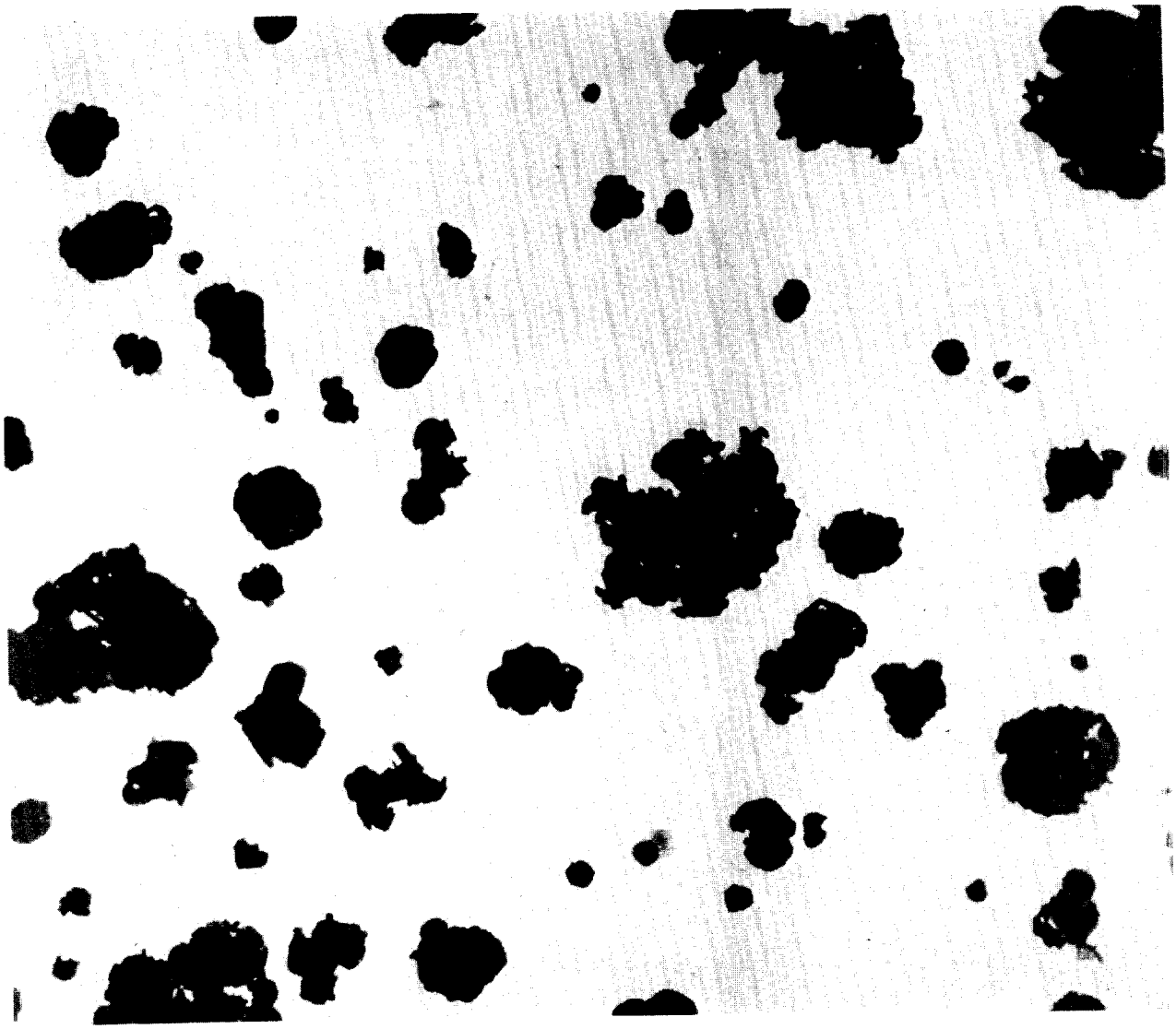

⊢⊣ 1 MICRON

FIG. 2 - TYPICAL ELECTRONMICROGRAPH OF COLLECTED AEROSOL

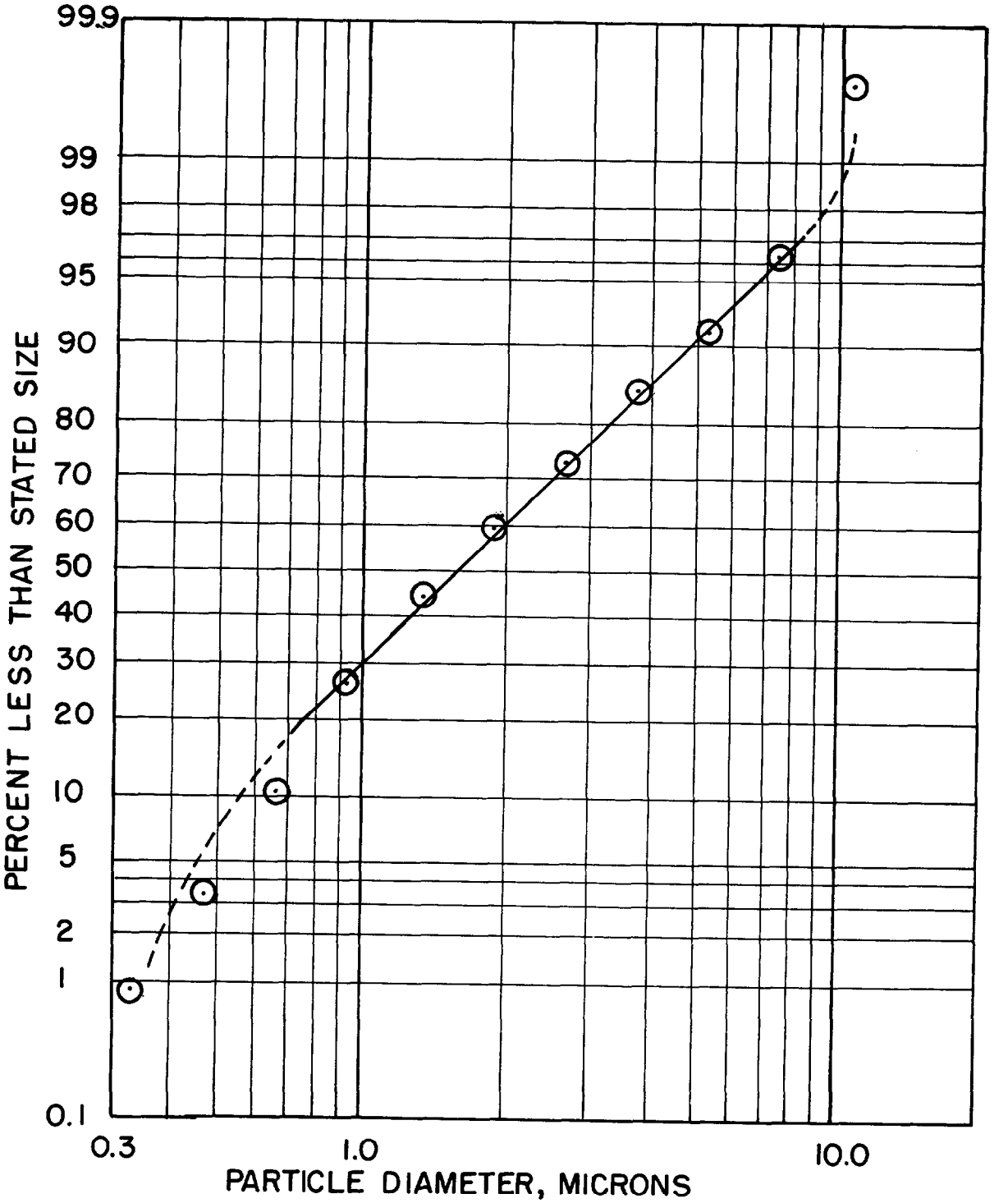

FIG. 3 - SIZE DISTRIBUTION PLOT OF AEROSOL MEASURED 195 MIN. AFTER START

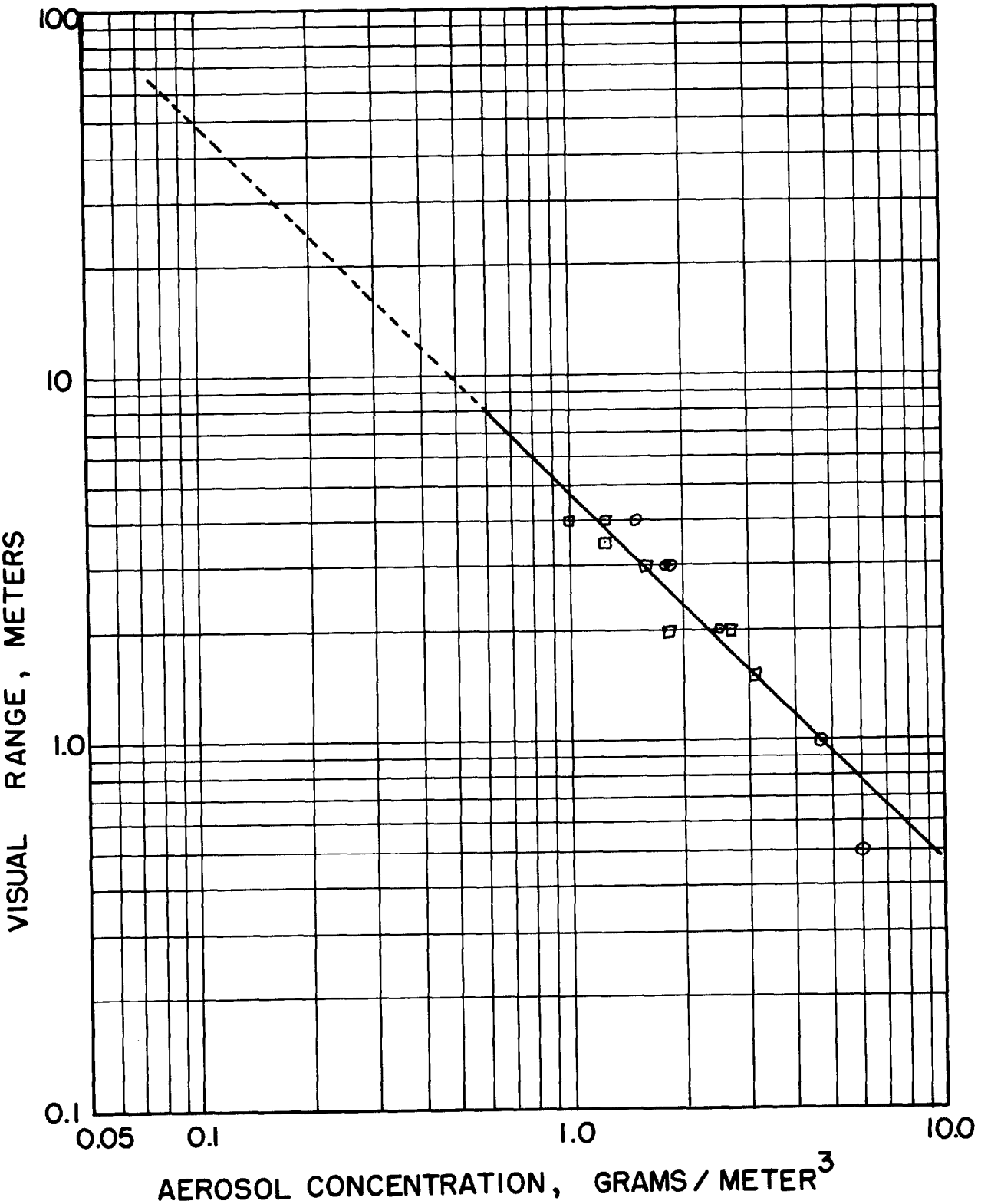

FIG. 4 - VISUAL RANGE IN SODIUM PEROXIDE CLOUD

(⊙ - 22% R.H., ⊡ - 46% R.H.)

when C_m is in grams per cubic meter, D is expressed in meters, and alpha has a value of 4.65. This equation implies that when the aerosol concentration is halved, the visual range is doubled.

Figure 5 shows the experimental arrangement of the observation targets and their relative visibility at various aerosol concentrations.

c. Light extinction

Light extinction measurements were made using a one milliwatt He-Ne laser which emitted monochromatic light having a wavelength of 0.6328 μ. This beam was directed across the aerosol chamber onto a photodetector, and the intensity of light reaching the detector was measured as a function of aerosol concentration. The beam can be seen in the lower part of Figure 5d. To insure that only extinction and not forward scattering was measured, the acceptance half angle was limited to 4 milliradians by one millimeter diameter apertures. This acceptance angle is consistent with the recommendations of Hodkinson(4).

The data for two runs are shown on Figure 6. There does not appear to be any significant difference between the data points for these two runs. The dotted line indicates expected transmittance if only single scattering occurs, and it is a straight line in accordance with Bouguer's Law. Deviations from the dotted line begin at a transmittance of about 70%, as pointed out by Van de Hulst(5). The effect of multiple scattering on transmittance is illustrated by the difference between the solid and dotted lines. As the aerosol concentration increases, the effect becomes more pronounced.

Bouguer's Law can be expressed in the form(6)

$$T = 100 \exp (-3C_m Qt/2\rho d)$$

where T is the percent transmission, C_m the aerosol concentration in grams per cubic centimeter, t the path length in centimeters through which the beam must travel, d the mass median diameter of the aerosol particles, and ρ the aerosol particle density. The latter two terms have the units of centimeters and grams per cubic centimeter, respectively. Q is the extinction coefficient which, according to Hodkinson(7) has a value of 2 for irregular particles larger than about 1.0 microns in diameter.

From the slope of the dotted line in Figure 6, and the measured particle mass median diameter, it is possible to estimate

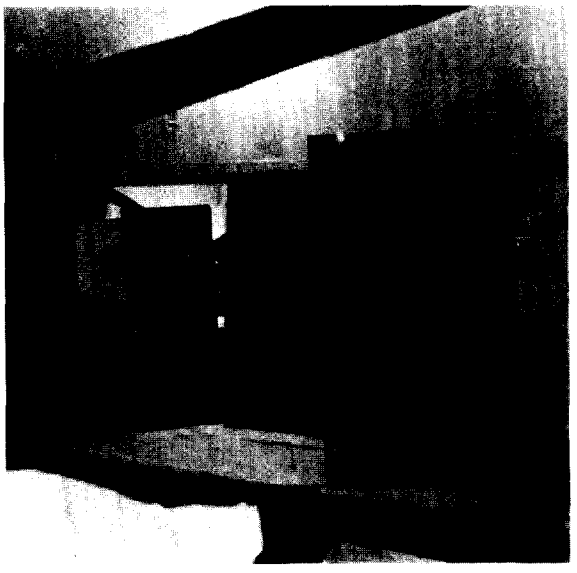

a. $C_m = 0$

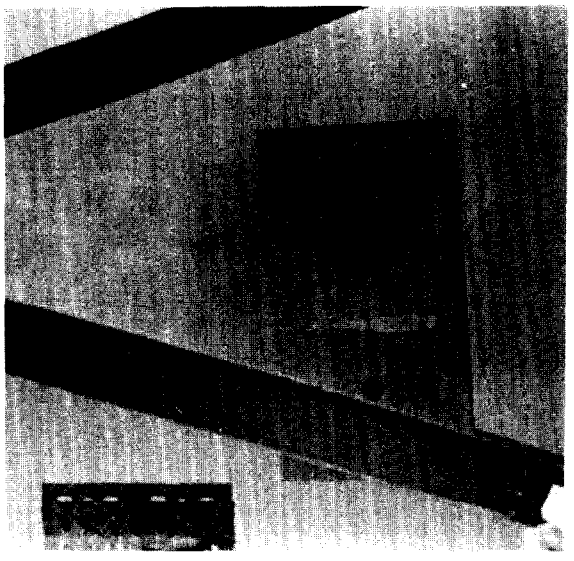

b. $C_m = 4.1\ gm/M^3$

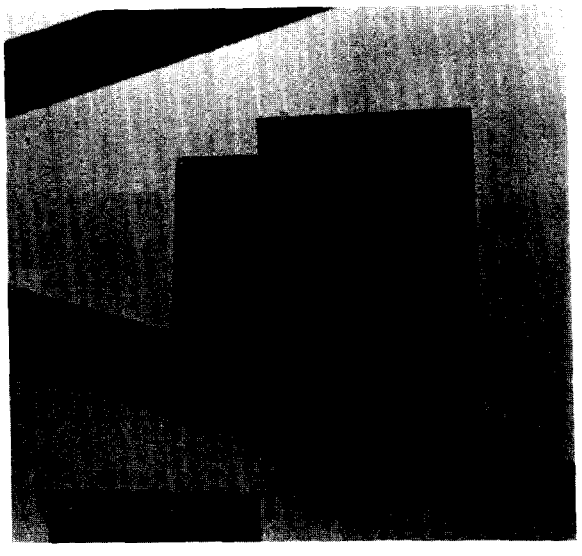

c. $C_m = 2.6\ gm/M^3$

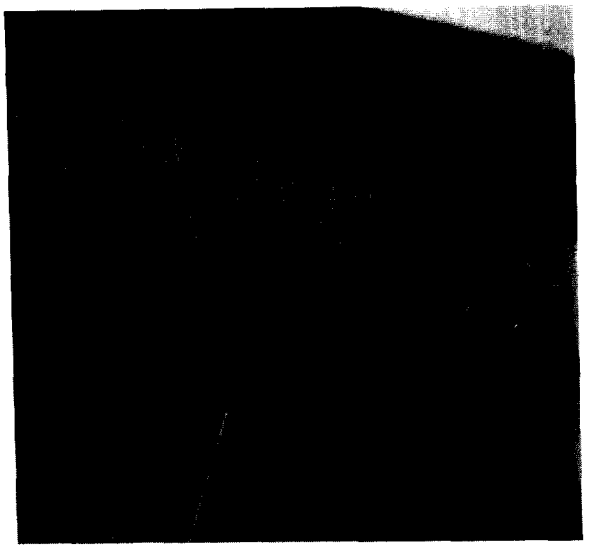

d. $C_m = 1.8\ gm/M^3$

FIG.5 - PHOTOGRAPHS OF VISIBILITY TARGETS AT VARIOUS AEROSOL CONCENTRATIONS

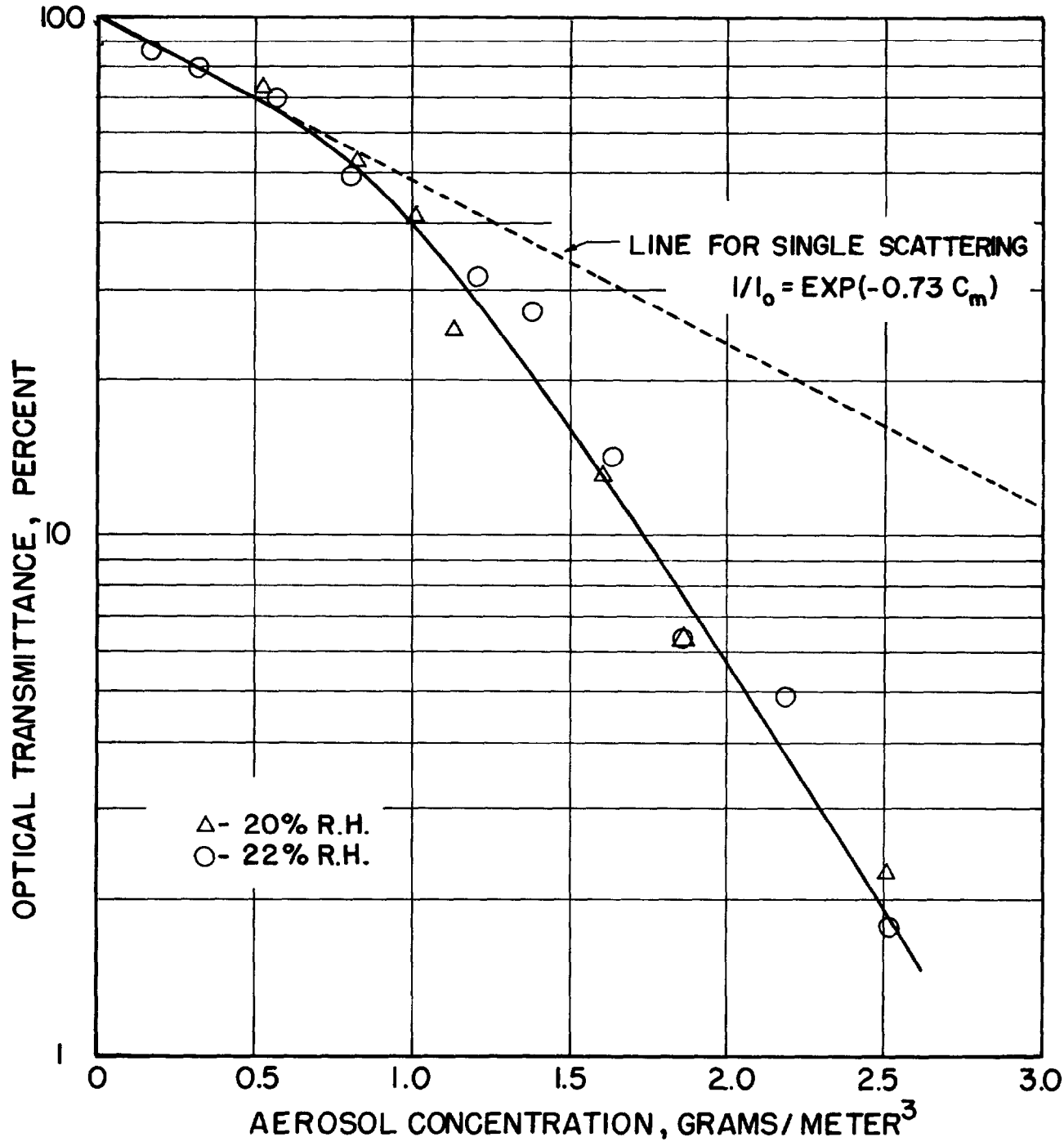

FIG. 6 - TRANSMITTANCE AND MASS CONCENTRATION THROUGH SODIUM PEROXIDE CLOUDS

particle density, i.e.,

$$\rho = 2.05\ Qt/d$$

Using this relationship, a particle density of 1.2 grams per cubic centimeter was deduced, which can be compared to a density of 2.8 gm/cm^3 for solid sodium peroxide. This reduced density (density ratio of 0.43) would be expected for aerosol particles produced by burning, although reported ratios for oxides of other metals are sometimes lower[8]. It is possible to partly explain this difference by considering methods of measurement used previously. For example, Whytlaw-Gray and Patterson[9] discussed experiments where density was determined from weighings of electrically precipitated smokes. The precipitated material, being an agglomeration of agglomerates, would have greater void space than the airborne particles. Thus, lower densities would be expected. When samples of our test aerosol were precipitated and the density determined in this manner, densities of 0.54 gm/cm^3 were determined, which gave a density ratio of 0.19, also consistent with reported data[8]. However, we feel that use of the light extinction technique is more representative of the airborne particles.

Samples of the test aerosol were collected on glass slides using a point-to-plane electrostatic precipitator and were then examined in a JELCO scanning electron microscope using secondary scattered electrons. Figure 7 shows the particles at a magnification of about 2000X. The flocculant nature of the particles is clearly evident, and they appear to be isometric flocs made up of many smaller, sphere-like particles. A density ratio of 0.43 does not appear to be inconsistent with the structure of these particles.

d. Light scattering

Light scattering measurements were made on the sodium peroxide aerosol using a Brice-Phoenix Light Scattering Photometer, modified for aerosols. Data were collected at twelve points within the interval of 7° to 140°, and included both plane and perpendicular polarization for green and white light.

Figure 8 shows a plot of the scattering intensity of the aerosol as a funciton of scattering angle for different times. The relative smoothness of these curves when compared to similar curves for spherical, nonabsorbing particles, is consistent with data of Hodkinson[7] for irregular particles having a broad size distribution. The experimental data are well represented by calculated points based on the measured size distribution at

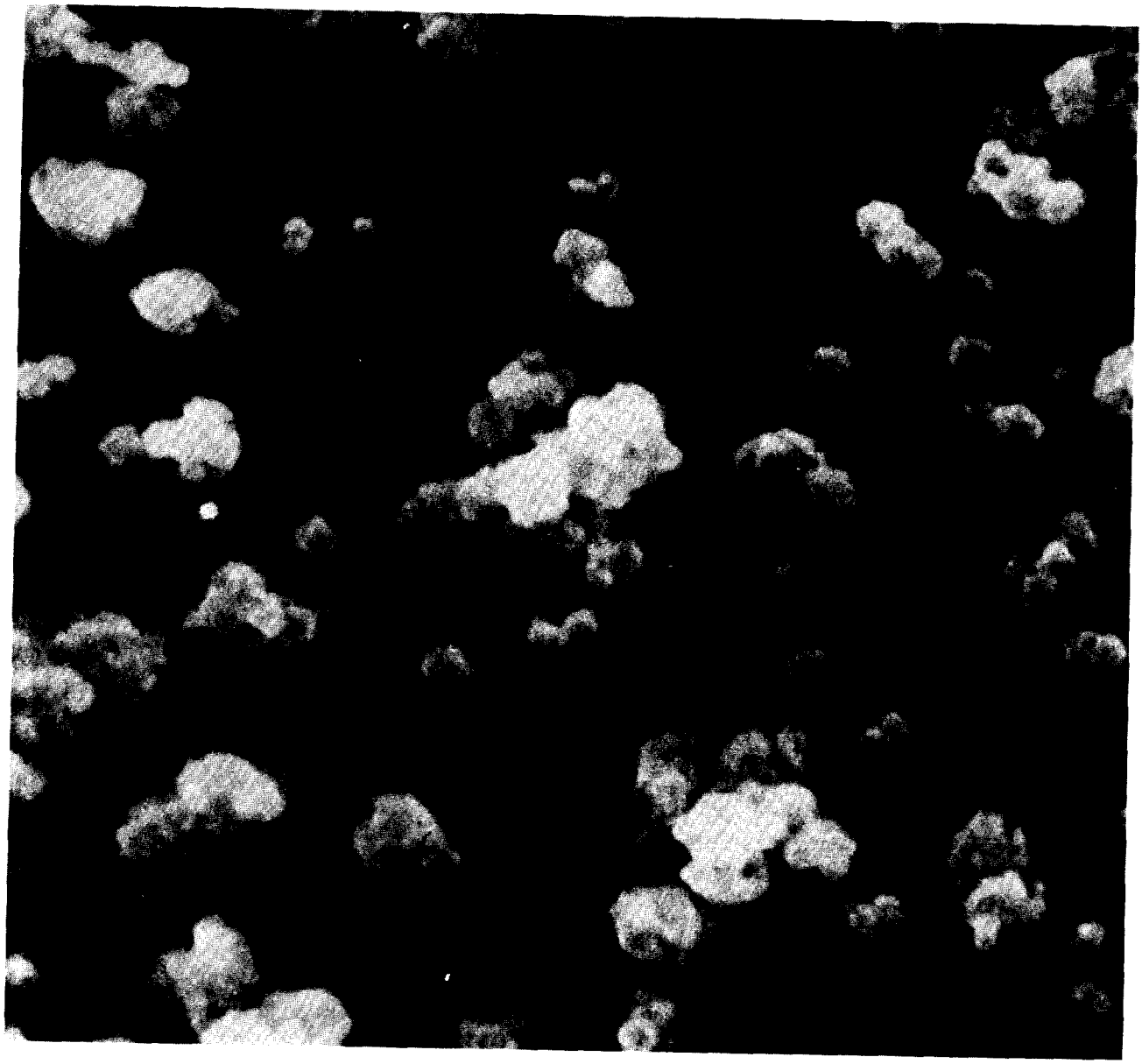

⟷ 1 MICRON

FIG. 7- SCANNING ELECTRON MICROSCOPE PHOTO OF COLLECTED AEROSOL PARTICLES (30° INCLINE)

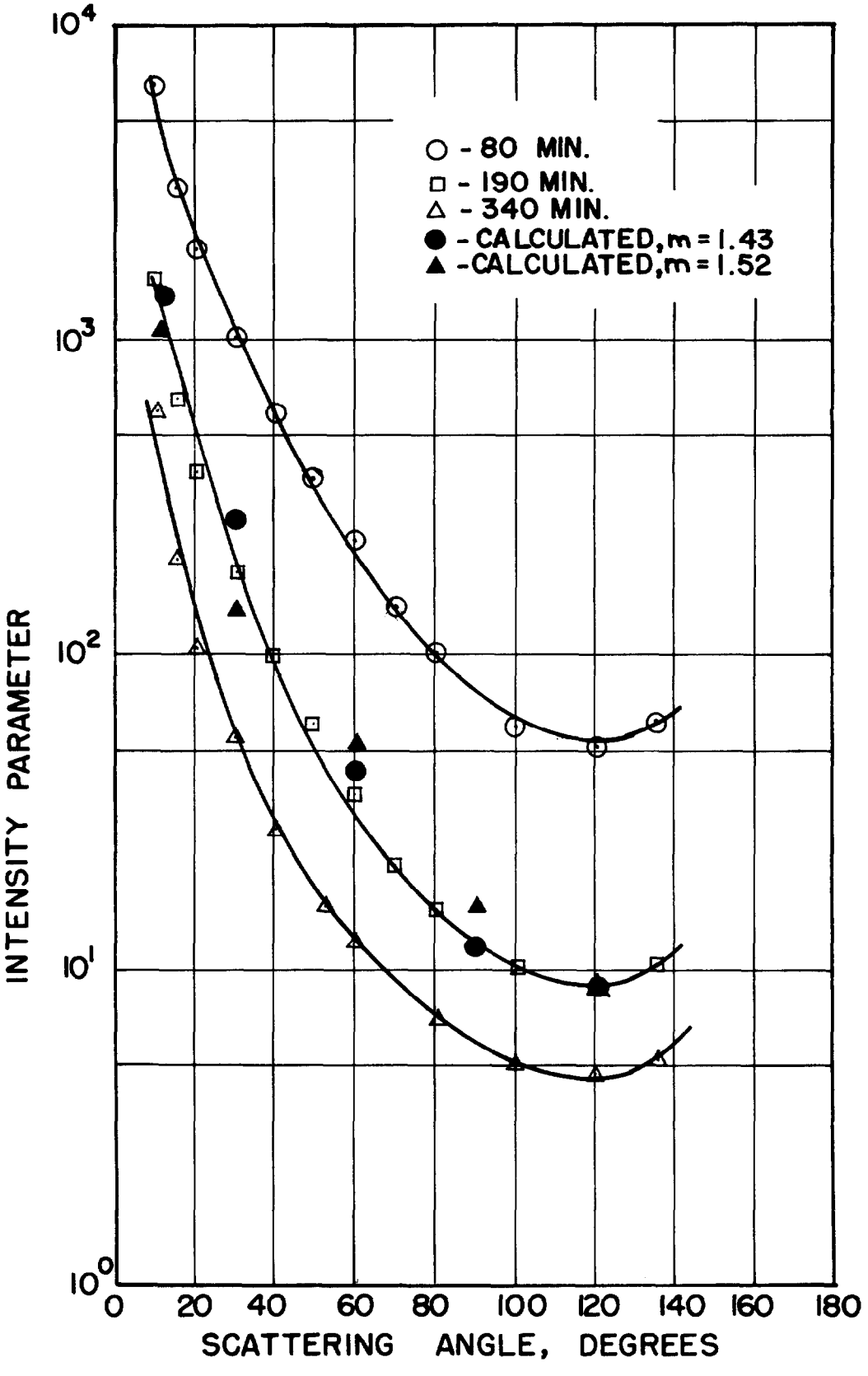

FIG. 8 - ANGULAR SCATTERING MEASUREMENTS OF SODIUM PEROXIDE AEROSOL

190 minutes and Mie theory using refractive indices of 1.43 and 1.52 for the aerosol particles.

The strongly forward scattering tendency of the sodium peroxide particles is apparent from Figure 7, with intensity variations of over three orders of magnitude. This variation is roughly the same as that reported for polydisperse coal dust[6].

Discussion of Data

In order to see an object, whether it is emitting light or not, there must be some degree of contrast between the object and its background. For an isolated object surrounded by a uniform and fairly extensive background Middleton[10] gives as a definition of contrast, C, the expression

$$C = \frac{B}{B'} - 1$$

where B is the luminance of the object and B' the luminance of the background. When the luminance of the object and background are the same, the constrast is zero and the object can't be seen; if the object is less luminous than its background C is negative, reaching a value of minus one for an ideal black object against a white background. When the object is brighter than its background, C can have any value up to infinity. For example, a light at night represents a case where C has a large value.

The minimum amount of contrast necessary for an object to be seen is the subject of much speculation, depending to a great extent not only on the physical properties of the medium through which the viewing is taking place, but also on the psychological state of the observer, the adaptation of his eyes to the general background light, etc. Therefore, the minimum contrast is difficult to predict without experimental visibility measurements for a given aerosol. Even the experimental numbers which we developed should be taken only as rough guides because of the human variables involved. Nevertheless, these data are consistent enough to be useful in estimating visibility at various aerosol concentrations.

It is possible to estimate the value of B/B' for a black object against a white background through the use of Koschmieder's Theory, which in its simplest form may be expressed as[10]

$$B/B' = 1 - e^{-\sigma t}$$

where σ is the extinction coefficient, defined as

$$\sigma = 3C_m Q/2\rho d.$$

Replacing Koschmieder's equation for B/B' in the contrast equation gives

$$C = - e^{-\sigma t}.$$

This equation says that with a short viewing distance ($t << 1$) or a very low aerosol concentration, ($C_m << 1$), C is equal to minus one, and we would have perfect viewing of the black object.

Suppose now we define a limiting value of C as ε, the threshold of brightness contrast; that is the contrast level at which we can just see a black object against the white background. Then using visibility data from Figure 4 and measured properties of aerosol size and density ε can be calculated for the sodium peroxide aerosol. These data are shown in Table 1

Table 1

ESTIMATED THRESHOLD OF BRIGHTNESS CONTRAST, ε

Visibility, Meters	Aerosol Concentration	ε
4.0	1.00	-0.468
3.5	1.25	-0.436
3.0	1.60	-0.402
2.0	1.85	-0.495
2.0	2.32	-0.414
1.5	2.55	-0.483
1.0	4.90	-0.395

Average ε is 0.44

For viewing distant objects through haze or fog, a value for ε of 0.02 is often used for daylight conditions although, as pointed out by Middleton[10], there is a great deal of variability in this number. Target size, type and amount of illumination as well as the relevant aerosol properties all affect this value, as do many psychological factors. The value which we determined of 0.44 is not unreasonable compared to the variety of values

reported in the literature, although it probably also reflects the extreme opacity of the sodium peroxide aerosol. It was mentioned earlier that the particles scattered light very strongly in the forward direction. This property would tend to reduce contrast around an object and thus require more contrast for viewing.

To answer the question of how to best improve visibility in a chamber containing sodium peroxide particles, we should consider the definition of C, the contrast. Since C can have very large positive values when viewing a light source, if objects, which are important to find after an accident, such as major valves, emergency switches or exits, were provided with strong light sources, their location could be more easily determined, even though the objects themselves still could not be seen. Even these lights would be essentially useless in aerosol concentrations above about 5 gm/M^3. If emergency workers were also provided with lights when they entered a dense aerosol cloud, these lights would aid them in keeping track of each other or signaling each other in the cloud, but the lights, or even strong flashlights, would be of little use to the individual in locating non-reflecting objects. Searchlights would also be of little value since the light would increase the relative illumination of the background as well as the target. One exception would be highly reflective surfaces. Since in strong illumination these surfaces are equivalent to sources of light, a flashlight or searchlight would help in locating them.

Summary

Tests were conducted with a sodium peroxide aerosol produced by open pan burning to investigate the dense optical nature of the resultant cloud. Aerosol concentrations ranged from 0.01 to 10 grams per cubic meter in a closed room which had a volume of about 100 cubic meters.

Samples of the cloud were collected for electron microscopy using an electrostatic precipitator and from these samples a count mean particle diameter of 1.6 microns was determined, with the log-normal distribution having a geometric standard deviation of 2.3.

Black discs on white targets were used to determine the visual range in the cloud. An empirical estimate of the range is given by:

$$D = 4.65\ C_m^{-1}$$

where D is in meters, and C_m is in grams per cubic meter.

Light transmission measurements were made using a laser light source. At high aerosol concentrations, multiple scattering was evident. At low concentrations, Bouguer's Law could be used to deduce the apparent aerosol particle density, which we found to be 1.2 grams per cubic centimeter. Scanning electron microscope photographs appear to confirm this conclusion.

Angular light scattering measurements were made, which showed that the aerosol particles scattered light very strongly in the forward direction. The angular pattern did not change with aerosol concentration, implying a reasonably constant particle size distribution at the different concentrations. Experimental data agree with calculated values when refractive indices of 1.43 and 1.52 were used for the sodium peroxide aerosol along with the measured particle size distribution.

All data indicate the opaque nature of the aerosol cloud. At concentrations above 1 gram per cubic meter, vision would be restricted to four meters or less, making walking through the cloud difficult and potentially hazardous. With concentrations of 0.1 gram per cubic meter, maximum visibility would be limited to about 40 meters, or roughly into the middle of a 200 foot diameter containment vessel. Typical overhead lights could be distinguished at distances three to four times greater than nonlit objects in the same cloud concentration.

Acknowledgements

The authors would like to thank Mr. T. Baldwin for his help in generating the sodium peroxide aerosol. This work was supported in part by U. S. A. E. C. Contract No. AT (30-1) 841, and USPHS Environmental Health Training Grant 5 T01 00016-10.

REFERENCES

1. Koontz, R. L., Nelson, C. T. and Baurmash, L., "Modelling Characteristics of Aerosols Generated During LMFBR Accidents", Treatment of Airborne Radioactive Wastes, IAEA Proceedings Series, p. 51 (1968).

2. Davies, R. J., "Estimation of Aerosol Concentration in a Nuclear Reactor Containment After An Accident", Presented at the International Congress on the Diffusion of Fission Products, Saclay, France, Nov. 4 - 6 (1969).

3. First, M. W. et al., "Semiannual Progress Report," Harvard Air Cleaning Laboratory, NYO-841-22, (1970).

4. Hodkinson, J. R. in Aerosol Science, C. N. Davies, Ed., Academic Press, New York (1966).

5. Van de Hulst, H. C., Light Scattering by Small Particles, John Wiley and Sons, New York (1957).

6. Conner, W. D. and Hodkinson, J. R., Optical Properties and Visual Effects of Smoke-Stack Plumes, PHS Pub. 999-AP-30, Cincinnati (1967).

7. Hodkinson, J. R., in Electromagnetic Scattering, M. Kerker, Ed. Pergamon Press, New York (1963).

8. Fuchs, N. A., The Mechanics of Aerosols, Macmillan, New York (1964).

9. Whytlaw-Gray, R. and Patterson, H. S., Smoke, Edward Arnold, London (1932).

10. Middleton, W. E. K., Vision Through The Atmosphere, U. Toronto Press, Toronto (1963).

DISCUSSION

BEATTIE: A scientific question this time. Can you say Mr. Hinds how these figures for visual range compare with those for water that is the visual range in clouds and so on with which I'm fairly familiar, please?

HINDS: We attempted to, in fact get some information on this affect to compare our results with, but we were unable to. So, I can't really say. My subjective evaluation is that at concentrations of about 1 gm per cubic meter the opacity exceeds the densest fogs possible.

BEATTIE: I could just add that I think that was my impression, thank you very much.

MOREWITZ: Was there any deposition on the visual targets you were looking at and might that not have affected your apparent range?

HINDS: We did not find such deposition, even after 2 runs, we buffed them off; there was insignificant amounts present.

CLOUGH: Could I ask you whether you consider the consequences of the chemical form of the particles which you've made and whether you're sure of their chemical form. Let me tell you why I ask. If you take a normal atmosphere with normal humidity, normal amount of carbon dioxide in it say 0.0003 at. pressure and you do the calculations for the rate of arrival of water vapor and the carbon dioxide, onto the particles and you assume the sticking probability is 1 then you can show that the rate at which sodium peroxide should be converted to hydroxide in the particle is less than a few seconds. If you go on to do the calculation for the rate of conversion of that particle into a solution, in fact it can be shown the sodium hydroxide would make itself into a drop at a relative humidity above 35% in a very short time. If you would then go on to do the next calculation for the rate of reaction of carbon dioxide with that droplet you will find that the rate of formation of sodium carbonate is controlled not by diffusion of the CO_2 gas in the atmosphere but by diffusion of the CO_2 gas in the liquid phase of the sodium hydroxide droplets. However, you still find that the rate of formation of the sodium carbonate is of the order of seconds. So what I'm saying is that in the normal atmosphere this is all very rapid and from the calculations one might expect that a sodium peroxide particle would almost immediately form itself into sodium hydroxide droplets; this is above relative humidity 35 percent. If the relative humidity wasn't above 92 percent the sodium carbonate formed in the droplet would subsequently cause the droplet to dry out again into a sodium carbonate particle.

That is more a statement than a question but I would appreciate some comments on it. May I just ask, do you know that those electron microscope pictures which you showed are sodium oxide particles and not tried-out hydroxide or carbonate?

HINDS: In answer to your last question -- we took electron-microscope, I mean electrostatic precipitator samples and kept them in dry nitrogen at all times to prevent any contamination. We feel they are representative of what existed in the chamber. As far as the chemical nature of the aerosol we didn't make any evaluation apart from observing the whitish yellow color of the filter sample which is the color of sodium peroxide. The chemical composition doesn't affect this analysis, if the particles are dry it doesn't make too much difference what they are except for the calculation of their density ratio and use of refractive index. In fact one set of points the refractive index used is 1.43 which is fairly close to that of the carbonate. I believe the other, 1.52, is what we think is correct for sodium peroxide. Both yield similar scattering diagrams.

FIRST: May I add a few words to what Mr. Hinds has said because his experiments were piggyback on some of mine and I know how the aerosols were generated. Your supposition is well founded. To overcome the problems which you have brought up, we would dehumidify the closed chamber before setting up the aerosol, getting down to a dew point of about 40°F. This was one way. In some of the later experiments we would, first, introduce a small amount of sodium and allow it to scavange the moisture and CO_2 out of the atmosphere as it settled and then start the experiment.

SODIUM AEROSOL FILTRATION STUDIES*

M. W. First and T. Baldwin

Harvard School of Public Health
665 Huntington Avenue
Boston, Massachusetts 02115

ABSTRACT

Industrial cleanable cloth filters have important advantages for sodium fume collection following accidental releases from liquid metal cooled fast breeder reactors. Glass filter fabrics have superior temperature resistance, but are attacked chemically by strong alkalies and are difficult to clean by gentle backflow. Teflon fabrics are stronger and can be cleaned of accumulated filter-cake by vigorous mechanical shaking. In addition, they have excellent chemical resistance and good cleaning characteristics. When Teflon is pretreated with an asbestos filter aid, it has high initial collection efficiency and may be cleaned satisfactorily for many cycles. This permits total filtration of large amounts of sodium fume per square foot of filter cloth.

I. INTRODUCTION

Accidental loss of coolant to the containment vessel spaces from any part of a sodium cooled nuclear reactor will result in rapid vaporization and oxidation of the hot metal (500-1050°F) to produce an airborne fume. The chemical nature of the reaction products will be determined by the partial pressures of oxygen and water vapor in the spaces affected and the quantity of sodium released. The fraction of the escaping sodium that becomes airborne will be influenced primarily by the method of release; sprays producing more airborne particles than spills.(1) Rapid capture and removal of sodium fumes is essential if the facility is to continue to operate in spite of minor malfunctions and avoid release of radioactivity to the environment in the event of a major, multi-ton spill.

Heat must be removed continuously from sealed cells containing primary and secondary sodium loop heat exchanger equipment and associated machinery to avoid equipment failures from overheating. Heat removal is also an important aspect of accident control in the fuel rod inspection cells and in the main containment area during fuel rod changing to avoid sudden severe tempera-

*The work reported upon herein was performed under terms of Contract AT (30-1) 841 between Harvard University and the U. S. Atomic Energy Commission.

ture increases following large sodium spills which may result in interior pressure increases that exceed structural safety limits. Recirculating contained air or nitrogen through refrigerated coils is a satisfactory method for extracting excess heat and reducing gas pressure, but airborne sodium particles that accompany the gas are likely to be deposited on the cooling surfaces by impaction, interception, and thermophoresis and interpose a severe interference to rapid heat flow.[2] Even moderate contamination of the air cooling heat exchanger surfaces can produce failures by the corrosive attack of the strong sodium hydroxide which may form on cold sodium oxide coated surfaces, even when humidity is maintained at a low level. Therefore, it is necessary to protect cooling surfaces and other equipment from sodium deposition by introducing a particle collecting device, such as a filter, upstream of the air cooler, air blower, etc.

Sodium aerosol particles, even when generated by different methods, usually have a mass median diameter between one and two microns when freshly formed and a wide spread of sizes (i.e., large geometric standard deviation)[3,4]. Agglomeration and flocculation occur spontaneously and rapidly when high particle concentrations are generated by oxidation of hot metallic sodium and this process produces an even greater spread in the sizes of particles that are present. When collected on filters, the particles produce rapid resistance rise because of their tendency to compact under slight pressure and the detrimental effects on porosity of even small chemical changes brought about by absorption of water vapor. These characteristics of sodium aerosols (i.e., small particle size, high concentration, and marked blinding or plugging characteristics when deposited in filters) require filters possessing high efficiency for small particles and the ability to store large quantities of material in the pores with only moderate pressure rise.

Previous studies of high efficiency, high capacity filters for sodium aerosols[4] have demonstrated that when deep bed filters are assembled so that the various grades of fibrous media are arranged in graduated fiber diameters and packing densities, and when followed by a pleated absolute filter, they are capable of collecting elemental sodium and sodium oxide fumes at high efficiency and storing large amounts of fume in the filter with acceptable resistance increases. One filter pack design is capable of collection efficiencies greater than 99.9% and sodium fume storage in excess of 0.5 lb of sodium per square foot of filter face area with filtration velocities of 6-12 ft/min and a terminal filter resistance of 20 in.w.g. Sodium storage values in excess of 0.75 lb/sq. ft. of filter face area were obtained when filtration was conducted at lower velocities, but the face area and total space requirements

increased proportionately. Although it is possible to install deep bed fixed filters of this type with high temperature resistance (~1,000°F) and adequate holding capacity for the largest design basis sodium spill, the space required for installation will probably exceed the amount available for this function. Therefore, there is considerable interest in the use of industrial cleanable cloth filters for protecting heat exchangers from fouling after large sodium spills. These filters are commercially available, are designed to handle heavy dust loadings, and are cleanable automatically without interrupting filtration. In addition, accessory equipment of many kinds is available to remove the collected material from the filters and convey it in enclosed tunnels to a prepared disposal site. This is an especially important safety measure when the collected aerosol particles contain a high percentage of unreacted elemental sodium. Cleanable fabric filters have other advantages over the deep bed single use filter, including lower cost and reduced space requirements, and seem a better choice for large reactors whereas the deep bed filter seems better adapted to research and test facilities in which the amounts of sodium in use are small and the size of the sodium spill is similarly limited.

Cleanable cloth filters are inferior to deep bed filters in temperature resistance. Glass filter fabrics are able to tolerate temperatures up to 550°F and have the best temperature resistance of all available fabrics*, but they are fragile and are rapidly degraded by strong alkalies such as sodium hydroxide. When the glass fiber surfaces become etched by contact with strong alkali, it becomes more difficult to clean accumulated filter cake during the cleaning cycles. Teflon fabrics are resistant to chemical attack by all concentrations of sodium oxides and hydroxide, they release the filter cake easily, are much stronger than glass (so they can be cleaned by vigorous shaking), and are superior in every respect except temperature resistance. The maximum temperature exposure for this fabric is approximately 450°F. Little is known about brief period heat resistance as industrial cleanable fabric filters are designed to have a service life measured in years under normal service conditions, but it seems unlikely that a significant increase in temperature will be compatible with dependable service and high collection efficiency. The worthwhile characteristics of cleanable industrial cloth filters make them of potential value for application to LMFBR reactors for control of accidental sodium releases.

*This temperature limitation is not because of the softening point of the glass (approximately 1000°F) but the loss of the silicone-Teflon lubricant which makes it possible to shake the filter bags without fracture of individual glass fibers.

II. EXPERIMENTAL ARRANGEMENTS

A. Generation of Sodium Aerosols

Sodium aerosols were generated by heating elemental sodium to 1000°F or higher in an inert atmosphere, sweeping the vapors out of the heated zone with heated nitrogen or other inert gas purge stream, and permitting condensation of sodium vapor to occur in a cool zone with or without the presence of oxygen.[3] Under these conditions of aerosol formation, particulate loading was low (<0.5 gm/M^3), pressure drop increase of the filter was rapid per gram of sodium deposited (per square meter of filter cloth), and filter cloth cleaning was difficult.

Other sodium aerosols were generated by spraying molten sodium at a temperature in excess of 500-600°F into an air atmosphere. Under these conditions, hot sodium droplets vaporized and burned to form particle loadings of sodium and sodium oxides in excess of 10 grams per cubic meter of air. Mean particle size was considerably greater than one micron but large numbers of submicron diameter particles were present, even though they represented but a minor fraction of the total weight of airborne sodium. Based on color, it was estimated that the temperature of the sodium flame produced by atomizing hot sodium with compressed, heated nitrogen through a two-fluid pneumatic nozzle was in excess of 2500°F. Atomization of hot sodium under pressure into a 3500 cu. ft. chamber resulted in high sodium airborne particulate loadings which most accurately reproduce anticipated accident conditions.

To simulate reactor operating conditions as closely as possible, molten sodium releases were made intermittently into the test chamber so that initially, the filter was subjected to a high sodium dust concentration, but this declined progressively as particles settled to the floor, deposited on walls and ceiling, and were removed by filtration. When the sodium concentration declined to 1-2 grams per cubic meter (g/M^3), a fresh charge of molten sodium was atomized into the chamber to elevate the concentration again. Cycle time for sodium introductions was about one hour.

B. Cleanable Fabric Filter

Figure 1 shows a diagram of the dual filter installation used for the sodium aerosol studies. The two filter bags, measuring 12 cm in diameter and 1.6 meters long, were sometimes used alternately so that one unit could be on stream while the other was being cleaned but at other times, the two were used in parallel to double the available filter area. The mechanical shaking arrangement is shown in Figure 1. When filtering with glass fabric bags, the shaking mechanisms were inactivated, and the bags were cleaned by back flow air, only.

FILTER BAG TEST APPARATUS

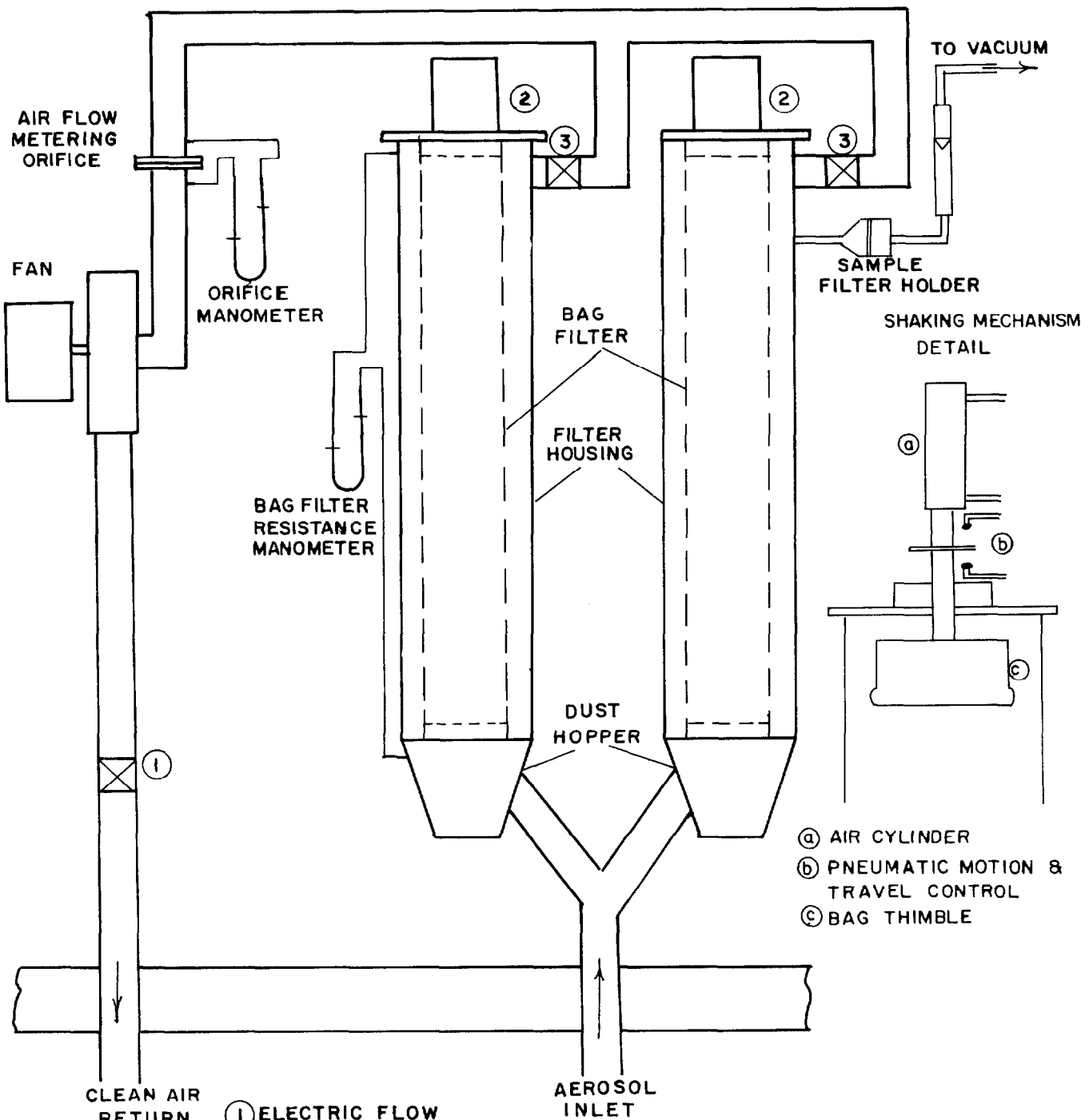

FIGURE I

III. EXPERIMENTAL RESULTS

A. Glass fabric filters cleaned by reverse air flow

Filter bags were tested without prior application of filter aids and after precoating with fine asbestos fibers called "floats"[5]. Initial studies were made on glass bags with an asbestos coating of 156 gm/M^2 of bag surface and a constant air flow rate through the bag of 0.37 M^3/min at NTP*. The air to cloth ratio was 0.61 M^3/M^2 and this was also the superficial filter face velocity in M/min. Inlet particulate sodium oxide concentrations ranged from 750 to 1900 mg/M^3 of air measured at NTP. A maximum pressure drop across the bag of 15 cm of water was selected to avoid stretching the fabric or fracturing the fibers and stitching. Following this practice, an initial run of 137 minutes was obtained on a new glass fabric bag preflocked with asbestos. After backflowing with clean air to remove the sodium deposit and reduce filter resistance, a second run of 64 minutes was obtained (without recoating the bag with asbestos). A third run (again, without new asbestos) lasted 10.75 minutes before the maximum pressure drop was reached. Removal efficiencies (calculated as Na) for this series of tests varied from greater than 99.79% for the initial cycle to greater than 99.40% for the third cycle, reflecting the substitution of an excellent particle retention sodium oxide filter cake for the asbestos filter aid as the filter fabric continued in service. The dashed lines of Figure 2 show the filter pressure drop data related to gas flow through the clean cloth, the application of asbestos filter aid, deposition of sodium oxide, and the three cleaning cycles. It will be apparent from Figure 2 that removal of the filter aid at the time of the first cleaning cycle permitted sodium oxide particles to penetrate into the interstices of the filter fabric during the next filtration cycle and to form a tenaceous surface cake that could not be cleaned satisfactorily. This resulted in a third and subsequent filtration cycles which were too brief to be of value.

Next, studies were conducted to explore the performance of glass fabric filter bags precoated with an asbestos filter aid and recoated with asbestos following each cleaning cycle. The objective was to extend the period of satisfactory bag service by maintaining an asbestos "parting layer" between fabric and deposited aerosol particles to prevent penetration of particles into the fabric structure where they become entrapped and, after chemical and physical changes, resist cleaning. The solid lines of Figure 2 show the results of filtration with this method of operation (i.e., with a precoating step preceding each filtration cycle). As may be noted, this procedure did

*20°C and 1 atm.

FIGURE 2 GLASS FILTER BAG PERFORMANCE (PRESSURE VS. SODIUM DEPOSITED)

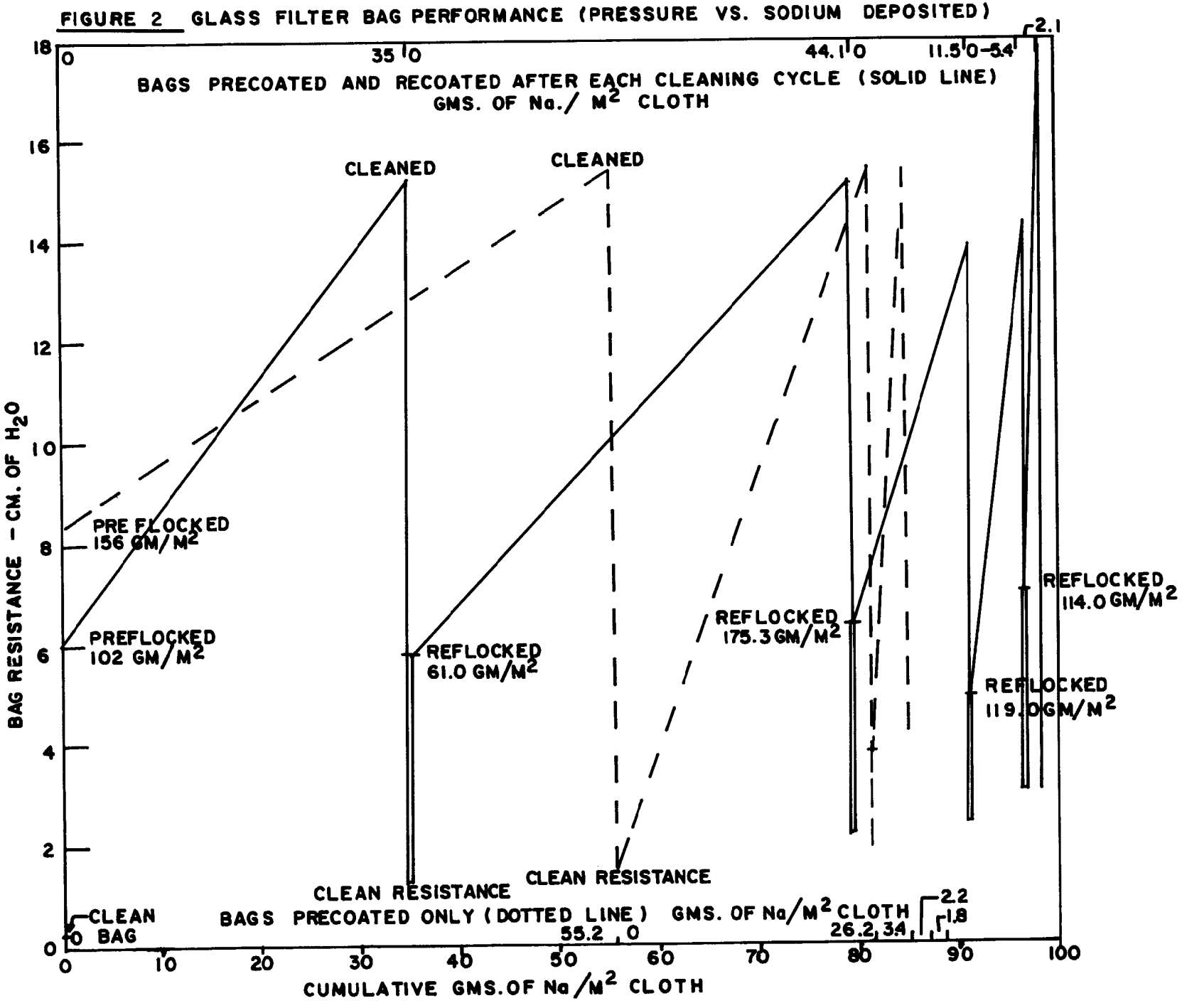

not result in any significant improvement in the performance of the bags.

During the final cleaning cycle, the glass fiber filter bag ruptured. It has not been determined if chemical damage to the glass from sodium oxide and hydroxide deposition was an important contributor to this failure. Nonetheless, based on this factor and the data obtained in the filter studies, it was concluded that glass fiber filter bags may not meet the needs of a cleanup system for a major sodium fire.

B. Teflon fabric filters cleaned by backflow air

Figure 3 shows that Teflon filters can be operated satisfactorily with only a single preflocking (to obtain initial clean bag high efficiency filtration) and that filters composed of this fabric, when compared with glass, will give twice or more the number of useful cleaning cycles without reflocking.

C. Teflon fabric filters cleaned by mechanical shaking

When using Teflon filter bags, it was possible to clean the filter cake from the bag surfaces by mechanical shaking. This proved more effective than gentle backflow air cleaning without shaking, which is required for glass fabric bags. As a result, it was possible to greatly reduce filter resistance each time the bags were cleaned and to permit a longer filtration cycle before reaching the maximum pressure drop of 15 cm of water.

A typical series of filtration cycles during a period when there were four sodium fires in the chamber is shown in Figure 4. It is particularly pertinent to note the greatly increased filtration cycles (numbers 8, 9, and 10) which resulted from vigorous bag cleaning. The last 3 cycles exceeded the initial cycle in length even though the bags were flocked with asbestos floats only before the first cycle. For this series, the total amount of sodium deposited was 750 gm/M^2 (one bag only) of filter face area. Filtration efficiency was in excess of 99% for all tests.

IV. DISCUSSION AND CONCLUSIONS

Experimental results show that aerosol particle size has an important effect on filter resistance increase per weight of particles deposited. High loadings (e.g., up to 30 grams per cubic meter of air) were associated with larger mean particle size and low pressure drop increase across the filter bag. At sodium fume loadings substantially below one gram per cubic

TEFLON BAG FILTER

(EVAPORATED FUME)

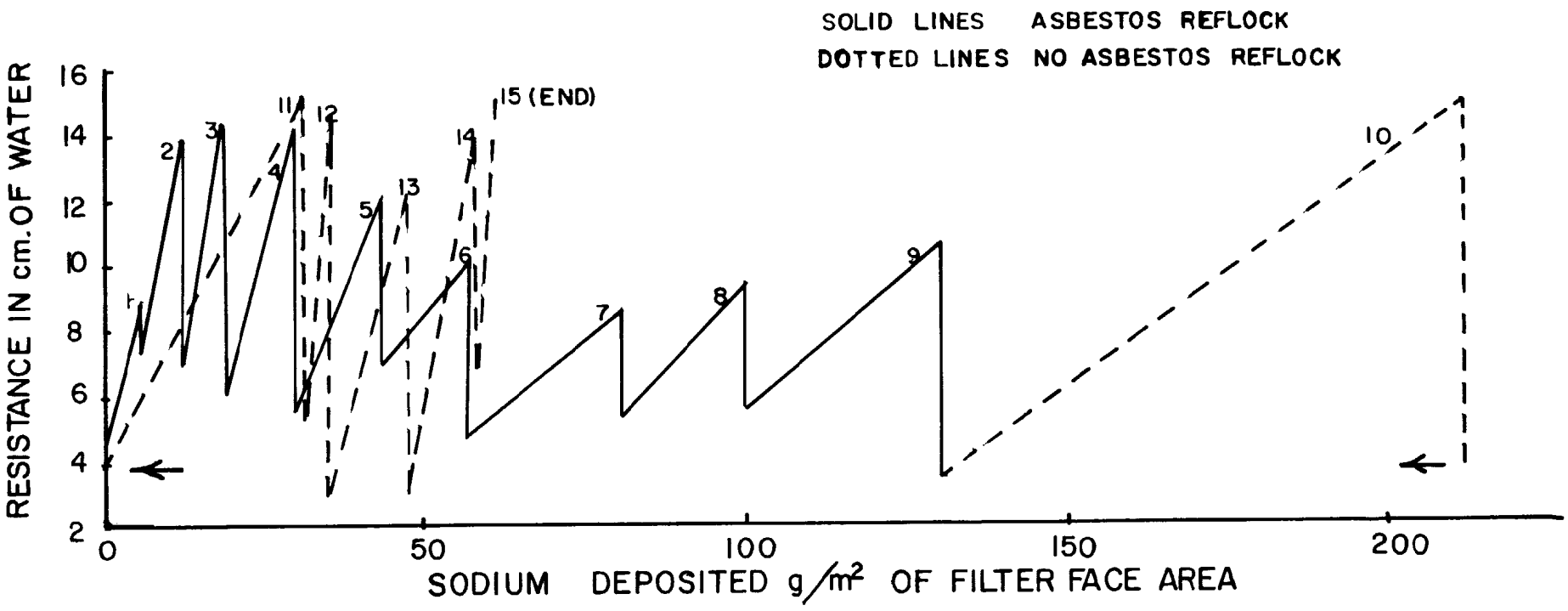

EXPERIMENTAL CONDITIONS

FILTER FACE VELOCITY 0.9cm./sec.
FUME M MD 1.1μ
CLEANING METHOD – BACKFLOW

Figure 3 Typical Series of Filtration Cycles Using Teflon Fabric Filters (Sodium Aerosol Source - Evaporated Fume).

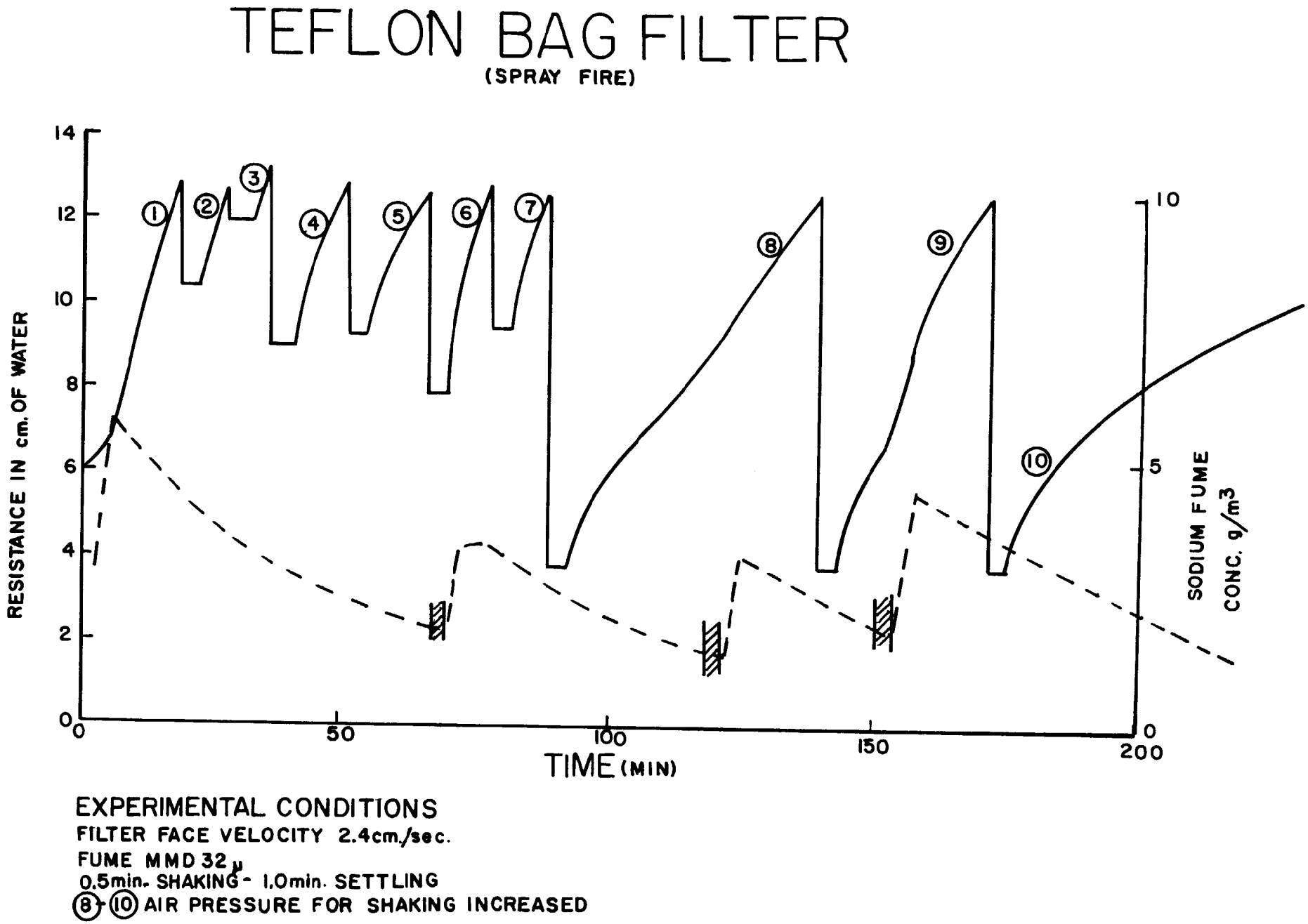

Figure 4 Typical Series of Filtration Cycles Using Teflon Fabric Filters (Sodium Aerosol Source - Spray Fire in Air)

meter of air, the mean particle diameters were close to one micron and a rapid filter pressure drop increase per unit of sodium deposited was observed. At sodium loadings well above 10 gm/M^3, a very high weight percentage of the particles were from 10 microns to well into the visible range (> 100 microns). These very highly agglomerated and porous particle clusters produced only modest pressure drop increases per unit of aerosol particle deposited. It is fortuitous that the higher the sodium compound loading on the filter, the slower the rise in pressure drop. This phenomenon is now being studied more closely because it has important implications for the design of accident control systems.

Also to be noted is the fact that withdrawal of 1% of the chamber gas volume per minute through the pilot-plant filter system (and return of the cleaned air to the chamber) had no perceptible effect on hastening the clearing of sodium particles from the chamber air. This tends to confirm the wisdom of using local exhaust ventilation rather than general ventilation for controlling the spread of sodium throughout the facility. This would prevent airborne sodium from depositing on surfaces and, by confining the evolving fumes to a small area and a limited air dilution, maintain very high dust loadings to the filter which should result in porous filter cakes and long filtration cycles between cleanings.

Studies are in progress to produce sodium fume loadings inside the test chamber up to at least 30 g/M^3 by both spray fires and pool fires to test the effect of loading on particle size, particle shape, and filterability. In addition, studies are being conducted to evaluate quantitatively the benefits to be derived from preflocking Teflon filter cloths with asbestos floats.

REFERENCES

1. First, M.W. "Contamination Control of Sodium Fires from Liquid-Metal Cooled Reactors" for presentation at the 18th Conference on Remote Systems Technology, American Nuclear Society, Washington, D.C. (Nov. 16-19, 1970).

2. First, M.W. and Yusa, H. "Heat Transfer Properties of Sodium Compounds Deposited on Surfaces from Aerosols", Proc. 11th USAEC Air Cleaning Conference, Conf. 700816, pp. 413-424, Clearinghouse for Federal Scientific and Technical Information, National Bureau of Standards, U.S. Dept. of Commerce, Springfield, Virginia. (Jan. 1971).

3. Viles, F.J. Jr., Himot, P. and First, M.W. "High Capacity --High Efficiency Filters for Sodium Aerosols," Harvard Air Cleaning Laboratory Report, NYO-841-10, Boston, Mass, (Aug. 1967).

4. First, M.W., et al. "Semiannual Progress Report, Sept. 1, 1969-Feb. 28, 1970," Harvard Air Cleaning Laboratory Report, NYO-841-22, Boston, Mass. (April, 1970).

5. Billings, C.E., First, M.W., Dennis, R., and Silverman, L., "Laboratory Performance of Fabric Dust and Fume Collectors", Harvard Air Cleaning Laboratory Report, NYO-1590, Boston, Mass., (August, 1954).

DISCUSSION

PALMER: I'm wondering if these filters would have any application for an accident in which organic coolant is burning? Here again we have quite a sticky mess. Could you comment on this?

FIRST: I believe it might if it had a coating of filter aids which would be selected to handle it. The reason I say this is that some years ago the Southern California Edison Company decided to make an installation for removal of the cloud that was emitted from their heavy oil burning stations. This white plume was largely sulfuric acid mist and, as you can imagine, when this material gets into a filter cloth it produces a very sticky wet mass. They found, however, that if they blew powdered limestone or dolomite into the fire box and let that go through the system, it not only had a beneficial effect on the corrosion of the boiler tubes, but when it came out and was deposited on the glass fabric it acted as a filter aid. The sulfuric acid was soaked up on the calcium-magnesium oxide mass. In this manner, they were able to use the bags successfully for many years. For this reason, I think it is possible, by using a system of filter aids, to handle many things which could not be handled with just a bare cloth.

BEATTIE: I've listened to what you have to say with great interest Dr. First, and to what your Mr. Hinds said before you. And I haven't come to pick a quarrel with you this time. I just wanted to add one or two thoughts that occurred to me which seem to carry some of these facts about sodium clouds together for me. In a fast reactor there are usually some sodium feed pipes. There have to be some in sodium equipment. At any rate, in the Dounreay fast reactor the one that has been operating for about 10 years, there were such pipes and the operators were worried about the possibility of a burst. And of course the system is pressurized with Argon so they were worried about what they called a gusher, which would be burning sodium coming out of a burst pipe. And if you think that a burst pipe in these circumstances is incredible, well, we don't believe in incredibility, and strange things do happen, as Dr. Epler of Oak Ridge has shown recently, in some papers. However, the Dounreay people did an experiment to satisfy themselves. Dounreay is in the northern part of Scotland, so there are very few people. They waited for a day when the wind was blowing towards the North where there was nothing but sea, icebergs, and the North Pole. And they took out onto the shore a vessel filled with I think, a kilogram or so of inactive sodium, heated and pressurized, opened the tap and stepped back smartly. What was observed was indeed a gusher, and the kind of dense cloud that your Mr. Hinds mentioned and here it would have the sort of density, particulate density that you were mentioning. Much denser than water clouds, that is optically dense. Denser than even the densest cumulus

clouds. And of further interest is the fact that the cloud drifted off over the sea depositing very very slowly indeed. It drifted a long way and was lost from sight, thinning out all the time. This takes me back to other papers on the deposition of sodium vapor in containment; of course this was in the open air, the experiment at Dounreay. But I did reflect then that if the deposition took so long in the open air, it could very well take a long time in a containment, if the concentration were low enough.

FIRST: I quite agree, of course. For the very rapid agglomeration and flocculation situations that we have been discussing, we refer to concentrations of grams per cubic meter. It's quite obvious that the rate at which the sodium is released is a very important factor in the size distribution which can be expected. By that I mean the total quantity of sodium lost is not the only important factor but, rather, the rate at which it is lost. Very slow evolution produces small particle sizes because the particles will deposit continuously by settling, thermophoresis, etc., and will only just be replaced by the slow rate of generation. I wonder if there is any significance to the fact that you British conducted the experiment just off the coast of Scotland?

BEATTIE: Being that I am a Scot myself, I did of course disapprove of it!

RIVERS: I believe you said that you did not measure efficiencies or penetration because they were uniformly very high, and therefore did not seem to be a matter of much concern.

FIRST: Let me clarify that. I said that I didn't report the results here, but we did measure collection efficiency and it was uniformly high. I thought it would not be interesting to show a lot of nines after the decimal point.

RIVERS: We have done a great deal of work in this line, measuring the performance of fabric collectors on metal oxides (chiefly zinc oxide). It always appears that there is an intimate relationship between the pressure rise across the cloth and the system operating parameters - the frequency of cleaning cycle, method of vibration and the penetration level considered acceptable. Generally engineers ignore penetration, because it is small in industrial situations. In nuclear applications, we may be required to deliver specified penetrations, and this factor will affect the design of the equipment. I would like to see penetration data for your experiments, and I want other people to understand that penetration is a design parameter.

FIRST: I quite agree with you. The efficiency or penetration is very important. I hope you will find that information in the preprint. If you do not, I will be glad to get the information for you and to repair that omission in the final copy that goes to the printer. It should be there of course.